SYNTHESIS AND REACTIVITY OF SOME Co-, P-CHIRAL Co(III) COMPLEXES

LIHUI SUN

Synthesis and Reactivity of Some *Co*-, *P*-Chiral Co(III) Complexes

by

© **Lihui Sun**

A thesis submitted to the School of Graduate

Studies in partial fulfilment of the

requirements for the degree

of Master of Science

Department of Chemistry

Memorial University of Newfoundland

St. John's, Newfoundland

Jan. 1998

Abstract

Chiral phosphorus compounds have attracted research interest due to their biological activity and potential applications. Asymmetric synthesis of chiral phosphorus compounds via transition-metal-mediated (TMM) chemistry, with its possibility to modify reaction conditions and to control stereochemistry of phosphorus through coordination, holds promise as a synthetic avenue for synthesis of new phosphorus materials. This thesis focuses on a novel method to synthesize chiral pentavalent phosphorus compounds via optical induction from transition metal complexes and examines the chemistry of the resulting inorganometallic phosphorus moieties for further transformations.

Three series of *Co*-, *P*-chiral Co(III) complexes are synthesized via transition-metal-mediated (TMM) Arbuzov reactions. The structures and spectroscopic properties are described and the reactivity of the synthesized chiral phosphonate moieties are examined. Unlike their organic analogs, the inorganometallic phosphonates are inert to nucleophiles. Reaction with PCl_5 or $SOCl_2$ under prolonged heating cleaves the Co–P bond. In the presence of BCl_3, the perfluoro-substituted *P*-phosphito Co(III) complex reacts with the nucleophile to give a novel product, which involves C–F bond cleavage.

The LUMOs of the inorganometallic phosphonates and their organic analogs are analysed at the Hückel level. The LUMOs of the inorganometallic phosphonates are metal-based while those of their organic analogs are dominated by the orbitals of phosphorus centre. The shift of the LUMO from phosphorus to metal explains the behavioural difference between organic and inorganometallic pentavalent phosphorus compounds.

Acknowledgements

I wish to express my thanks to my supervisor, Professor Chet R. Jablonski, for his guidance, interest, suggestions, patience and financial assistance during my studies at Memorial University of Newfoundland. I learned a lot from our discussions. He has contributed significantly to the quality of this thesis.

I am very grateful to the administrative and technical staff who have helped in one way or another in the course of this research. Special thanks are due to Dr. Brian Gregory and Miss Marion Baggs for measurement of Mass spectra, to Dr. John N. Bridson for collection of X-ray crystallographic data and to Mr. David O. Miller for X-ray analysis and NMR spectroscopic measurements. I also wish to thank Dr. C. R. Lucas and Dr. A. R. Stein for their patience in reading through this thesis, and helpful comments and suggestions in shaping this thesis. Many thanks are also extended to Memorial University of Newfoundland for award of a graduate fellowship.

Finally, I greatly appreciate my husband, Qing Wang, for his understanding, encouragement and support.

To My Husband, Qing Wang,

and My Parents

Contents

List of Tables and Schedules

Chapter 1

Chapter 2

Chapter 3

Chapter 4

List of Figures

Chapter 1

Chapter 2

Chapter 3

Chapter 4

List of Abbreviations

AChE	acetylcholinesterase
ALS	acetolactate synthase
BINAP	2,2'-bis(diphenylphosphino)-1,1'-binaphthyl
CACAO	computer aided composition of atomic orbitals
CAMP	cyclohexylanisylmethylphosphine
CHIRPHOS	2,3-bis(diphenylphosphino)-butane
CIP	Cahn–Ingold–Prelog
Cp	η^5-cyclopentadienyl
Cp*	η^5-pentamethylcyclopentadienyl
de	diastereomeric excess
DIOP	4,5-bis(diphenylphosphino)-2,2-dimethyl-1,3-dioxolane
DIPAMP	1,2-bis[(*o*-methoxyphenyl)phenylphosphino]-ethane
EHC	extended Hückel calculation
EHMO	extended Hückel molecular orbital
ee	enantiomeric excess
FDA	Food and Drug Administration
FMO	fragment molecular orbital
h	hour

HOMO	highest occupied molecular orbital
IR	infrared
L	levo
LUMO	lowest unoccupied molecular orbital
Men	menthol
MO	molecular orbital
mp	melting point
NMR	nuclear magnetic resonance
NORPHOS	2,3-(bisdiphenylphosphino)bicyclo[2.2.1]hept-5-ene
OMPA	octamethylpyrophoramide
PNH	(*S*)-diphenyl-((1-phenyl)amino)-phosphine, $PPh_2NHC^*H(Me)Ph$
PYRPHOS	3,4-bis(diphenylphosphino)-pyrrolidine
RAMP	(*R*)-(+)-1-amino-2-(methoxymethyl)pyrrolidine
RP	phosphinidene
SAMP	(*S*)-(–)-1-amino-2-(methoxymethyl)pyrrolidine
TEPP	tetraethyl pyrophosphate
THF	tetrahydrofuran
TLC	thin layer chromatography
TMM	transition metal mediated
TPP	thiamine pyrophosphate

Chapter 1.

Introduction

1.1 Significance and Methodology for Preparation of Homo-Chiral Molecules

Biological systems, in most cases, specifically recognize a single enantiomer because of the inherent chirality of enzymes. The need for specificity is implied in the basic definition of the word "chirality", as coined by Lord Kelvin nearly 100 years ago.[1] In chemistry, the term refers to molecules which, like a right and left hand, exist in two forms that are mirror images of each other. Chiral molecules may contain chiral centers, axes, and/or planes. Mirror image isomers (enantiomers)[1,122] are identical under achiral conditions, hence have identical spectra and solubility, but behave quite differently in chiral environments. For example, each enantiomer rotates the plane of plane polarized light in opposite directions.

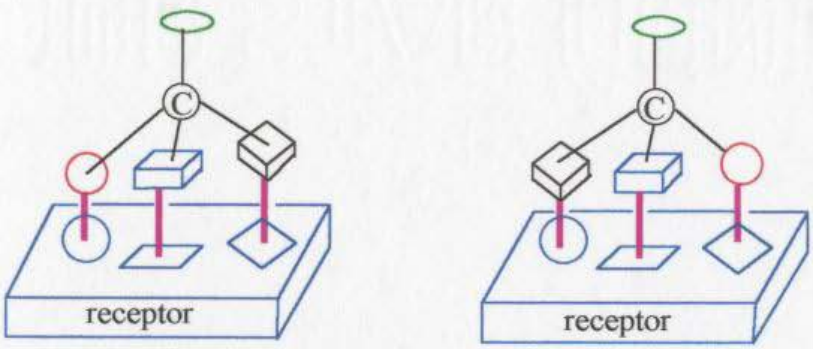

Figure 1.1 Chirality recognition by a chiral biological receptor[1]

Many enzymes are themselves chiral and accept only molecules with

"matching" chirality (Figure 1.1).[1] Hence, each enantiomer can have quite different biological activity. For example, (+)-estrone (Figure 1.2) is a female hormone whereas its enantiomer (–)-estrone has no hormonal activity. The tragedy resulting from the consequence of the stereochemical impurities in thalidomide is another convincing example of the relationship of pharmacological activity to absolute configuration[122] or handedness. The *R*-isomer of thalidomide (Figure 1.2) is a sleeping aid whereas the *S*-isomer is teratogenic. The commercial application of the racemic mixture to pregnant women in the 1960's caused birth defects, which established a new "enantiomer consciousness" as far as drugs are concerned.[1,10] The

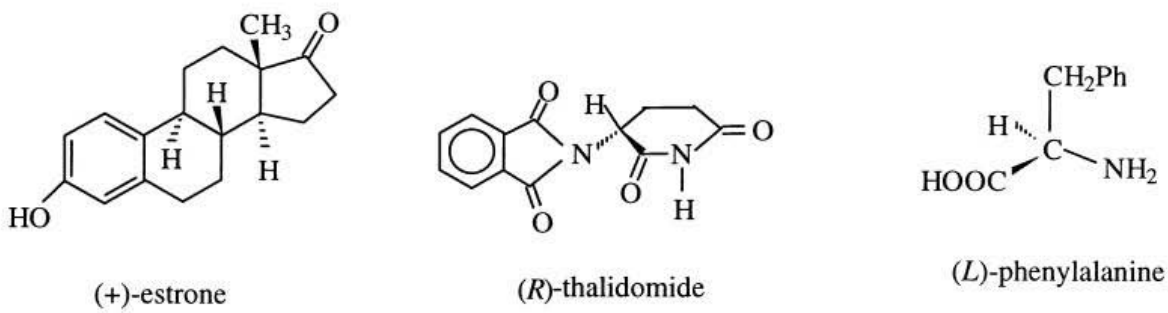

(+)-estrone (*R*)-thalidomide (*L*)-phenylalanine

Figure 1.2 Chiral compounds with biological activity[3]

same situation holds for other fields such as human food additives, animal food supplements and agrochemicals. For example, the new sweetener aspartame, used in cola-mix beverages, is synthesized using *L*-phenylalanine (Figure 1.2).

The awareness of the increasing importance of optically active compounds has

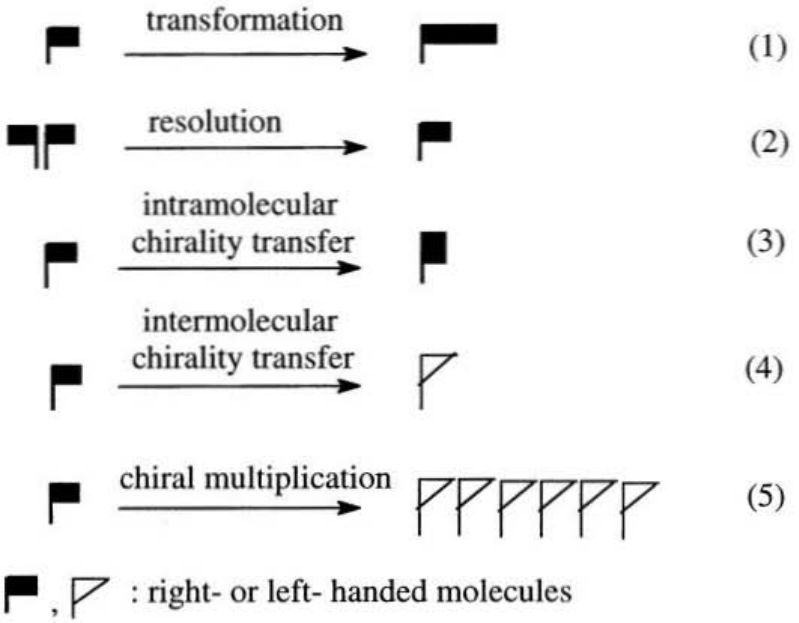

Figure 1.3 General routes to chiral molecules

challenged chemists to design and develop new approaches for the synthesis of chiral molecules in enantiomerically pure form.[28] Recent rulings of the Food and Drug Administration (FDA) in the United States concerning use of chiral drugs have heightened the interest in this area.[1,34] Arduous work has resulted in a myriad of excellent methods of producing optically pure compounds;[2-5] these can be classified into three basic methodologies including *i*) derivatization of chiral building blocks, *ii*) resolution and *iii*) stoichiometric or catalytic asymmetric synthesis (Figure 1.3).[6] Success of the three methodologies is measured by the enantiomeric excess, or optical yield (% ee), which is defined as the percentage proportion of the major enantiomer less that of the minor enantiomer (% ee = [(major – minor) / total] × 100).

1.1.1 Derivatization of Chiral Building Blocks

Derivatization of chiral building blocks involves modification of naturally occurring chiral materials, which are available cheaply and in large quantities from the natural chiral pool,[2] in a series steps to arrive at the desired products (equation 1, Figure 1.3). Common chiral building blocks include amino acids,[7] amino alcohols, hydroxy acids, alkaloids, terpenes, sugars, etc.[2] A successful application of this method is the synthesis of unnatural amino acids.[8]

Materials derived from the "natural chiral pool" are abundant and inexpensive. However, this method ultimately relies on the availability of naturally produced chiral entities. Frequently, both enantiomers, which may be required as starting materials, are not available. For example, *L*-rhamnose is inexpensive while its *D*-enantiomer is not commercially available. Moreover, design and execution of modified reactions to retain optical purity is an additional requirement for optical purity of the products, which, therefore, limits the range of accessible target molecules.

1.1.2 Resolution

Classic resolution (equation 2, Figure 1.3) had been used as the primary method to obtain enantiomerically pure compounds until the 1970's. The principle is to transform enantiomers of the synthesized racemic mixture into diastereomers with optically active reagents (resolving agents). The resolving agents are usually

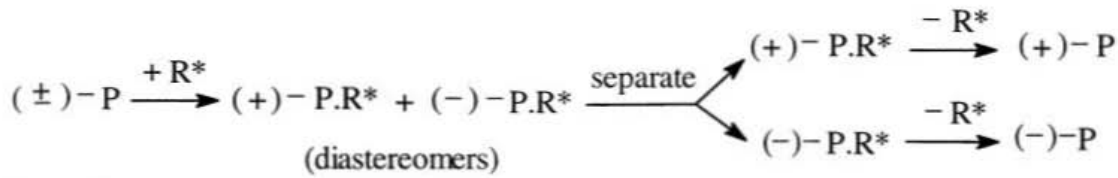

P: product

R*: homochiral resolving reagents

Figure 1.4 Resolution method

naturally occurring, enantiomerically pure compounds such as tartaric acid, camphor sulphonic acid, quinine, etc.[4] The resulting diastereomers, unlike enantiomers, are no longer simply related as object and mirror image. They have different chemical and physical properties and may be separated, most commonly by fractional crystallization, chromatography or distillation. Finally, the separated diastereomers are treated to liberate the two original enantiomers. The resolving agents can usually be recovered and reused (Figure 1.4).

Other resolution techniques include chiral chromatography,[4] which employs columns with a chiral stationary phase or chiral eluents on achiral supports via formation of short-term diastereomeric interactions with the enantiomers, and kinetic resolution,[9] which depends on different reaction rates of each enantiomer with an enzyme or a chiral chemical reagent.

Resolution can produce materials of relatively high enantiomeric purity and hence is a valuable method, especially on an industrial scale. (1*R*)-*cis*-permethric acid, the starting material of the important insecticide cypemethrin, is prepared via

this method.[4] Further, both enantiomers can be obtained, which is an important consideration in biological studies. Unfortunately, resolution remains largely an empirical science, and the maximum yield of a single enantiomer is 50% except for kinetic resolution.

1.1.3 Asymmetric Synthesis

Asymmetric synthesis shows promise as an efficient tool to obtain enantiomerically pure or enriched compounds without the disadvantages resulting from the limited natural chiral pool or resolutions. A chiral unit is used as a template to generate a new element of chirality from a prochiral precursor (chiral induction). This method is general, efficient and flexible and has, therefore, received substantial consideration.[2,3,5]

1.1.3.1. Stoichiometric Asymmetric Synthesis

First generation asymmetric syntheses, or stoichiometric asymmetric syntheses (equations 3 and 4, Figure 1.3), involve installation of a simple chiral fragment in enantiomerically pure form into one of the reactants, either the substrate or the attacking agent. The attached chiral auxiliary establishes a diastereomeric relationship with the new stereocenters and, following one or more diastereoselective steps, is ultimately cleaved.

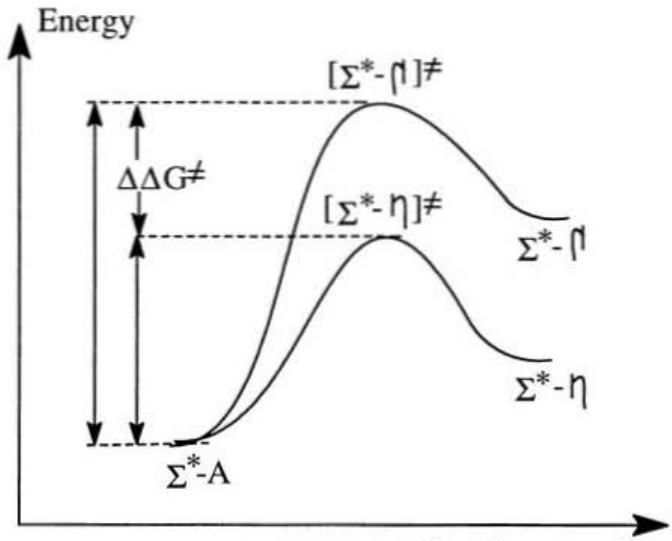

Σ* : chiral auxiliary
Σ*-A : starting material
Σ*-Π / Σ*-Η : product enantiomers
ΔΔG≠ : energy difference

Figure 1.5 Reaction coordinate diagram for chiral induction

The interpretation of chiral induction by the chiral fragment relies on transition state theory.[10,122] For prochiral reagents, there are two possible reaction paths to enantiomeric products. The chiral auxiliary, Σ*, causes each path to form distinct, diastereomeric transition states with different energies, $[\Sigma^*\text{–}\Pi]^{\neq}$ and $[\Sigma^*\text{–}\eta]^{\neq}$, as a result of steric effects, hydrogen bonding, chelation and electrostatic interactions. Under conditions of kinetic control, the reaction path with the lower activation energy occurs faster, leading to the observed stereoselectivity (Figure 1.5).[10] The guidelines for determining the outcome are based upon: *i*) steric or stereoelectronic bias to the environment of the reaction site(s) established by the chiral auxiliary and, *ii*) a sufficient difference (a minimum of 2 kcal mol^{-1}, ca. 8 KJ mol^{-1}, is desirable) between the free energy of two possible transition states, $\Delta\Delta G^{\neq}$.[122] Generally, chiral auxiliaries are either natural products or compounds derived from natural products

which are available in both enantiomeric forms by classical, high yield transformations.[4]

This strategy has been used with great success. For example, asymmetric alkylation of aldehydes and ketones was commercially developed by Enders[2] using the hydrazine SAMP, (*S*)-(–)-1-amino-2-(methoxymethyl)pyrrolidine, and its enantiomer RAMP, with optical yield up to 99.5% ee (Figure 1.6). The very high diastereomeric selectivity is not yet fully understood, but it is quite clear that the hydrazone anion has a rigid, internal chelated structure involving the lithium cation and the methoxy oxygen, making the R_e and S_i faces[122] highly nonequivalent.

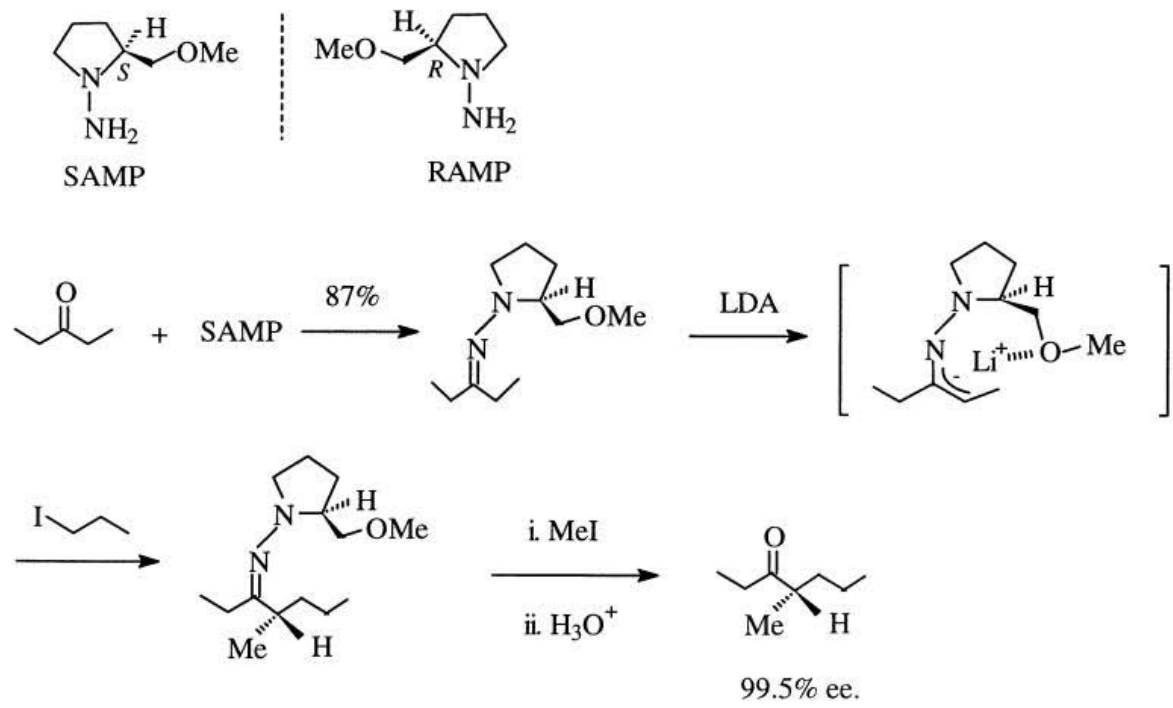

Figure 1.6 Asymmetric alkylation of aldehydes[2]

Since the generation of a new asymmetric center does not occur on the chiral auxiliary, the reactions are extremely versatile and a wide variety of reactants are possible. Hence, the method can produce chiral compounds which are fairly difficult to obtain by other methods. Another major advantage for this strategy is the relative ease with which enantiomers may be obtained pure (e.g. through chromatography of diastereomeric intermediates) and the degree of purity established. The disadvantage is that the enantiomerically pure chiral auxiliary is required in stoichiometric amounts because, in many cases, the chiral auxiliary is actually destroyed during the cleavage reaction to produce the final product and hence cannot be recycled.

1.1.3.2 Asymmetric Catalysis

Asymmetric catalysis is both elegant and economical compared with the first generation asymmetric syntheses because it results in multiplication of the chirality contained in the optically active catalysts (equation 5, Figure 1.3). In asymmetric catalysis, the catalysts, which are enantiomerically pure compounds, act as templates to transfer the chiral information to prochiral substrates. In general many catalytic cycles are possible, resulting in recovery of the chiral catalysts, hence chirality is multiplied and sub-stoichiometric amounts of catalyst are enough to produce large amounts of optically pure or enriched products. The efficiency of the catalyst is expressed as the turnover frequency (formerly "turnover number"),[16] which is the

ratio of the rate of the catalysed reaction to the concentration of the catalyst.

Enzymes are the perfect natural chiral catalysts since they produce optically active substances needed for life processes in very high optical yield with high efficiency and under mild conditions. Efforts to mimic enzymes led to the use of alkaloids as catalysts. An elegant example is the use of the alkaloid cinchonodine as the catalyst in the asymmetric conjugated addition of thiophenol to cyclohexenone.[5] However, enzymatic reactions are often restricted to natural substrates, and reactivity, as well as stereoselectivity, rapidly decreases when the substrate is varied.[3,126,127]

Studies of synthetic, enantioselective catalysts led to use of chiral transition-metal complexes.[85] Chiral transition-metal complexes have now found wide application throughout the chemical industry to produce many tons of "value added" homochiral products.[11,12]The application of transition metal complexes as catalysts is a result of their versatile ability to bond, wide range of oxidation states, variable coordination number and the broad choice of ligands. Almost any organic compound containing a donor group can coordinate with transition metals. The reactivity of organic compounds is often altered and regulated on bonding to a transition metal, hence exciting, novel approaches to target molecules under relatively mild conditions are possible. Furthermore, the geometrical restrictions on bonding of ligands in transition metal complexes effectively determine alignment of reacting species brought together by the metal and in turn provides control of stereoselectivity as well

as of chemical selectivity.[96,98]

More recently, transition metal complexes containing a chiral auxiliary have been found to act catalytically and to result in multiplication of chirality.[6] According to the position of stereogenic center, transition metal complexes as asymmetric catalysts can be divided into two groups. The first group uses chiral ligand auxiliaries while the second group involves the chiral-at-metal auxiliary.

1.1.3.2.1. Chiral Ligand Auxiliary

The first successful homogeneous asymmetric catalysis using soluble transition metal complexes with chiral ligands was reported in 1966.[13] The Cu(II) complex of the chiral salicylimine Schiff base shown in Figure 1.7 was found to catalyse the enantioselective carbenoid reaction between styrene and ethyl diazoacetate to give *cis*- and *trans*-2-phenylcyclopropanecarboxylates in <10% ee. In spite of the low optical yield, this observation demonstrated chiral induction from the bound, optically active ligands to the coordinated prochiral precursor and opened a new area in asymmetric synthesis.[126-128] Subsequently, optically active phosphines became the ligands of choice because of their steric and electronic variability. The pioneering introduction of the monodentate Horner phosphine P*PhPrMe, containing a phosphorus chiral atom, into a rhodium complex which catalysed enantioselective hydrogenation of C=C bond[13-15] initiated a flood of research.

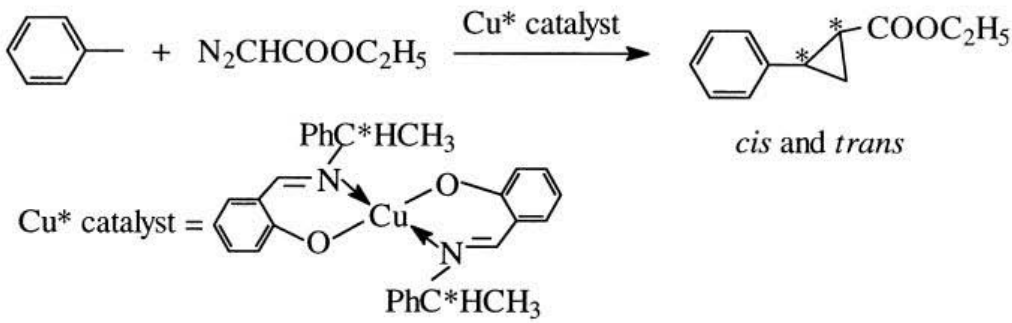

Figure 1.7 Carbenoid reaction catalysed by a Cu(II) complex with chiral ligand

Soon, however, diphosphine ligands took over. [3] The majority of bidentate phosphines applied in asymmetric catalysis contain a stereogenic center, plane or axis as the crucial component of the P–P backbone linkage. Chiral induction is generally believed to be a result of "transmitter groups" attached at phosphorus which are normally aryl residues. Owing to the chelating ring and the symmetry of the backbone, the number of possible diastereomeric reactive intermediates and transition states is dramatically reduced compared with two unidentate ligands. The rigidity of the conformation of the chelating ring and the arrangement of fully aromatic "chiral transmitters" pass chiral information from the chiral centers in the ligand skeleton to the catalytically active site of the catalyst. Most of the diphosphines are air-stable solids which are commercially available. Figure 1.8 shows some frequently used diphosphines. Transition metal complexes with chiral diphosphine auxiliaries have been widely applied in asymmetric catalysis such as hydrogenation, oxidation, hydrosilylation, aldol-type reactions and isomerization.[2,21,22] A notable application

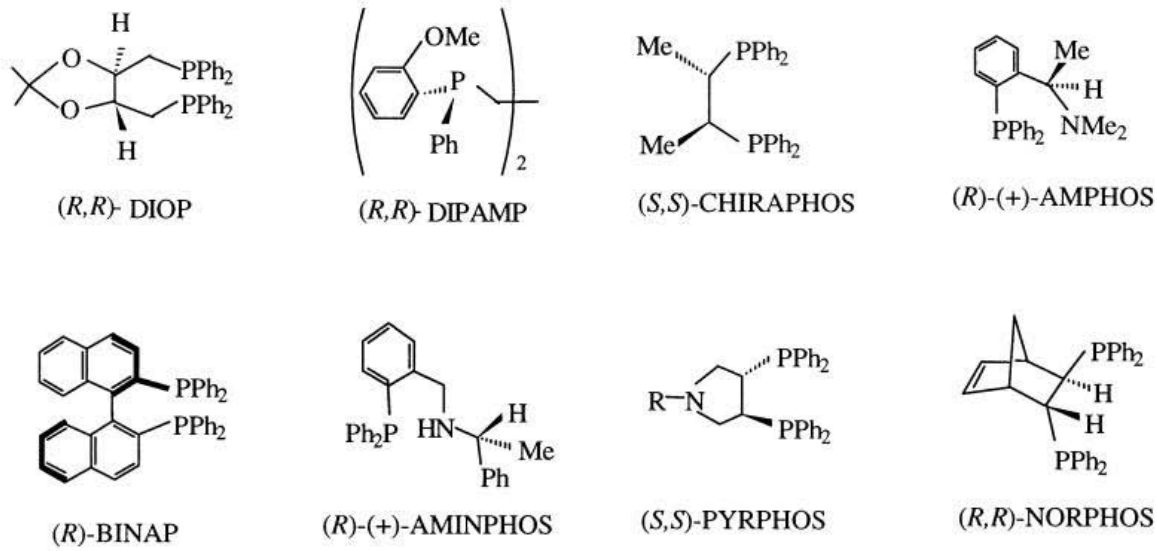

Figure 1.8 Chiral diphosphine moieties

is the synthesis of *S*-DOPA, an anti-Parkinson drug needed in amounts exceeding 200 tons per annum, which is catalysed by a rhodium (*R,R*)-DIPAMP complex.[17-19]

1.1.3.2.2 Chiral Metal Auxiliaries

Chiral-at-metal complexes are an intriguing area of study in the field of asymmetric organometallics. Few chiral-at-metal systems have been developed.

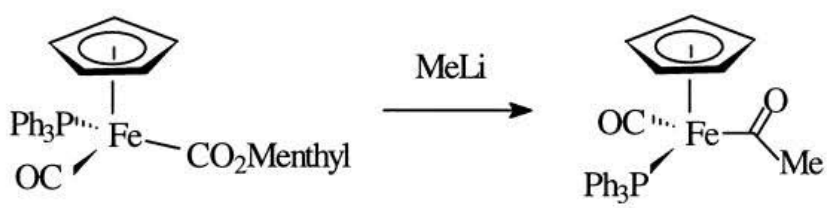

Figure 1.9 Chiral iron comples

Brunner prepared the chiral iron-acyl complexes shown in Figure 1.9 from the corresponding

menthyl esters by the addition of methyl lithium.[149] A great deal of work on chiral iron complexes has been carried by Liebeskind[26] and by Davies [25] with compound B shown in Figure 1.10 as the model. Gladysz[24] synthesized related chiral rhenium compounds (A of Figure 1.10). Chiral-molybdenum-π-allyl compounds have also been reported.[23] All these models contain octahedral metals with three of the six coordination sites occupied by the cyclopentadienyl group and three other ligands occupying the remaining coordination sites. Hence the transition metal center can be viewed as pseudo tetrahedral with four different ligands. These compounds are air-stable and thus easy to handle. They are also highly crystalline, coloured and easily purified by chromatography or crystallization. Furthermore, compared with the chiral ligand auxiliary in which the chiral source is "distal" to the prochiral target, the chiral transition metal atom is "proximal" to the prochiral moieties (Figure 1.11). It is obvious that the "proximal" centre has the potential to exert a more direct and therefore stronger influence (chiral

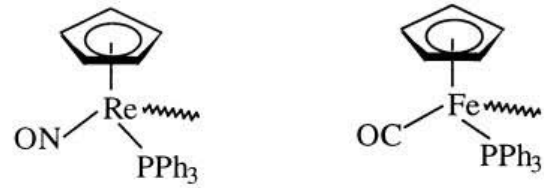

A B

Figure 1.10 Transition metal chiral-at-metal auxiliaries

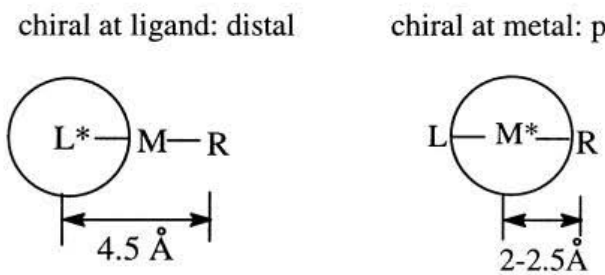

Figure 1.11 Chiral induction of two groups of transition-metal compounds

induction) on the target molecules than the "distal" one.

Results in last ten years have shown that chiral metal auxiliaries can exert significant stereochemical control in a wide range of asymmetric synthetic transformations. For instance, Gladysz used chiral rhenium-ketone complexes to prepare optically active alcohols in high enantiomeric excess (Figure 1.12).[23,24] Chiral iron complexes have been used by Davis for asymmetric synthesis of organic

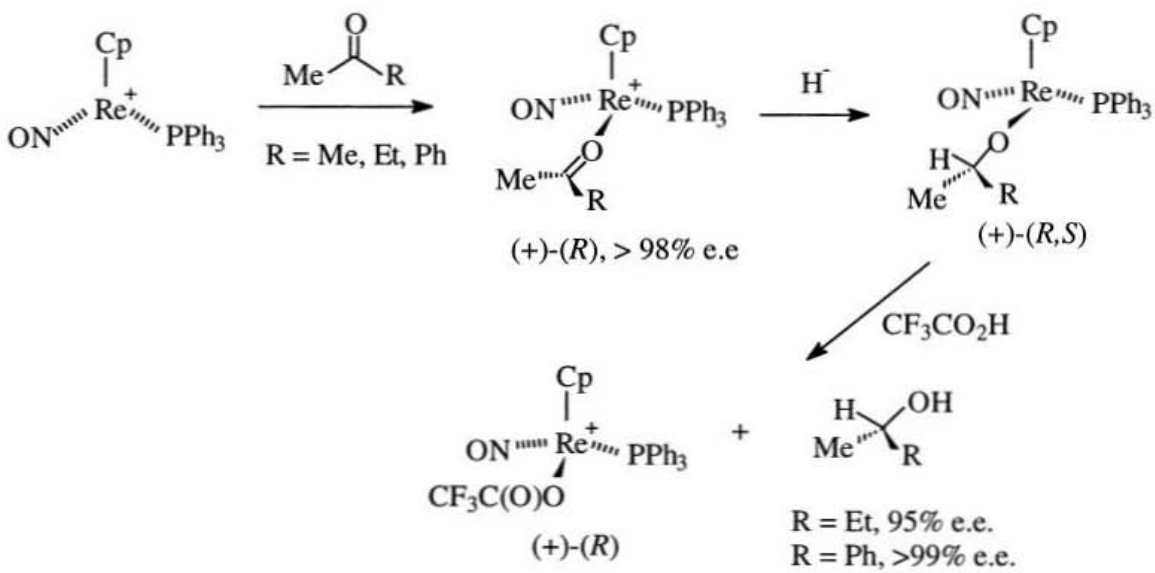

Figure 1.12 Application of chiral Rh-ketone complex[23,24]

compounds through C–C formation reactions such as alkylation, aldol condensation, Michael addition alkylation, Diels-Alder reaction, etc.[23,124] Alkylation of iron–acyl complexes, as shown in Figure 1.13, is a typical demonstration of the stereoselectivity resulting from the chiral metal centre.[25] The homochiral iron–acyl complex is first

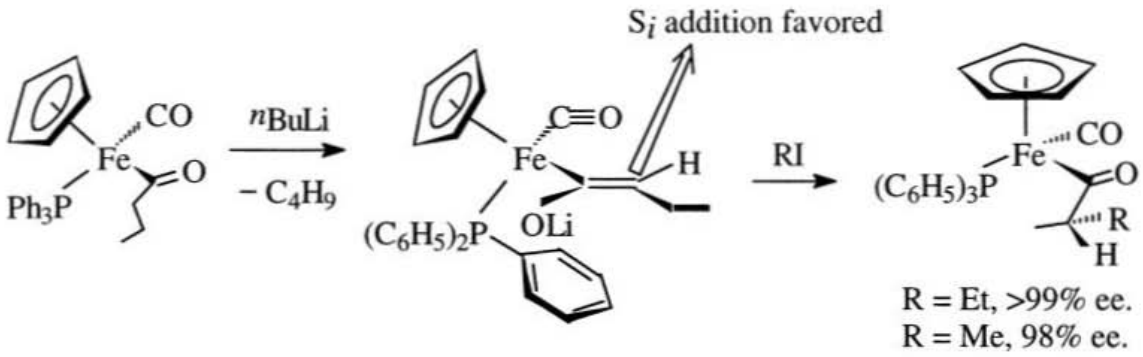

Figure 1.13 Diastereoselective alkylation of a chiral iron acyl complex

deprotonated by base to form an enolate intermediate. The intermediate enolate anion has the *E* configuration and adopts a conformation in which the negatively charged oxygen of the enolate intermediate is antiperiplanar to the CO ligand so that the alkyl group of the acyl avoids the very bulky phosphine auxiliary. Electrophilic attack at the enolate in the next step occurs only from the unhindered face of the enolate, giving stereo-controlled formation of a new chiral carbon centre.

Chiral-at-metal auxiliaries produce good chiral induction and subsequent cleavage of M*–C bond affords chiral carbon compounds in relatively high optical yield.[25] However, application of chiral-at-metal complexes is predominantly stoichiometric. Research of the development of chiral-at-metal auxiliaries into asymmetric catalysts is still in process.

In summary, asymmetric catalysis is a valuable methodology in asymmetric synthesis as chemical industry and society are seeking ways to conserve energy and

to make the best possible use of available resources.

1.2 Significance of Organic Phosphorus Compounds

Research on the chemistry of phosphorus was first undertaken by Lassaigne who prepared phosphate esters in 1820.[27] Since then, the work of Michaelis, who developed chemistry of compounds containing the P–N bond, and Arbuzov, who investigated trivalent phosphorus compounds and discovered the famous Arbuzov rearrangement reaction to form a P–C linkage, established the foundation of this field.[27,115] The driving force for continued research in this area is the wide practical use of organophosphorus compounds in various developing areas, for example, as lubricants, oil additives, water treatment cleaners, flame retarding agents, fertilizers, plasticisers and pesticides.[29,30]

Phosphorus compounds are also recognized to have important biological functions.[31,35] Organophosphorus compounds are the essential constituent of protoplasm.[31] Phosphate esters $[(RO)_nO_{3-n}P(O)]^{(3-n)-}$ $(n = 1 - 3)$ are profoundly endogenous chemicals, forming the backbone of many of the most important molecules in life, such as the oligonucleotide polymer DNA, RNA and phosphatide,[31,159] and hence play a critical role for

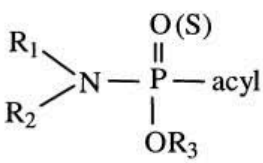

$R_1, R_2, R_3 = R^-$

acyl = Cl^-, F^-, SCN^-, CH_3COO^-

Figure 1.14 Biologically active organophosphorus compounds discovered by Schrader

maintenance of life. In 1932, Lange and Krueger first found that diakylphosphorofluoridates demonstrated physiologically abnormal effects.[32] Related organophosphorus compounds are known nerve toxins which were especially important during World War II.[33,45] Schrader and co-workers' discovery, in 1937, of contact insecticidal activity in some organophosphorus compounds of the general formula shown in Figure 1.14[31] led to a variety applications.

Many organophosphorus compounds have been synthesized and their biological properties tested as candidate pesticides. For example, the systemic insecticide, octamethylpyrophoramide (OMPA), later named Schradan, was discovered by Schrader in 1941. A number of insecticidal organophosphorus esters, including the first practical insecticide "Bladan" which contained tetraethyl pyrophosphate (TEPP), were also discovered in 1947. Structure-activity relationship studies indicated that almost all the biologically active phosphorus compounds, some of which had been prepared long ago without knowledge of their toxicity, are neutral esters of phosphoric or thiophosphoric acids (Figure 1.15) which are characterized by the presence of a stable phosphorus-oxygen or sulfur double bond.[27] This conclusion is consistent with both the result first proposed by Schrader and the fact that all phosphorus compounds in nature are P(V)

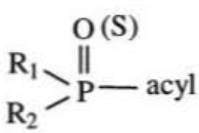

$R_1, R_2 = R^-, RO^-, R_2N^-,$
$acyl = Cl^-, F^-, SCN^-, CH_3COO^-$

Figure 1.15 General formula of biologically active phosphorus compounds

oxyacid derivatives. Table 1.1 shows examples of several types of phosphorus compounds with known biological activity.

The pesticidal activity and mammalian toxicity of organic pentavalent phosphorus esters, first found by Adrian and Ball in 1940's,[31,36] are attributed to their phosphorylation and alkylation properties which result from the positive charge on the phosphorus atom of the polarized phosphoryl group. Organophosphoric esters can inactivate serine enzymes in the nerve system via phosphorylation of a serine hydroxyl group at the catalytic site of the enzymes and thus disturb the normal nervous function, finally resulting in the severe and often lethal damage to the organism.

Table 1.1 Some Examples of Organophosphorus Compounds with Biological Activity

Structure	Use	Chemical type
$(CH_3O)_2P(O)(OCH{=}CCl_2)$	insecticide	phosphate
$(i\text{-}C_3H_7O)_2P(O)(SCH_2C_6H_5)$	fungicide	phosphorothiolate
$(CH_3O)P(S)(Ph)(OPh\text{-}p\text{-}NO_2)$	insecticide	phosphorothionate
$(CH_3O)_2P(O)(CH(OH)CCl_3)$	insecticide	phosphonate
$(OH)_2P(O)(CH_2NHCH_2CO_2H)$	herbicide	phosphonic acid
$(C_4H_9CH(C_2H_5)CH_2)_2P(O)(OC_2H_5)$	herbicide	phosphinate
$CH_3P(O)(OCH(CH_3)_2)F$	nerve gas	phosphonofluoridate

The major target enzyme of the organophosphorus compounds, including insecticides and nerve gases, is acetylcholinesterase, a serine enzyme.[13] Acetylcholinesterase (AChE) is one of the hydrolytic enzymes for acetylcholine, a transmitter in the nerve system, and plays an important role in the nerve system. AChE breaks down acetylcholine into inactive acetic acid and choline after the acetylcholine has transmitted a signal from one nerve cell to another nerve cell or from a nerve cell to a muscle cell. The mechanism of hydrolysis of acetylcholine by AChE is shown in equation 1 of Figure 1.16. The enzyme and the substrate first combine to form an enzyme-substrate complex, followed by transferral of the acyl group to the AChE molecule to form the acylated enzyme, which, in turn, is rapidly hydrolysed with recovery of the enzyme, AChE. The hydroxyl group of serine in AChE plays an important part in biological activity. Organophosphorus compounds inactivate AChE via irreversible phosphorylation of the serine hydroxyl group at the

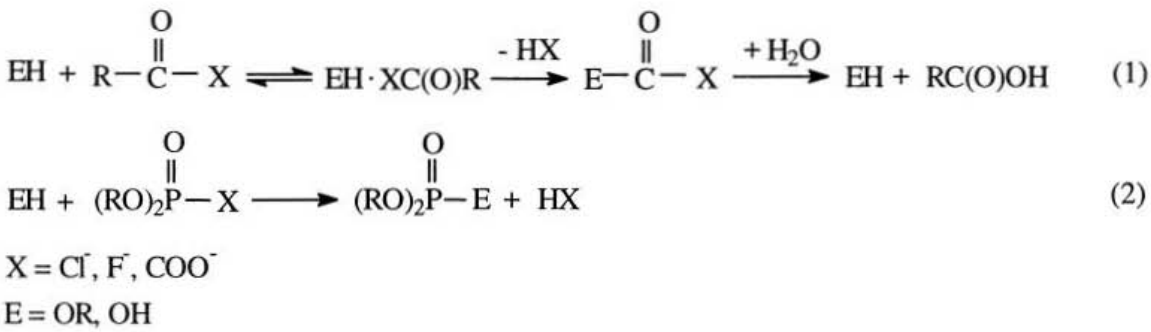

Figure 1.6 Reactions of AChE

catalytic site to give a very stable product (equation 2, Figure 1.16). Inhibition of AChE blocks the decomposition of acetylcholine and results in a severe disturbance of nervous function, for example, the respiratory system,[45] leading to death.

The target enzymes of the organophosphoric esters are not strictly limited to AChE; they also react with other enzymes which control growth of insects, such as hormone esterases, pheromone esterase, etc. Due to their relatively high effectiveness and low persistency in the natural environment,[44] hundreds of organophosphorus compounds have had applications as insecticides,[38,39] herbicides,[40,41] antibacterial agents,[42] plant growth regulators,[50,51] fungicides,[43] etc. for over four decades.

Enzymes targeted by pentavalent organophosphorus compounds, such as AChE, hormone esterase, etc., control not only metabolisms of insects but also those of mammals including humans and viruses. Therefore, organophosphorus compounds also have potential applications for metabolic regulation. For example, phosphate-containing nucleoside analogues were used in cancer and viral chemotherapy in the early 1960's.[46] Recent work has found that α-hydroxy phosphonates and phosphonic acids are excellent inhibitors of enzymes, including renin,[35,47] EPSP synthase[48] and HIV protease,[49] which highlights the importance of organophosphorus compounds in biological systems. Moreover, pentavalent organophosphorus compounds with biological activity are small molecules, and, therefore, development of these compounds to oral delivery drugs is possible.[46] All these achievements establish

organophosphorus compounds as attractive targets in the pharmaceutical industry.

1.3 Role and Function of Pentavalent Phosphorus-Chiral Compounds

Both trivalent and pentavalent phosphorus compounds can display chirality. Only the chirality of pentavalent phosphorus is discussed here, due to the biological function of the phosphoric esters mentioned above.

Tetrahedral, pentavalent phosphorus compounds demonstrate bioactivity similar to carbon compounds. Firstly, enzymes are the common targets of phosphorus compounds and carbon compounds. Secondly, the phosphoryl group mimics a carbonyl group in some enzyme reactions. The above mentioned AChE inhibitory organophosphorus insecticides can be considered the phosphorus analogs of acetylcholine since they compete with acetylcholine for AChE. Thirdly, nucleophilic substitution reactions on the phosphorus center of pentavalent phosphorus compounds proceed via $S_N1(P)$, $S_N2(P)$ and addition-elimination mechanisms,[37] which parallel those of tetrahedral carbon compounds.

Pentavalent, tetrahedral phosphorus can then be viewed as an analog of carbon and modification of the activity of organophosphorus compounds is based on the known properties of carbon. For instance, phosphonic analogs of morphactins and peptides have been studied as plant growth regulators.[51] Acetylmethylphosphinic acid, a phosphorus analog of pyruvic acid, is an active-site-directed inhibitor of

acetolactate synthase (ALS), which is a thiamine pyrophosphate (TPP)–dependent enzyme functioning to catalyse the condensation of two pyruvate molecules in the leucine and valine biosynthetic pathway, and thus has significant herbicidal activity.[98] In light of the similarity to tetrahedral carbon and the well-known stereospecificity in reactions of carbon-chiral compounds with enzymes, it is surprising that the effect of phosphorus-chirality on the biological activity of organophosphorus compounds had been scarcely investigated until the late 1950's.

Tetrahedral carbon contains four sp^3 hybridized orbitals with each valence electron occupying one orbital, and can therefore form four σ-bonds with other functional groups. A chiral carbon center results when the four functional groups are different. Pentavalent phosphorus in phosphoric esters have a characteristic "posphoryl" bond often represented as P=O. The P–O–P bond angles in phosphoric acid (PO_4^{3-}) are 109°,[27] indicating that phosphorus, like carbon, can also exhibit tetrahedral symmetry corresponding to sp^3 hybridization (Figure 1.17). However, both the higher bond energy (125 – 156 kcal/mol) and shorter bond distance (1.44 – 1.55Å) of the phosphorus-oxygen bond of the phosphoryl group compared to the corresponding values of the P–O single bond (86 kcal/mol, 1.71Å) support contribution from $p\pi$-$d\pi$ bonding. The π-bonding presumably arises from the donation of the nonbonding

Figure 1.17 Chiral C(IV) and P(V)

2*p*-electron of the negative charged oxygen atom into a vacant 3*d*-orbital of phosphorus. This bonding model accounts for the existence of optically active compounds in which the phosphorus atom serves as an asymmetric center is possible. The first resolution of an optically active pentavalent phosphorus compound, ethylmethylphenylphosphine oxide, was performed by Meisenheimer in 1911.[52] Unfortunately, the result did not arouse research interest in phosphorus-chiral compounds because the natural substrate of AChE, acetylcholine, is itself achiral.

AChE was first found to be able to recognize the chirality of organophosphorus compounds by Michel who observed, in 1955, that enantiomers of sarin (Figure 1.18) reacted with AChE at different rates.[53] The chirality of the phosphorus atom is the most reasonable source of the difference in activity. Since then, several enantiomers of biologically active organophosphorus compounds have been isolated and examined for their inhibitory activity on enzymes.[31,51] It is amazing to note that AChE activity is highly stereospecific for asymmetric organophosphorus compounds although its natural substrate has no asymmetric centre. The biological activity of organophosphorus compounds is greatly affected by phosphorus-chirality. For example, (*S*) (–)-Salithion (Figure 1.18) has a higher insecticidal activity than the (*R*) (+)-isomer.[54] The $(R)_p$-isomer of methamidophos (Figure 1.18) is more toxic to the housefly than is the $(S)_p$-isomer. Four diastereomers of *O*-*sec*-butyl *S*-2-(ethylthio)ethyl ethylphosphonothiolate (Figure 1.18), with both phosphorus and

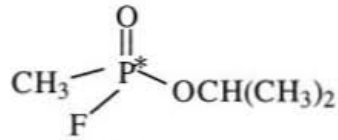

Sarin

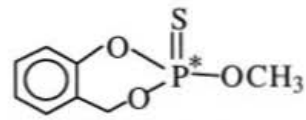

(*S*) (-)-Salithion

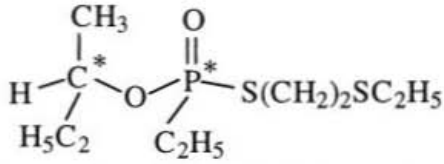

O-sec-butyl *S*-2-(ethylthio)ethyl ethylphosphonothiolate

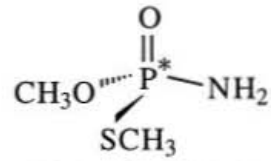

(*R*)-methamidophos

Figure 1.18 Examples of chiral pentavalent phosphorus compounds

carbon chiral centres, have also been tested for toxicity.[55] The dextro-C-levo-P isomer and levo-C-levo-P isomer are very toxic whereas the dextro-C-dextro-P isomer and levo-C-dextro-P isomer are almost harmless. Thus, the chirality of phosphorus dominates that of carbon in determining biological activity in this case.

The nature of the chirality for phosphorylated AChE is still uncertain, but recent investigations of the mechanism of reactions between AChE and organophosphorus compounds showed that steric effects play a pronounced role in the recognition of chirality by AChE.[37,56-58] When organophosphorus inhibitors react with AChE, the negatively charged oxygen atom of the phosphoryl group hydrogen bonds with the hydrogen of the NHs on the backbone of the AChE enzyme. The enantiomer of organophosphorus compounds with less steric hindrance for formation of the hydrogen bonding thus gives a more stable complex with AChE and therefore is preferred.

Homochiral organophosphorus compounds can be expected to have important

practical applications. Development of strategies for the synthesis of enantiomerically pure or enriched phosphorus-chiral molecules is, thus, a challenge to be addressed.

1.4 Synthetic Methodology for the Production of Phosphorus-Homochiral Compounds

The importance of the chirality of phosphorus compounds in biological systems and in catalysts for asymmetric synthesis suggests that synthetic routes to homochiral phosphorus compounds would be highly desirable. Unfortunately, not all of the general routes for chiral synthesis are suitable for phosphorus-chiral compounds. Phosphorus-chiral organophosphorus compounds cannot be found in the natural chiral pool [59] and hence derivatization of the chiral building blocks, the straightforward route to carbon-chiral compounds, is impossible for preparation of phosphorus-chiral compounds. Nowadays, homochiral phosphorus compounds are generally obtained by resolution and stereoselective synthesis.

1.4.1. Resolution

Resolution involves initial conversion of the prochiral phosphorus compound to phosphorus racemic compounds which are subsequently resolved. In principle, preparation of phosphorus-chiral compounds usually starts with selective step by step displacement of the X groups of PX_3 or $O{=}PX_3$ (X = Cl, Br, OR, etc.). Many

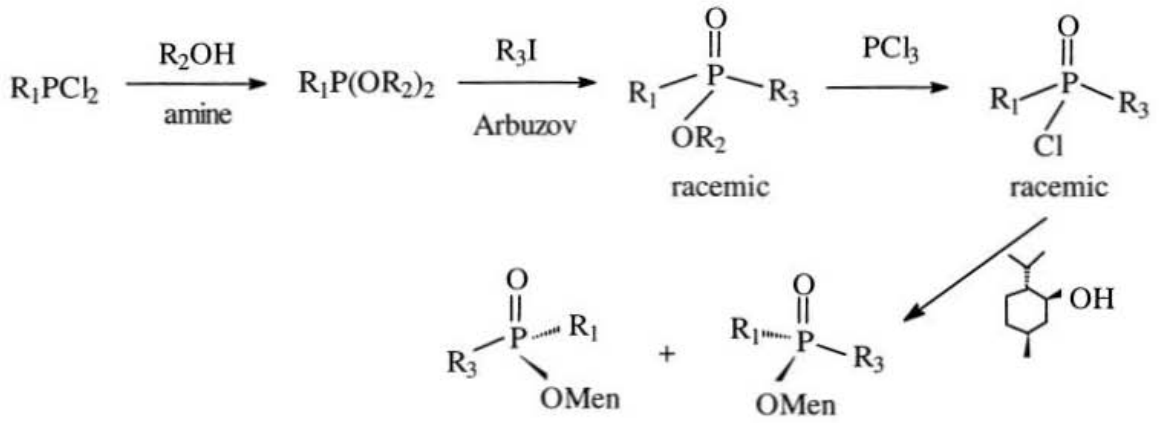

Figure 1.19 Resolution of phosphorus compounds with menthol as resolving agent

$PR_1R_2R_3$ or $O{=}PR_1R_2R_3$ alkyl and aryl dichlorophosphines are commercially available,[60] and both direct displacements (Figure 1.19) and Arbuzov reactions (Figure 1.20) are commonly used to form the P–C bonds.

Menthol, cholesterol, camphorsulfonic acid, tartaric acids and their derivatives are common resolving agents. Menthol substitutes one functional group of the chiral pentavalent phosphorus, affording diastereomers (Figure 1.20).[2] Commercial applications of this method produces cyclohexyl-(*o*-anisyl)methylphosphine (CAMP)[129,130] and 1,2-bis-(*o*-anisyl)phenylphosphino)ethane (DIPAMP)[131] which are commercially important ligands for the enantioselective catalytic hydrogenation. Acids with chiral anions can either protonate the phosphorus-oxygen double bond of the P(V) compounds (Figure 1.19) or form ionic salts with phosphines (Figure 1.20).[61,62] A point worthy of attention is that, although phosphines are resolved by chiral acids, synthetically useful preparation is usually limited to benzylphosphonium

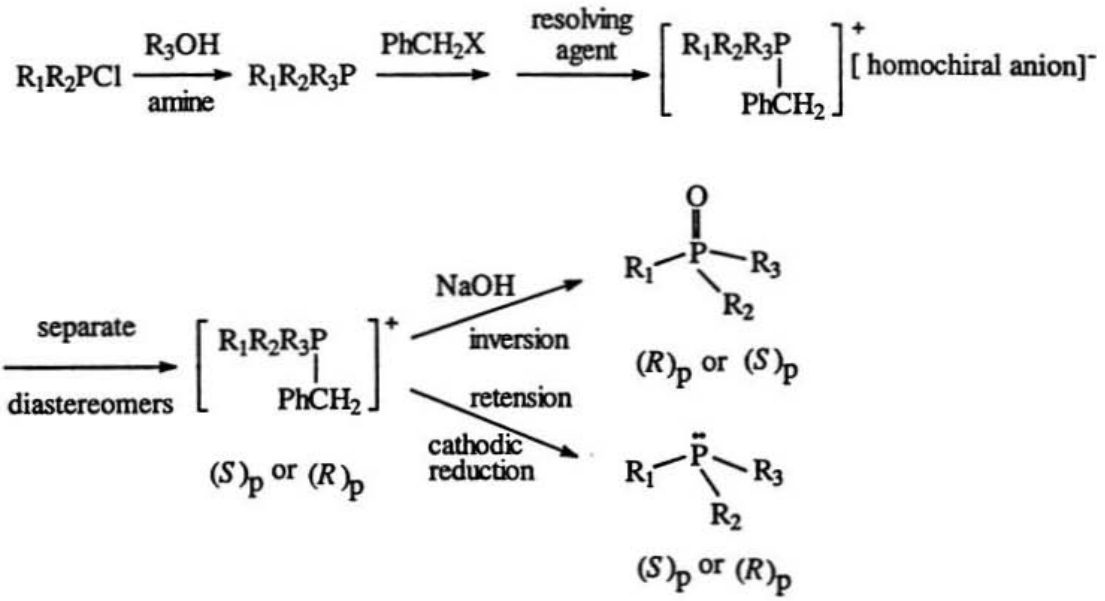

Figure 1.20 Resolution of phosphorus compounds via diastereomeric salts

(CAMP)[129,130] and 1,2-bis-(*o*-anisyl)phenylphosphino)ethane (DIPAMP)[131] which are commercially important ligands for the enantioselective catalytic hydrogenation. Acids with chiral anions can either protonate the phosphorus-oxygen double bond of the P(V) compounds (Figure 1.19) or form ionic salts with phosphines (Figure 1.20).[61,62] A point worthy of attention is that, although phosphines are resolved by chiral acids, synthetically useful preparation is usually limited to benzylphosphonium salts because predominant loss of benzyl group in the following liberation step gives a single product in good yield. Competition of other alkyl or aryl groups with benzyl as the leaving group results in varying optical yield with reagents and conditions. Although the many possible stereochemical results provides considerable folder for mechanistic chemists, they tend to reduce the value of the phosphonium salt method

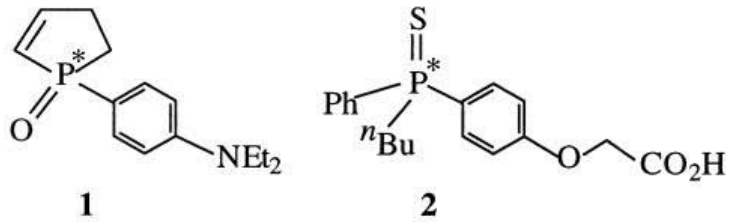

1 2

Figure 1.21 Resolution of phosphorus via backbone functions

gave separable salts with (+) and (–)-1-phenylethylamine. In the later case, sulfur in the P=S group is so weak a protic base that introduction of an added functionality for the purpose of resolution was necessary. Weak P=S basicity is probably the reason why no further examples of direct resolution of phosphine sulfides are found in the literature.

In the early 1970's, the Otsuka [65,66] and the Wild groups [67-70] developed a new procedure to directly resolve chiral phosphines with organometallic complexes containing a chiral ligand auxiliary. One of the procedures, which was developed by Otsuka and co-workers, relied on chiral palladium(II) complexes having homochiral

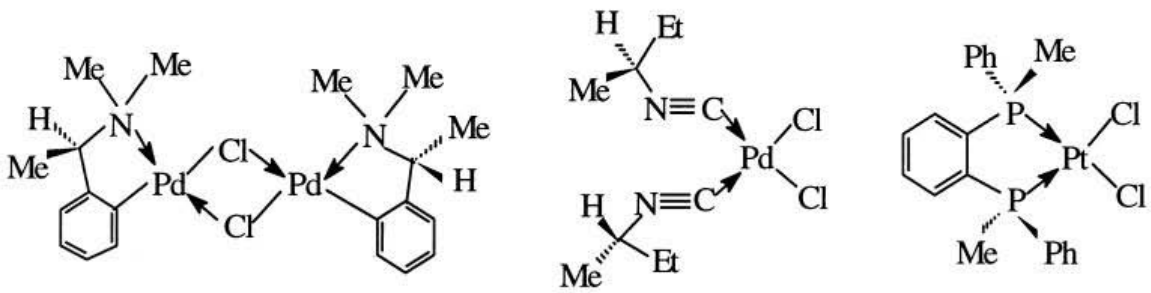

3 4 5

Figure 1.22 Resolving organometallic complexes with chiral ligands

ligands, such as diphosphines, 1-phenylethylamines, 1-naphthylethylamines, *sec*-butylisonitrile, etc. as the resolving agents (Figure 1.22) to form the diastereomeric transition-metal complexes with chiral phosphines. After separation of the diastereomers via fractional crystallization or chromatography, the chiral phosphines were easily displaced by other ligands with stronger coordination ability. The chloro-bridged Pd dimer complex (compound **3** in Figure 1.22) was found by Wild and co-workers to be especially well suited for the resolution of bidentate phosphines. The remarkable application to efficiently resolve *o*-phenylenebis(methylphenylphosphine) (compound **6** of Figure 1.23) is detailed in Figure 1.23. Nearly complete precipitation

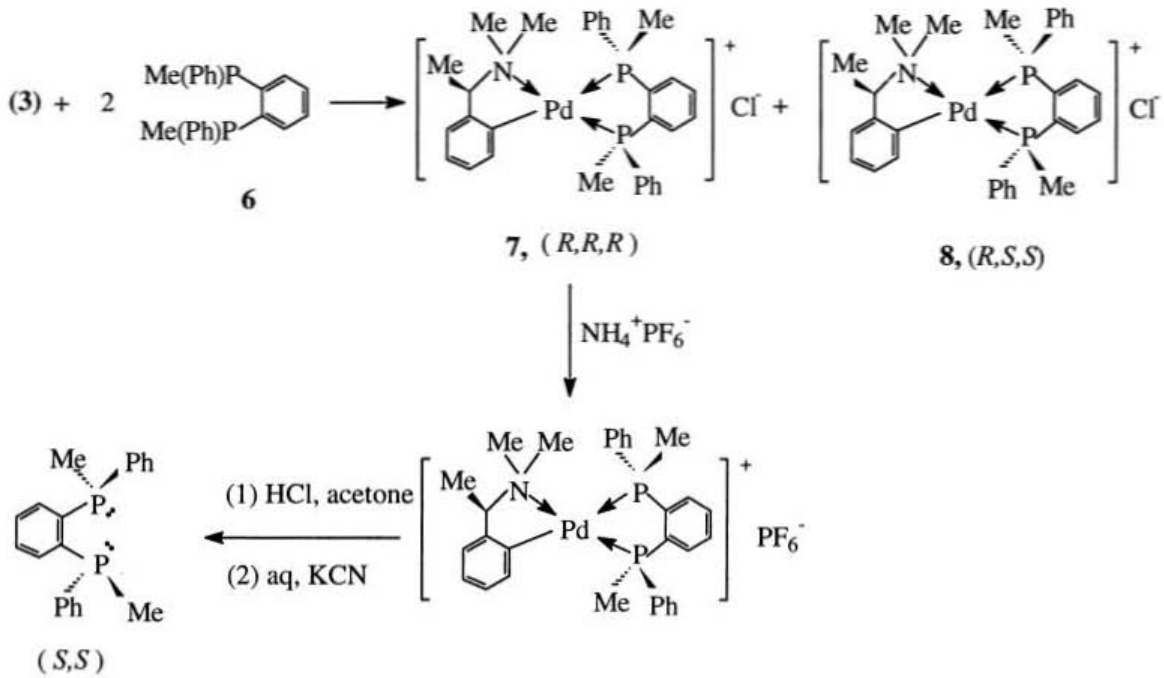

Figure 1.23 Resolution of chiral phosphine with chiral transition metal complexes

of a single complex, *(R,R,R)*-**7** in Figure 1.23, followed by effective two-step decomplexation, allowed the isolation of the optical pure (*S,S*)-isomer of compound **6** in 85% overall yield and recovery of the optically pure (*R,R*)-isomer from the mother liquors in even higher than 90% overall yield. Nickel,[71] iron,[72] platinum [73] and rhodium[74] complexes have been reported to successfully resolve chiral phosphines. Structures of several diastereomerically pure phosphine palladium intermediate complexes have been confirmed by X-ray structure determinations which also provide the important absolute configuration assignment. Although matching suitable transition metal complexes with the phosphorus compounds is frequently required, the method has been proven to be a direct, efficient and reasonably general synthetic route to phosphines of high enantiomeric purity.

1.4.2 Asymmetric Synthesis

A search for more flexible and general methods to prepare optically active phosphorus compounds has led to the development of methodologies for enantioselective synthesis. The reported methods cover chiral induction and derivatization of resolved phosphorus compounds.

1.4.2.1 Chiral Induction

The typical procedure involves installation of a chiral-carbon centre into the

reagents, which not only controls the stereochemistry of reactions with prochiral phosphorus compounds but also directly affords the diastereomeric products for easy resolution. The chiral auxiliaries are classified into two groups based upon whether the reaction intermediate is acyclic or cyclic.

Among the acyclic examples is a report by Naylor and Walker[75] of the alkylation of sodium methylphenylphosphide with (+)-1-phenylethyl chloride. Oxidation of the crude product with H_2O_2 leads to the formation of scalemic phosphine oxides with an optical yield of 26% ee (Figure 1.24). Some amines with chiral carbon [76,81-83] are also of the acyclic group. For example, proline was used as

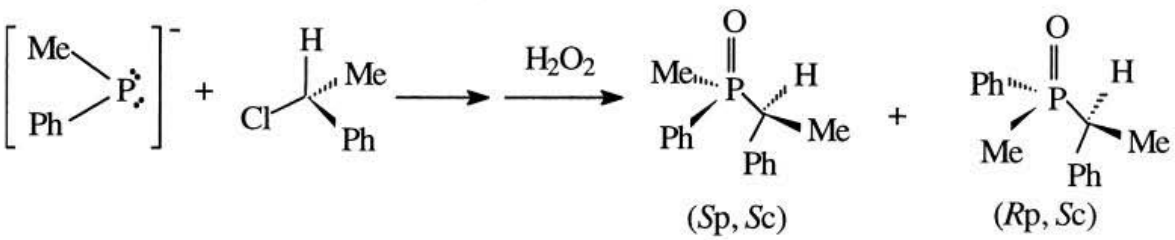

Figure 1.24 Asymmetric synthesis of *P*-chiral molecules via acyclic covalent diastereomers

a template to prepare chiral dialkylphenylphosphates and alkylphenylphosphonates (Figure 1.25). However, the application of amines as chiral auxiliaries is limited by the fact that the acid-catalysed P–N cleavage in the last step to release the chiral phosphorus fragment is stereospecific only for alcoholysis with simple primary alcohols.

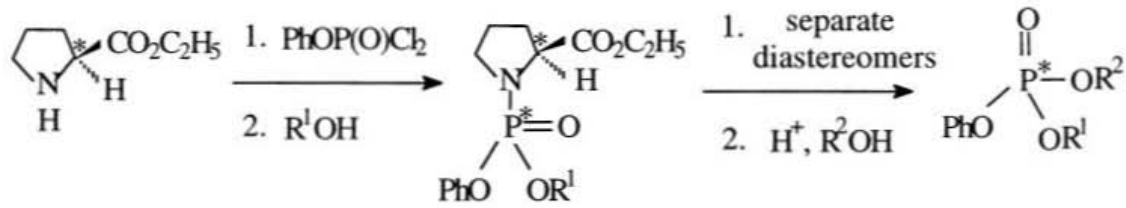

Figure 1.25 Asymmetric synthesis of P-chiral molecules via proline as the template

Carbohydrates and chiral β-aminoalcohols such as (–)-ephedrine have also been used as templates in asymmetric synthesis of four-coordinate *P*-chiral compounds.[77,109] The intermediates in these syntheses are cyclic covalent diastereomers with the chiral phosphorus atom incorporated into the ring. The phosphorus configuration determines the geometric isomers formed. Separation of the geometric isomers is relatively easy and subsequent ring opening and cleavage

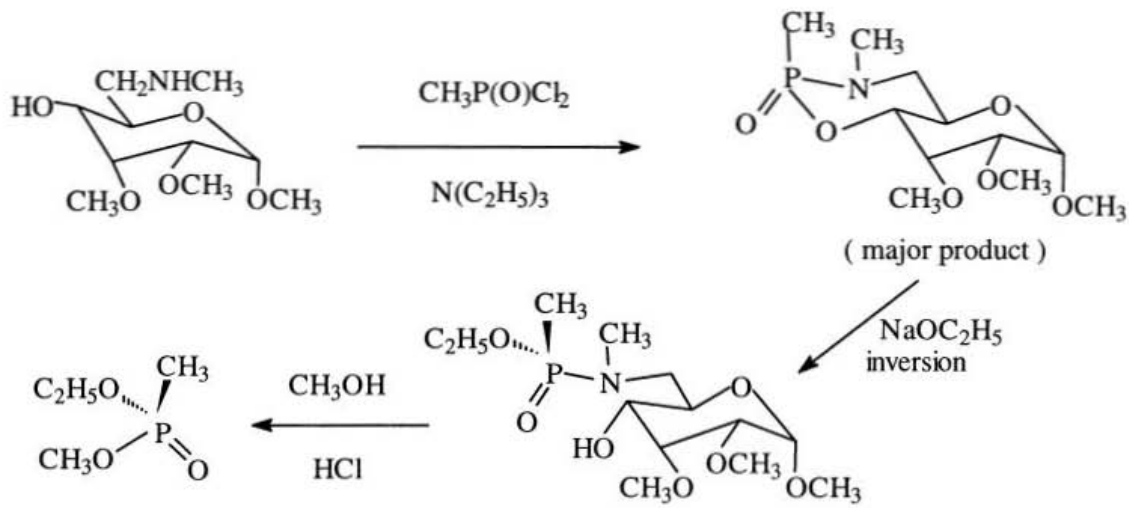

Figure 1.26 Asymmetric synthesis of P-chiral molecules via cyclic covalent diastereomers

give the chiral phosphorus product. The ring conformation exerts influence on direction of attack by nucleophiles and the geometry of possible transition states and intermediates. An example of this method is shown in Figure 1.26. Unfortunately, the diastereoselectivity of this method is not satisfactory. Stereochemical results for carbohydrate-derived reactions are given in Table 1.2.[2]

Table 1.2 Stereochemistry of Ring Opening of Cyclic Covalent Diastereomers:[2]

Leaving Group Axial

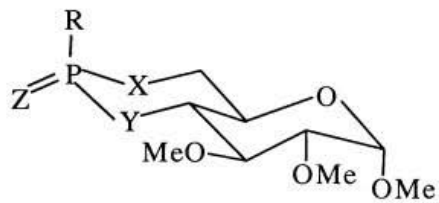

Ring heteroatoms			Leaving group	Nucleophile	Stereochemistry[a]
X	Y	Z	(R)		
O	O	O	Cl	EtOH	Inversion (93:4)
O	O	S	Cl	NaOEt/EtOH	Retention (65:31)
O	O	O	Cl	Me_2N/PhH	Inversion (87:9)
NMe	O	O	Cl	PhMgBr/Et_2O/PhH	Inversion (46:4)
S	O	O	Cl	NaOPh-*o*-NO_2	Inversion (53:-)
O	S	O	Cl	NaOEt/EtOH	Retention (28:-)
NMe	O	S	Cl	NaOEt/EtOH	Inversion (87:-)
O	O	O	SPr	NaOEt/EtOH	Retention (77:-)

[a] % yield of major and minor isomers where isolated

1.4.2.2 Derivatization

Some stereoselective syntheses are based on use of resolved phosphorus compounds as starting materials. Homochiral phosphorus compounds are functionalised, hence the method ultimately relies on the chemistry of available, resolved phosphorus compounds. Such an approach requires a suitable phosphorus-resolved precursor possessing one or more potential leaving groups and stereospecific reactions to create new bonds. The pioneering work in this area is due to Nudelman and Cram [78] and to the Mislow group.[79,80] They first demonstrated that homochiral phosphine oxides could be obtained via alkylation of resolved chiral menthylphosphinates, RR´P(O)OMen, with Grignard reagents. The reactions proceed with inversion of configuration at the phosphorus atom. This work led directly to the synthesis of the ligand DIPAMP, {(*R*,*R*)-1,2-bis[*o*-methoxyphenyl(phenyl)phosphino]ethane}, by the Monsanto group (Figure 1.27), which has on balance been the most successful of all diphosphines in its application to rhodium-complex-based asymmetric hydrogenation.[21] Using analogous reactions a pool of chiral phosphorus substrates has been created and various substitution reactions on chiral phosphorus centres, which are either stereospecific or highly stereoselective under some conditions, have been found.

The functional substituents on the backbone of the chiral phosphorus compounds, such as alkene, alkyl chloride, diene, aldehyde, etc., are also very useful

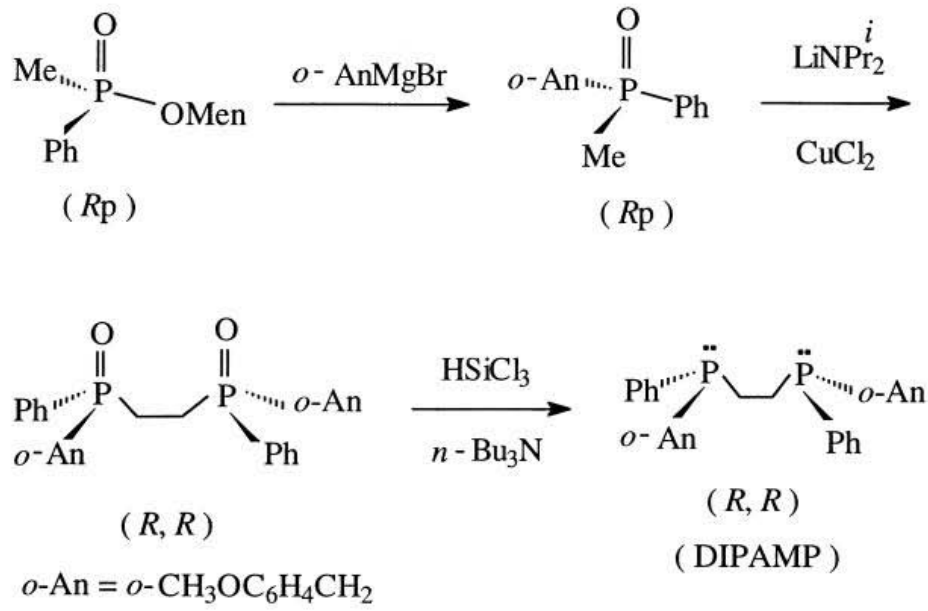

Figure 1.27 Synthesis of DIPAMP

as a "handle" for the derivatization, which offers a large variety of possibilities for structural modification on the basis of the versatile chemistry of the active groups.[59] A typical application of this method has been demonstrated by the use of a resolved α,β-unsaturated phosphine oxide as shown in Figure 1.28.

Derivatization affords desired phosphorus molecules with high chemical and optical yield, but the stereochemistry of the phosphorus compounds varies with reagents and reaction conditions. Therefore, for a specific target, investigation of the reagents and conditions is necessary.

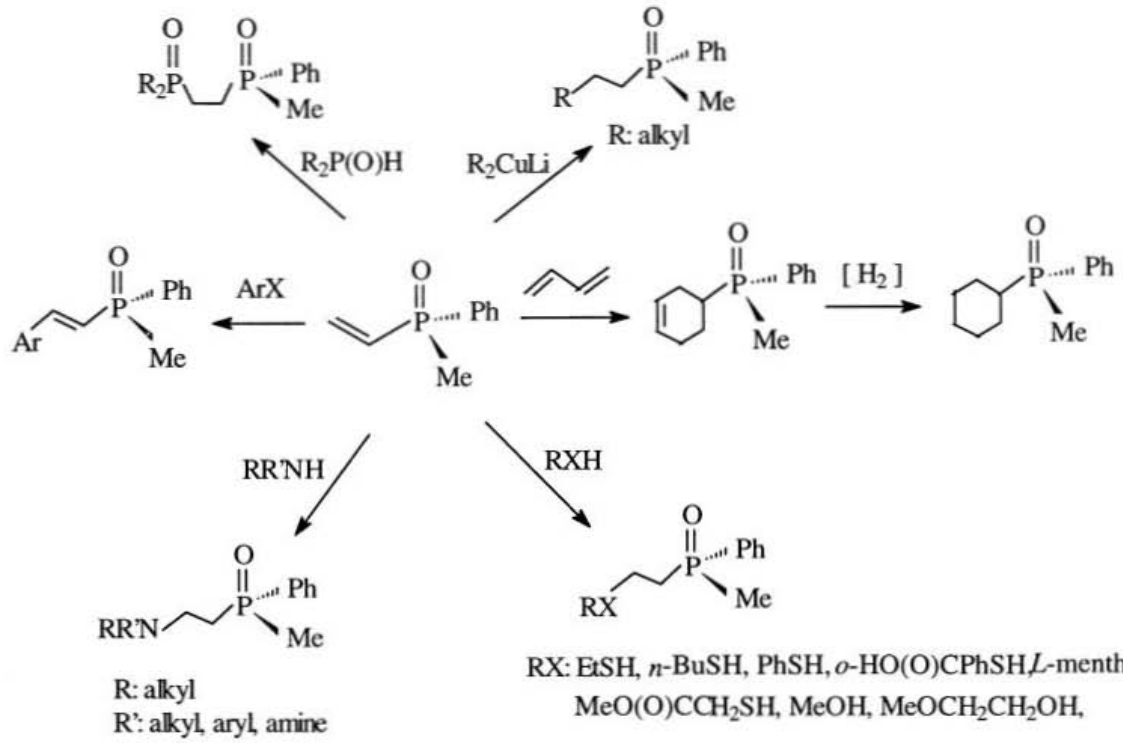

Figure 1.28 Derivatization reaction of α,β-unsaturated phosphine oxide

1.5 Applications of Transition-Metal Mediated (TMM) Chemistry to Phosphorus Compounds

Although organometallic complexes have been used as aids in the resolution and derivatization of chiral organophosphorus compounds,[84] the development of transition-metal mediated synthetic methodology for chiral organophosphorus still remains undeveloped. Given the wide application of transition-metal complexes to organic chemistry, it is not surprising to find a broad range of phosphorus reactions which are mediated by transition metals. Applications fall into three categories: *i)*

resolution of chiral phosphorus compounds as has been previously discussed;

ii) stabilization of otherwise unstable phosphorus species. For example, metal phosphinidenes (RP) have been recognized as transient species for several years, but they are so reactive that the first transition-metal-complex stabilized angular terminal phosphinidene was not isolated until 1987.[86] Hitchcock isolated a bent two-electron phosphinidene terminal ligand of the molybdenum complex shown in Figure 1.29.[86] Later, Cowley and co-workers reported isolation of a phosphinidene tungsten complex in which the phosphinidene acts as a linear four-electron donor (Figure 1.29).[87] In both cases, complexation supplements the use of bulky substituents such as *2,4,6*-tri-*tert*-butylphenyl which provide some kinetic stabilization. Phosphinous acid (H_2POH)[88] and aminophosphinidene oxides ($R_2NP{=}O$) [89] are stabilized in a similar fashion. Investigation of the effectiveness of the various metals for the stabilization of active phosphorus species indicates tungsten(0) has a definitive advantage over other metals.[93] The P–W(0) bond is strong and complexes are relatively inert at low temperature;

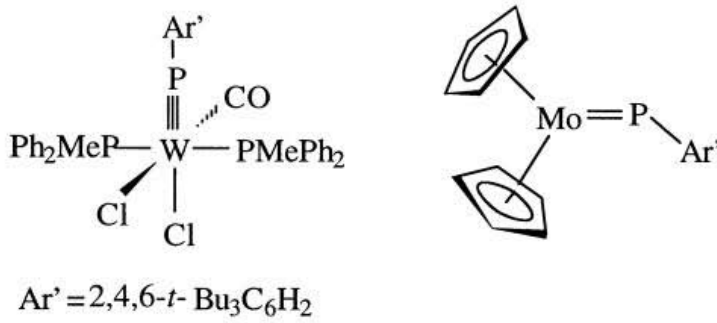

Figure 1.29 Phosphinidene transition-metal complexes

iii) modification of the chemistry of phosphorus compounds. Coordination of phosphorus with a transition metal often alters the chemistry compared to the corresponding free organic phosphorus compounds. New types of reactivity often result to give phosphorus compounds which are difficult to obtain by classic reactions.[100-106]

a) Masking of Phosphorus Reactivity by Complexation

In classical tetravalent phosphorus compounds, both the highest occupied molecular orbital (HOMO) and the lowest unoccupied molecular orbital (LUMO) are highly localized at phosphorus.[93] Thus, both electrophiles and nucleophiles tend to react at the phosphorus atom. Complexation is a highly effective technique to protect the phosphorus reactive centre so that chemistry can be transferred to another atom in the molecule. Several examples illustrate this point.

3,4-Dimethylphospholes easily react with dimethyl acetylenedicarboxylate via the phosphorus lone pair to give ring-expanded products.[107] However, Mathey and his co-workers showed that the phosphorus lone pair can be blocked by complexation with a transition metal, resulting in a [2+4] cycloaddition with the dienic system of the ring (Figure 1.30).[90] The cycloaddition selectively takes place on the side of the cycle opposite to the metal for obvious steric reasons. Complexation plays a critical role in the stabilization of the phosphorus heterocycle product.

Phosphorus complexation has also proven useful in developing the chemistry

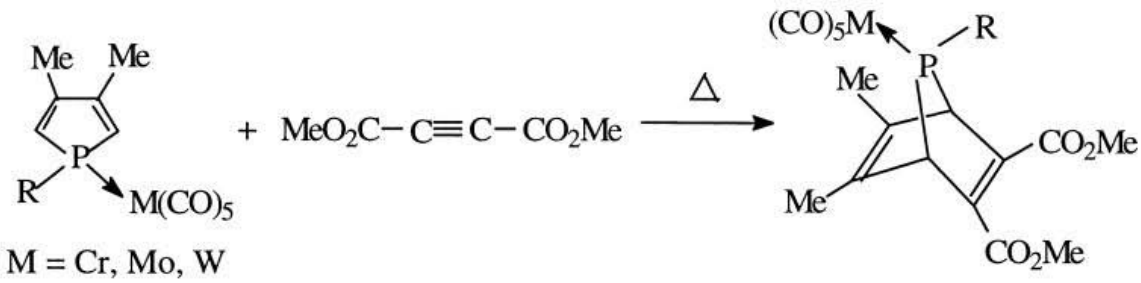

Figure 1.30 [2+4] cycloaddition of 3,4-dimethylphosphole complex

of the P=C double bond. The two highest occupied molecular orbitals of phosphaalkenes correspond to the lone pair and the P=C π-bond.[109] As a result, electrophilic reagents tend to attack both sites without selectivity. Blocking the lone pair of the phosphorus centre through coordination with transition metals allows the development of a regio-selective chemistry at the double bond. The first demonstration of this idea was the direct epoxidation of phosphaalkene complexes (Figure 1.31).[91-93] The epoxidation takes place with retention of stereochemistry at the double bond, compared with oxidation of free phosphaalkenes which leads to the cleavage of the P=C unit.[110]

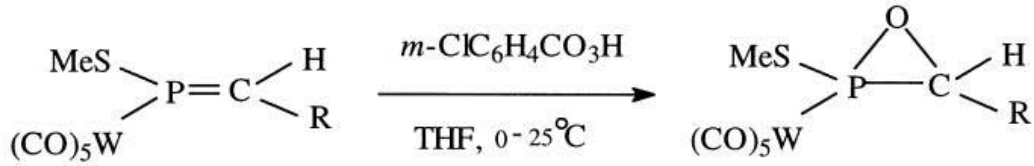

Figure 1.31 Selective epoxidation of a P=C double bond

Template syntheses of polydentate phosphines have also been made via P–H and alkene or alkyne condensation in coordination sphere.[94,95] In most cases, however, the resulting phosphorus compounds are achiral.

b) Stereochemical Control via Complexation

Some transition metal complexes have been used in the asymmetric induction of prochiral phosphorus compounds. A striking example is *L*-menthylphosphaalkene molybdenum complexes which selectively react with cyclopentadiene on their S_i faces (Figure 1.32).[111] The origin of the selectivity is ascribed to steric effects. Rotation of the menthyl group around its bond with phosphorus is blocked by the bulky complexing group. In the less hindered conformation, the isopropyl

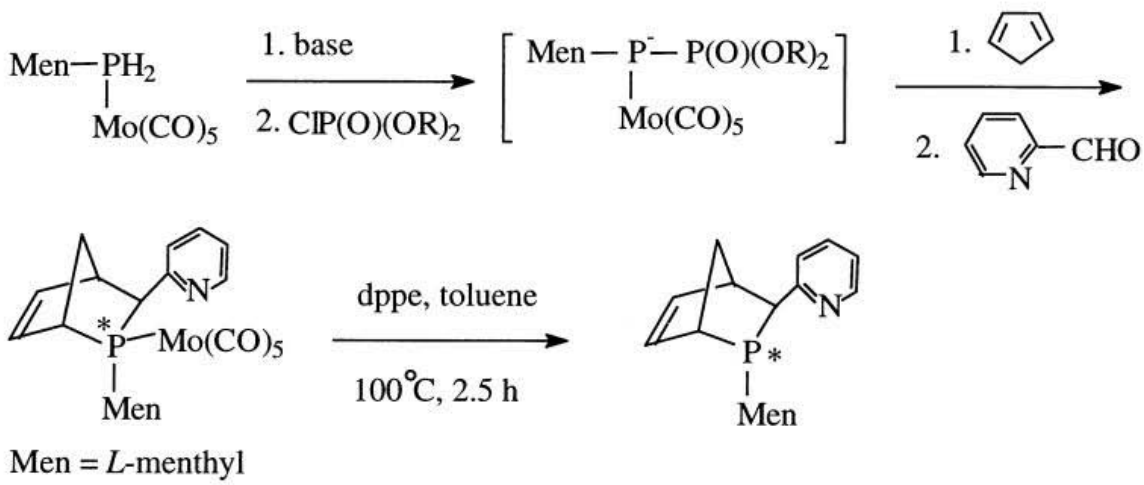

Figure 1.32 Stereochemical control of phosphorus compounds via complexation

substituents of the menthyl group shields the R_e face[111] of the phosphaalkene.

Nakazawa and his coworkers adopted iron complexes to prepare pentavalent phosphorus compounds via Arbuzov-like dealkylation. Substitution at phosphorus in inorganometallic amidophosphonates (L_n[M]–P(O)(NR_2)(OR)) occurs easily in the presence of the Lewis acid, BCl_3. Subsequent treatment with suitable nucleophiles gave derivatives of the phosphonate (Figure 1.33).[112] However, the resulting chiral phosphorus complexes are not resolved and, hence, stereoselectivity was not studied.

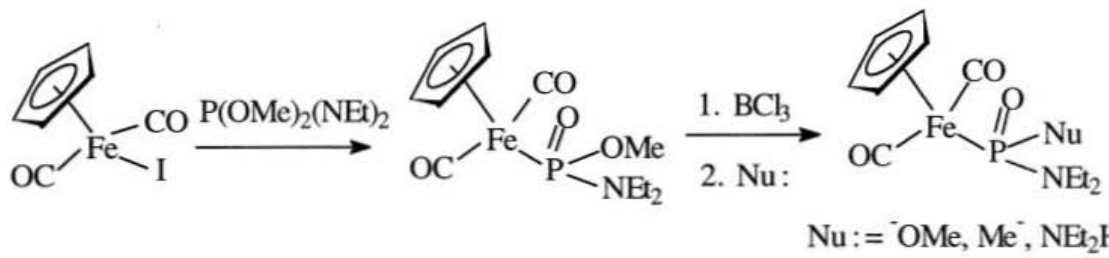

Figure 1.33 Stereochemistry of chiral phosphonate ligands

Transition metal complexes used to alter stereoselectivity of phosphorus chemistry have been based on the presence of a chiral auxiliary ligand. Application of chiral-at-metal transition metal complexes in this area has not been developed. Considering the chemical and stereoselective influences of complexation on chemistry of phosphorus moieties, asymmetric synthesis of chiral phosphorus compounds within the coordination sphere of a chiral transition metal seems promising.

1.6. Project Description

This research is directed toward the development of a new synthetic strategy for the preparation of phosphorus-chiral molecules. Since pentavalent phosphorus compounds have demonstrated extensive applications in various fields because of their biological activity and phosphines can be produced by stereospecific conversion from pentavalent phosphorus compounds, the target compounds selected are pentavalent compounds with a phosphoryl (P=O) group.

The goals of this research are to synthesize chiral phosphorus moieties through chiral induction by transition metal complexes, to examine the chemistry of the chiral phosphorus moieties and, finally, to establish routes leading to the cleavage of the metal-phosphorus bond in order to release new chiral phosphorus compounds. This thesis discusses the results obtained for the first two parts.

Jablonski et al have examined the synthesis of chiral pentavalent phosphorus moieties via transition-metal-mediated (TMM) Arbuzov reactions[125,145] and found that the chiral transition metal influences the stereochemistry at phosphorus. This thesis focuses on development of synthetic methods to chiral phosphorus compounds via TMM chemistry. Three types of pseudo-tetrahedral "piano-stool" cobalt(III) complexes containing cobalt and phosphorus chiral centres, L_n[Co*]P(O)(X)(Y), have been synthesized and separated (Figure 1.34). These compounds were previously named as covalent metalloderivatives of P(V) oxo esters to emphasize the

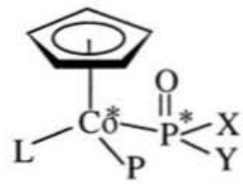

L = C_3F_7, P = $PPhMe_2$, X = OMe, Y = Ph; NEt_2
L = I, P = (*S*)-α-$Ph_2PNHC(H)MePh$, X = OMe, Y = NEt_2
L = C_3F_7, P = $PPhMe_2$, X = OEt, Y = SPh

Figure 1.34 Model compounds

relationship with classic Arbuzov organophosphorus chemistry. For example, $L_n[M]–P(O)(OR)_2$ is viewed as a metallo-substituted dialkyl phosphonate. This formalism requires that cobalt be assigned as Co(I). However, the cobalt complexes discussed here are chemically better described as Co(III). In order to avoid formal oxidation state ambiguities, the compounds shown in Figure 1.34, in which the phosphorus centres are formally P(III), are named respectively as *P*-phosphonito, *P*-amidophosphito and *P*-thiopheylphosphito complexes.[125] Structures of new complexes have been confirmed by ^{1}H, ^{31}P, ^{13}C, ^{19}F NMR, IR , MS and X-ray analysis. The functions of the supporting ligands and the chemistry of these complexes have been studied. Compared to their organic analogs, the inorganometallic phosphonates studied are inert to nucleophilic reagents.

Chapter 2

Transition-Metal-Mediated (TMM) Synthesis of *Co*- and *P*-Chiral Co(III) Complexes

2.1 Introduction

Following systematic work on asymmetric synthesis of chiral-carbon compounds in the last 30 years, recognition of the potential biological activity of phosphorus-chiral molecules has increased interest in developing reliable, stereoselective synthetic routes to chiral phosphorus compounds.

Asymmetric synthesis of chiral phosphorus compounds via transition-metal-mediated chemistry (TMM) has received little attention since there were more established routes to chiral phosphorus molecules. However, TMM synthesis, with its possibility to modify reaction conditions and to control stereochemistry of phosphorus through coordination, holds promise as a synthetic avenue for the synthesis of new *P*-chiral phosphorus materials. This chapter discusses a novel method to synthesize optically active phosphorus compounds via chiral induction from transition metal complexes.

Although both trivalent and pentavalent tetrahedral compounds have been

found to display chirality, this research focuses on pentavalent phosphorus moieties with a P=O double bond due to their potential biological activity. The overall strategy is to synthesize the chiral phosphonate moieties via TMM chemistry, followed by transformation and release of the chiral phosphorus moieties from the metal complex. This chapter focuses exclusively on the synthesis of the chiral phosphonate substrates via the transition-metal-mediated (TMM) Arbuzov reaction.[114] Subsequent transformations, which develop the chemistry and release the *P*-chiral target, will be discussed in the next chapter.

The TMM Arbuzov reaction, as the analog of the classic Arbuzov reaction for formation of a P–C bond,[112,113] occurs between a transition metal complex ($L_n[M]X$) containing a labile nucleophilic ligand such as a halogen (X) and trialkyl phosphites,

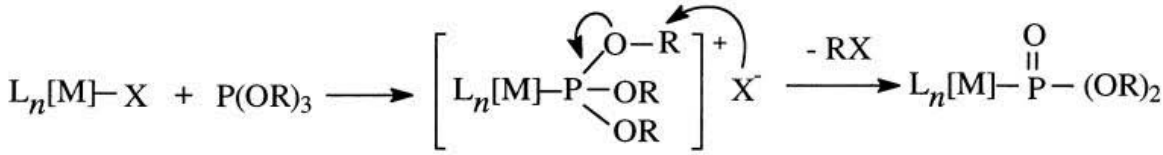

L = supporting ligands ; M = transition metals ; X = halide

Figure 2.1 Mechanism of transition-metal-mediated (TMM) Arbuzov reaction

ultimately producing a metal-phosphonate complex. Importantly, the transition-metal-mediated Arbuzov reaction occurs under milder conditions compared to the classic reactions.[112] The variety of metal complexes engaging in the reaction is surprisingly wide.[114] Most TMM Arbuzov reactions follow an ionic pathway[115,116] in which the

halide is first replaced by the phosphite to give a cationic intermediate, $[L_nM\{P(OR)_3\}]^+$, which is then subject to nucleophilic attack at the α-carbon of the coordinated phosphite by the released halide anion, affording the final phosphonate complex (Figure 2.1). The mechanism indicates that, in principle, a reaction of $L_n[M]X$ with a trivalent phosphorus compound having at least one alkoxy group can yield an Arbuzov-like dealkylation product. Hence, phosphines of the form $P(OR)_nR_1(R_2)_{2-n}$ (n = 1, 2) can produce chiral phosphonate moieties.

Several series of *Co*- and *P*-chiral η^5–cyclopentadienyl, η^5–pentamethylcyclopentadienyl, η^5–indenyl, etc. three-legged piano-stool complexes have now been successfully synthesized as the chiral auxiliaries via the Arbuzov-like dealkylation of prochiral phosphonates. The chiral cobalt center critically influences the stereochemistry of the nascent chiral phosphorus center and the reactions have

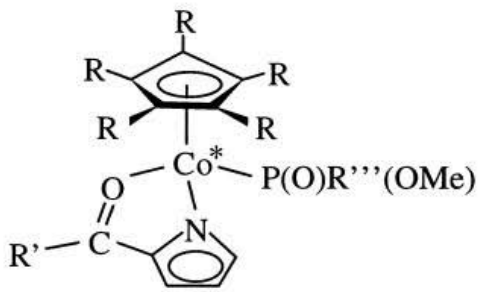

R = H, R' = H, R''' = Ph;
R = H, R' = Me, R''' = Ph;
R = Me, R' = Me, R''' = Ph

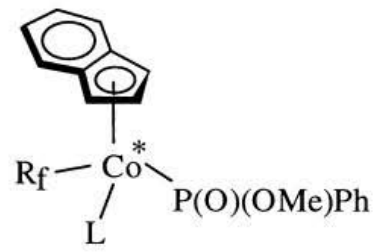

L = PMe_3, P = $PPh(OMe)_2$, $P(OMe)_3$
R_f = C_3F_7, C_6F_{13}

Figure 2.2 Chiral induction of cobalt atom on phosphorus moieties

been proven to proceed via an ionic mechanism.[145] Steric requirements of the spectator ligands and the entering phosphonites are crucial in determining the chiral induction. Some examples are shown in Figure 2.2.

Nakazawa has recently reported that substitution at phosphorus in inorganometallic amidophosphonates ($L_n[M]$–$P(O)(NR_2)(OR)$) can occur with the assistance of a Lewis acid.[111] Therefore, *P*-amidophosphito Co(III) complexes have been chosen as precursor target substrates for this study. As well, the chloride, methoxy and thioester substituted organic phosphonates easily undergo nucleophilic substitution. It is conceivable that the same will happen for the inorganometallic phosphonates. Hence, $P(OMe)_2Cl$, $P(OMe)_2Ph$ and $P(OEt)_2(SPh)$ have also been used in the transition-metal-mediated Arbuzov reaction in order to introduce functional groups which may increase the susceptibility of the pentavalent phosphorus center to subsequent nucleophilic attack.

2.2 Results and Discussion

P-chiral Co(III) η^5–cyclopentadienyl *P*-phosphonito complexes were synthesized via a chiral modification of the transition-metal-mediated Arbuzov reaction. Starting materials, $(\eta^5\text{–}C_5H_5)Co(X)(L)(I)$ (**1.** X = C_3F_7, L = $PPhMe_2$; **9.** X

= I, L = (S_C)-(−)-$PPh_2NHCH(Ph)(Me)$), were prepared following the literature route[155] by oxidative addition of XI (**1.** X = C_3F_7; **9.** X = I) to (η^5-C_5H_5)Co(CO)$_2$ to afford (η^5-C_5H_5)Co(CO)(X)(I), followed by preferential substitution of labile CO with supporting phosphine ligands, L. The starting materials were purified via chromatography with benzene as eluent.

2.2.1 Synthesis of *P*-phosphito Co(III) Complexes

2.2.1.1 $P(OEt)_2Cl$ as the Trivalent Phosphorus Reagent

Diethyl chlorophosphite was used as the trivalent phosphorus ester to react with the starting material **1**, (η^5-C_5H_5)Co(C_3F_7)($PPhMe_2$)(I), in order to introduce the chloride function into the cobalt *P*-phosphito complex. It was anticipated that introduction of a chloride into the pentavalent phosphorus moiety would provide useful versatility for further chemical transformation because of its ability to act as a good leaving group.

Treatment of compound **1**, (η^5-C_5H_5)Co(C_3F_7)($PPhMe_2$)(I), with 1.3 equivalents of $P(OEt)_2Cl$ in benzene at refluxing temperature for 20 hours gave no reaction (viz ^{1}H NMR and TLC). Since S_N2 reaction at the −OEt group[121] is more difficult than at the −OMe group, more forcing conditions were attempted. However, after refluxing in toluene for three days, ^{1}H NMR indicated that no reaction had

occurred. Separation of the crude mixture by chromatography recovered the starting material **1** in near quantitative yield.

There are two possible reasons for inertness of diethyl chlorophosphite in the transition-metal-mediated Arbuzov reaction. First, as mentioned before, coordination of the trivalent phosphorus ester with the cobalt center is the necessary coordination for Arbuzov-like dealkylation. The electron density on the phosphorus center of $P(OEt)_2Cl$ may be too low to substitute the iodide ligand of the cobalt complex due to the presence of strong electron-withdrawing functions. Alternatively, nucleophilic attack of I^- on the α-carbon atom of coordinated $P(OEt)_2Cl$ may be difficult because S_N2 reaction is more difficult at the 2° carbon center as observed by Nakazawa in the reaction of the cyclopentadienyl iron complex, $(\eta^5\text{-}C_5H_5)Fe(CO)_2(Cl)$.[121] Reaction with $P(OEt)Ph_2$ results in formation of the cationic complex, $\{(\eta^5\text{-}C_5H_5)Fe(CO)_2[PPh_2(OEt)]\}^+Cl^-$, the product of simple substitution at iron.

The coordinating ability of diethyl chlorophosphite, $P(OEt)_2Cl$, was examined via the sequence shown in Figure 2.3. Abstraction of iodide ligand from compound **1** with $AgBF_4$ in acetone gave the solvent complex **2**. Subsequently, diethyl chlorophosphite was added to compete with the solvent molecule for the coordination site. Addition of one equivalent of $AgBF_4$ to compound **1** in d_6-acetone gave a yellow precipitate. The ^1H NMR spectra of the greenish brown filtrate showed that the signal

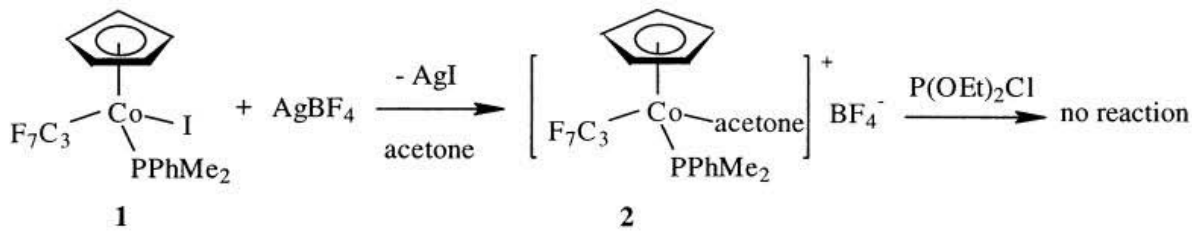

1 2

Figure 2.3 Coordination reaction of $P(OEt)_2Cl$

for -Cp was shifted from 5.08 ppm to 5.46 ppm and that two sets of doublets, assigned to the methyl group of $PPhMe_2$, shifted from 2.15 ppm and 2.11 ppm respectively to 2.14 ppm and 1.94 ppm. These observations suggested that the ionic intermediate was produced. ^1H NMR spectra after addition of $P(OEt)_2Cl$ indicated that chemical shifts of all functional groups remained unchanged, which showed that the coordinated acetone molecule is not replaced by diethyl chlorophosphite. Hence, the failure of the $P(OEt)_2Cl$ reactions was due to the lack of initial chlorophosphite coordination.

2.2.1.2 $PPh(OMe)_2$ as the Trivalent Phosphorus Reagent

Dimethyl phenylphosphite was used to synthesize an inorganometallic phosphonate containing a phenyl function in order to probe substituent effects on nucleophilic transformations.

2.2.1.2 i. Synthesis

Reaction of a brown solution of starting material **1** with 1.2 equivalents of dimethyl phenylphosphite in refluxing acetone afforded a reddish brown mixture. Separation of the crude product via preparative thick-layer radical chromatography gave four products **2-1a, 2-1b, 2-1c** and **2-1d** in the order of decreasing R_f value. The orange product **2-1a** and yellow product **2-1b** are the major products in which **2-1a** dominates over **2-1b**.

2.2.1.2 ii. Characterization

The four isolated reaction products **2-1a**, **2-1b**, **2-1c** and **2-1d** were characterized by elemental analysis, IR and ^{1}H, ^{13}C, ^{31}P and ^{19}F NMR (Tables 2.1.1-2.1.3). ^{1}H, ^{13}C, ^{31}P and ^{19}F NMR chemical shifts for **2-1a** and **2-1b** were those expected for diastereomers of *P*-phosphito Co(III) complexes containing $PPhMe_2$ supporting ligand while **2-1c** and **2-1d** were diastereomers of *P*-phosphito Co(III) complexes containing $PPh(OMe)_2$ supporting ligand.

A rationale for formation of **2-1c** and **2-1d** is that $PPh(OMe)_2$ is also a good coordinating ligand and, thus, substitutes not only iodide ligand (route **a** in Figure 2.4) but also $PPhMe_2$ to afford compound **5** (route **b** in Figure 2.4) which subsequently undergoes an Arbuzov reaction to produce the by-products as shown in Figure 2.4. Another possibility is that the $PPh(OMe)_2$ replaces the $PPhMe_2$ ligand of the cationic

intermediate **3** to give the intermediate **6** (route **c**) for dealkylation. Structures of by-products **2-1c** and **2-1d** have been confirmed by rational synthesis (route **d** in Figure 2.4). Reaction of $(\eta^5\text{-}C_5H_5)(C_3F_7)Co(CO)(I)$ with 2 equivalents of $PPh(OMe)_2$ gave the same products, which suggests that route **b** is correct. The *P*-phosphito Co(III)

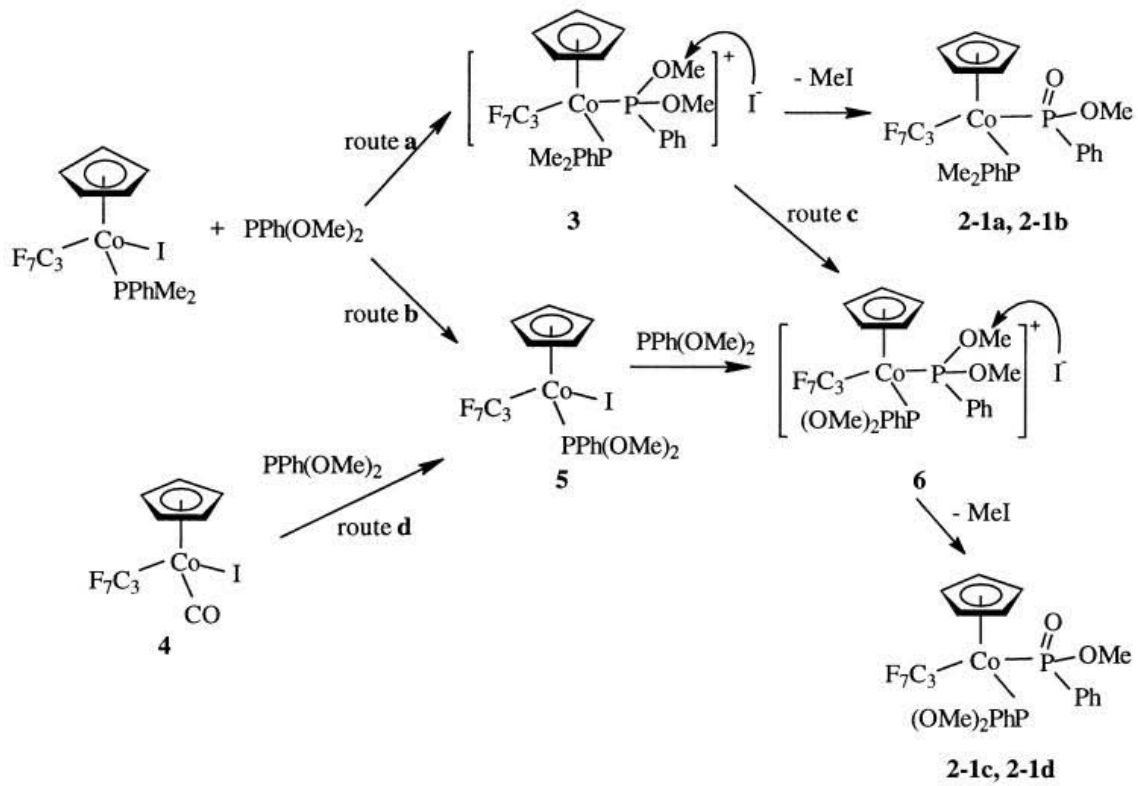

Figure 2.4 Synthesis of *P*-phosphito Co(III) complexes

complexes are both air and configurationally stable at room temperature in the solid state and in solution.

The presence of chiral cobalt and phosphorus centers results in diastereotopic germinal P(O)*Ph* and *P–Me* which are reflected in their NMR spectra as pairs of *ipso,*

ortho, meta and *para* ^{13}C resonances and as doublet of doublets in the proton NMR, respectively. The compounds also showed well-resolved AB ^{31}P NMR patterns corresponding to the presence of phosphonate (P(O)(OMe)Ph) and phosphine ($PPhMe_2$) or phosphinate ($PPh(OMe)_2$) as shown in Table 2.1.1.

2.2.1.2 iii. Solid-State Structure, Absolute Configuration and Chiral Induction

The solid-state structure of diastereomer **2-1a** was determined by X-ray diffraction in order to verify connectivity and establish absolute configuration. A single crystal of compound **2-1a** was obtained via diffusion of pentane into a solution of **2-1a** in dichloromethane at room temperature. The molecular structure (Figure 2.5) demonstrated that **2-1a** is the typical "three-legged piano-stool" complex with approximately 90° interligand bond angles (P(2)–Co–P(1) = 93.33(2)°, P(2)–Co–C(16) = 91.52(6)°, P(1)–Co–C(16) = 94.02(6)°). The η^5–coordinated cyclopentadiene occupies three *fac* coordination sites of the octahedral geometry while perfluoroalkane, dimethylphenyl phosphine and phosphonate complete the coordination sphere. The structure data determined from the X-ray analysis are shown in Tables 2.1.4 – 2.1.7.

The relative configuration of **2-1a** at cobalt and phosphorus was unequivocally assigned from the X-ray structure as shown in Figure 2.5. Consideration of the

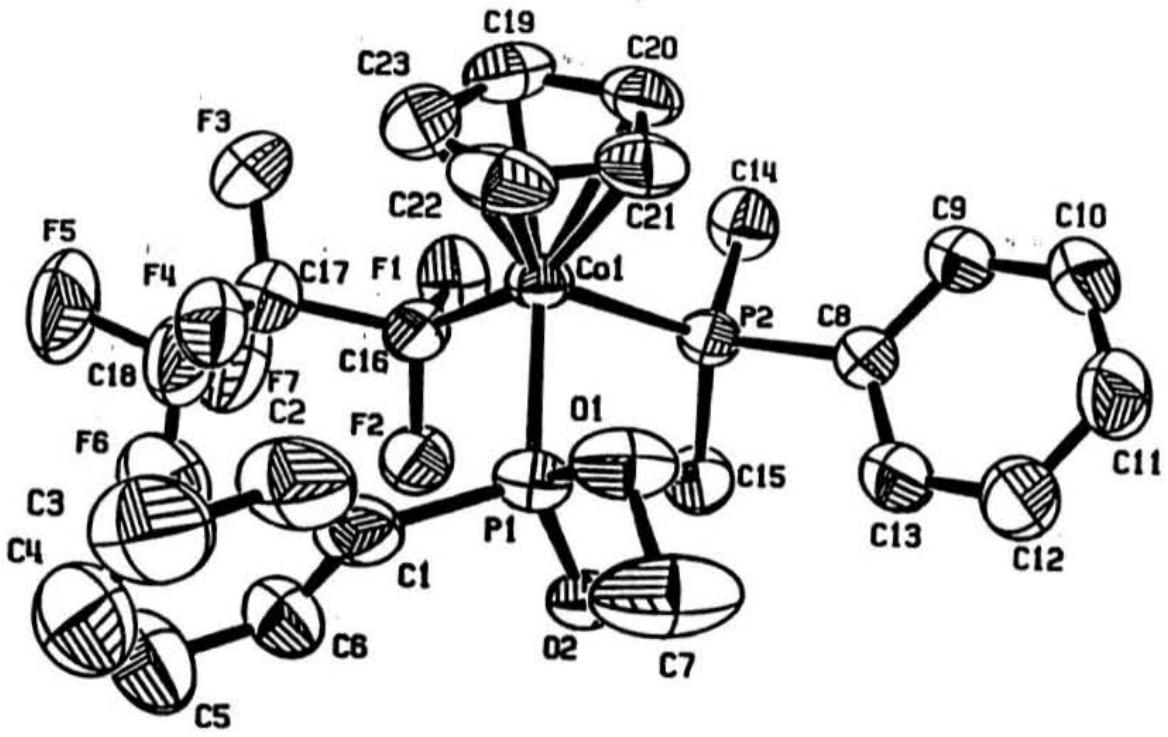

Figure 2.5 Molecular structure of P-phosphito Co(III) complex 2-1a

complex **2-1a** as a pseudotetrahedral case with η^5–Cp occupying one coordination site and the use of modified Cahn–Ingold–Prelog (CIP) rules[125,146-148] with the ligand priority series η^5–Cp > P(O)(OMe)Ph > $PPhMe_2$ > C_3F_7 for cobalt and Co > OMe > O > Ph for phosphorus specifies the relative configuration of **2-1a** as S_{Co},S_P / R_{Co},R_P. Hence, the relative configuration of the diastereomer **2-1b**, which has a lower R_f value, is assigned as S_{Co},R_P / R_{Co},S_P.

The diastereomeric excess is 42.9%, based upon the isolated products, with diastereomer **2-1a** as the major product, which suggests a modest chiral induction from Co* to P. The stereoselectivity may be related to the steric requirements of the

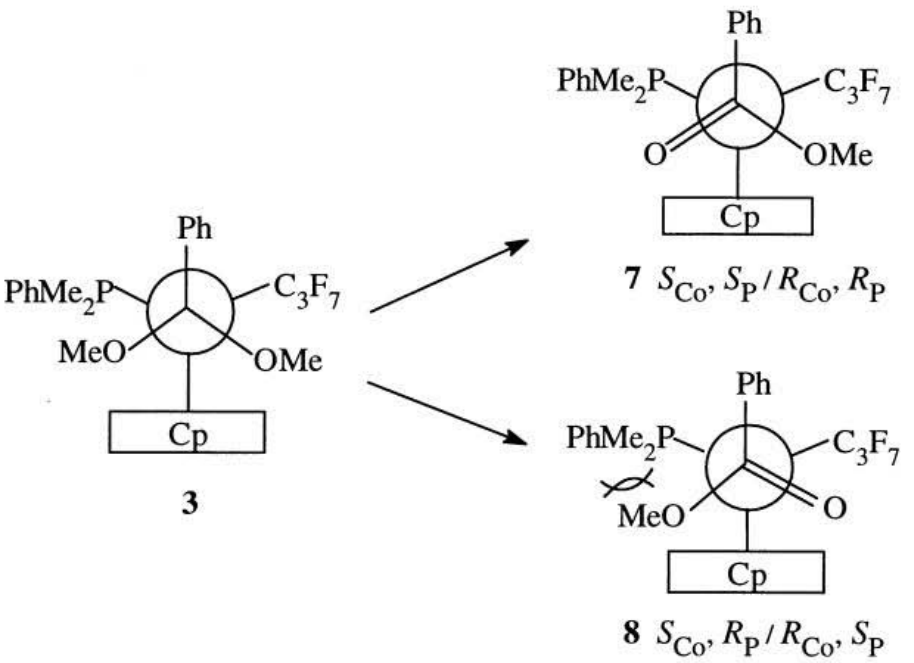

Figure 2.6 Chiral induction of *P*-phosphito Co(III) complexes **2-1**

product. Substitution of iodide in **1** by $PPh(OMe)_2$ gives a product-like intermediate **3** which undergoes dealkylation on the diastereotopic methoxy group to afford diastereomeric products **2-1**. The ligands on the cobalt center decrease in size in the order of η^5–Cp (cone angle 136°) > $PPhMe_2$ (cone angle 122°) > C_3F_7.[16] Hence, the most stable arrangement in the transition state is with the bulky phenyl group of the phosphite between the two least sterically demanding substituents on the cobalt (that is, between the phosphine, $PPhMe_2$, and the perfluoroalkane, C_3F_7), as shown in Figure 2.6.[162] Under conditions of kinetic control, a well developed P=O double bond will be controlled by the steric interactions between the phosphine and the P(O) substituents in the product. Therefore, product **7** will be the major product due to less severe C_3F_7 / OMe vs. $PPhMe_2$ / OMe interaction.

2.2.1.2 iv. Attempted Resolution of ***2-1a***

(1*R*)-(−)-10-Camphorsulfonic acid was tested as a potential resolving agent for the diastereomers in **2-1a** via protonation of the P=O function. Addition of one equivalent of (1*R*)-(−)-10-camphorsulfonic into a solution of **2-1a** in chloroform gave a ^1H NMR spectra in $CDCl_3$ which indicated that the Cp peak was split into two resonances at 5.14 ppm and 5.13 ppm. The –OMe doublet, resulting form coupling with the phosphorus center, shifted and split from 3.42 ppm to 3.62 ppm and 3.58

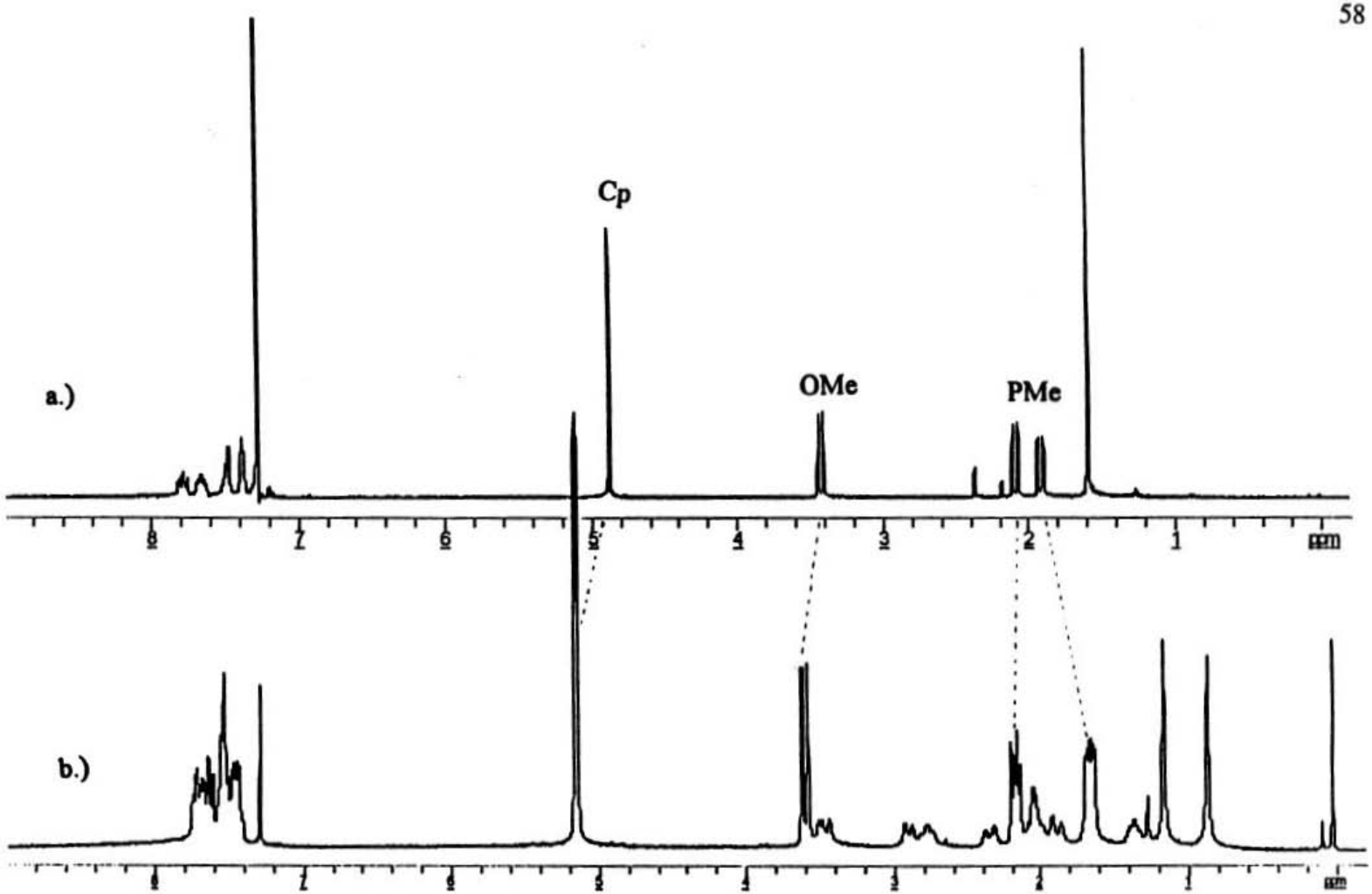

Figure 2.7 300 MHz ^{1}H NMR of a.) complex **2-1a** and b.) reaction of **2-1a** with camphorsulfonic acid

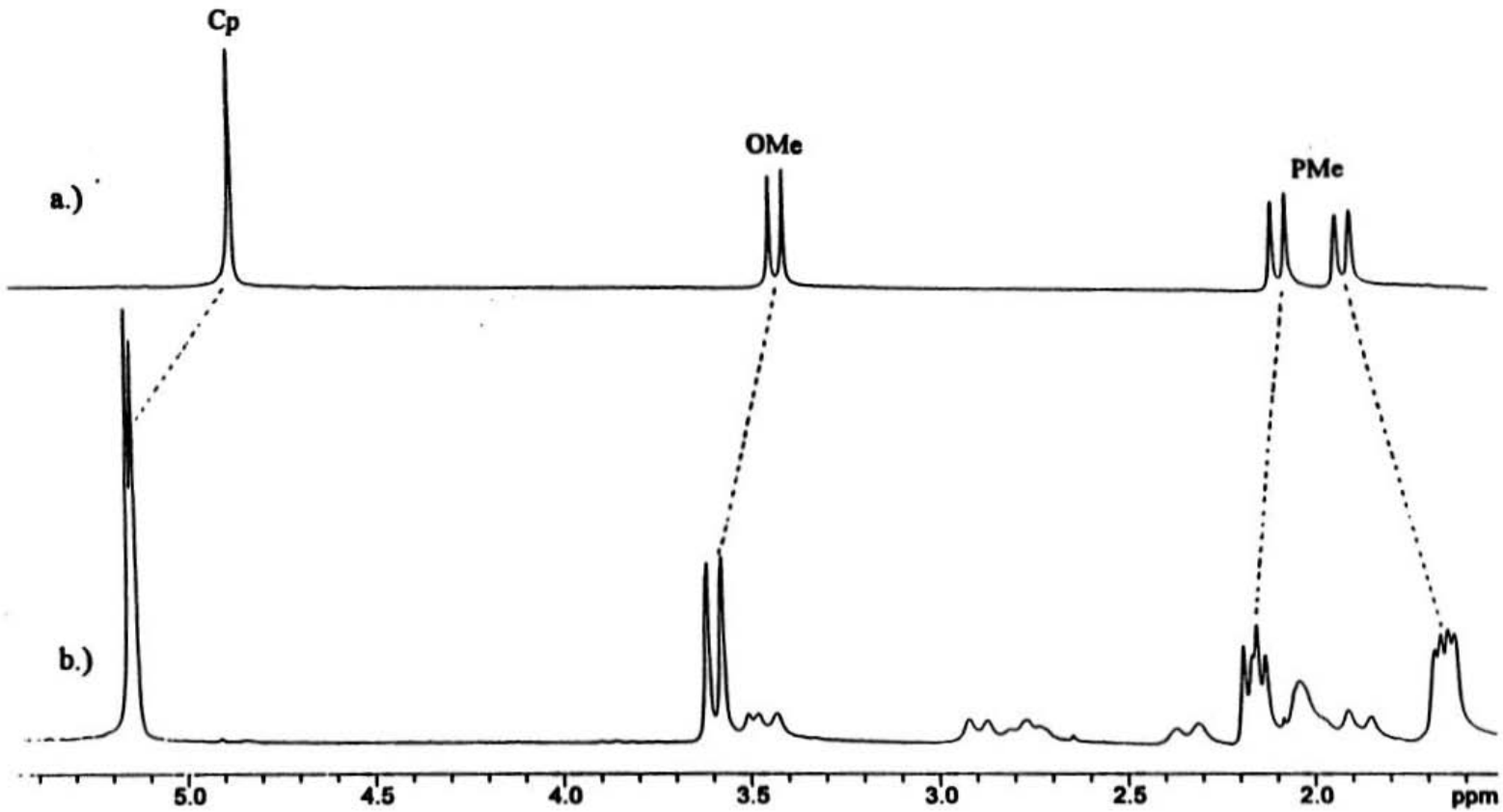

Figure 2.8 300 MHz expanded ^{1}H NMR of a.) complex **2-1a** and b.) reaction of **2-1a** with camphorsulfonic acid

ppm. The doublet of doublets of the two unequivocal methyl groups in $PPhMe_2$ appeared as four sets of doublets at 2.19 ppm, 2.14 ppm and 1.67 ppm, 1.64 ppm as shown in spectrum **b** of Figure 2.7. The expanded ^1H NMR is shown in Figure 2.8. The spectral changes indicated that protonation occurs to afford new diastereomers. Unfortunately, the diastereomers appear to have similar solubility and a suitable solvent for fractional crystallization was not found.

2.2.2 Synthesis of *P*-amidophosphito Co(III) Complexes

Inorganometallic *P*-amidophosphites were reported[111] to undergo nucleophilic substitutions with aid of the Lewis acid, BCl_3. In order to test this chemistry as a potential phosphorus elaboration mechanism, the *P*-amidophosphito cobalt (III) complexes shown in Figure 2.9 were synthesized. Two series of *P*-amidophosphito Co(III) complexes have been synthesized, with iodide (**2-2 a – d**) or perfluoroalkane

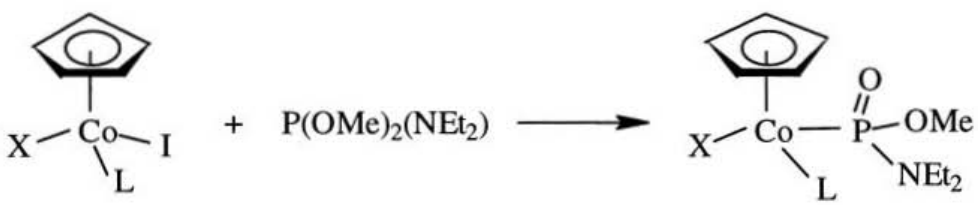

9, 2-2 a-d : L = PNH, X = I
1, 2-3 a-b : L = $PPhMe_2$, X = C_3F_7

Figure 2.9 Synthesis of *P*-amidophosphito Co(III) complexes

(**2-3 a, b**) as the supporting ligand, in order to compare the electronic effects on the susceptibility of the pentavalent phosphorus center toward nucleophilic attack.

2.2.2.1 Synthesis of $P(OMe)_2(NEt_2)$

Dimethyl (diethylamido)phosphite was used as the phosphite for the transition-metal-mediated Arbuzov reaction. It was prepared by reacting $(Et_2N)PCl_2$, which is prepared from the reaction between PCl_3 and Et_2NH in diethyl ether, with MeOH in Et_3N according to the literature method for $Me_2NP(OMe)_2$.[126] ^1H NMR of the crude product indicated good conversion to $Et_2NP(OMe)_2$, however, distillation under 0.1 mmHg pressure gave a very low yield (21.4 %). Increasing pressure in order to achieve higher distillation temperature failed to increase the yield and resulted in the formation of an unidentified orange oil at a pot temperature above 70°C.

Alternatively, $(Et_2N)PCl_2$ was stirred overnight with two equivalents MeONa in methanol at room temperature. After removal of the solvent, water was added and diethyl ether was used to extract the organic product which was obtained in 63.0 % yield and was used without further purification.

2.2.2.2 Synthesis of *P*-amidophosphito Co(III) Complexes

P-amidophosphito PNH Co(III) diastereomers, **2-2a – d**, were prepared by the

literature route[126] with the reaction of the purple compound **9**, $(\eta^5\text{-}C_5H_5)Co(PNH)(I)_2$ (PNH = (S_C)-(−)-$PPh_2NHCH(Me)Ph$), with one equivalent of $(NEt_2)P(OMe)_2$ at ambient temperature. Introduction of PNH directly transforms all final products into diastereomers for easy resolution. The optical yield, based upon isolated products, is 88% de, with compounds **2-2a** and **2-2b** as the major products. Spectroscopic data obtained for the four diastereomers are shown in Tables 2.2.1– 2.2.3.

The *P*-amidophosphito Co(III) dimethyl phenylphosphine complexes were synthesized by a similar reaction starting from **1**, $(\eta^5\text{-}C_5H_5)Co(PPhMe_2)(C_3F_7)(I)$. Separation, by preparative thick-layer radical chromatography, afforded diastereomers **2-3a** and **2-3b** in the order of decreasing TLC R_f values. The diastereomeric excess, based upon isolated products, is 53.7% with compound **2-3a** as the major product. Spectroscopic data of the products **2-3** are shown in Tables 2.3.1 – 2.3.3. Compounds **2-3 a, b** are air stable in the solid state and in solution. However, they decompose in solution after exposure in air for several days.

2.2.3 Synthesis of *P*-thiophenylphosphito Co(III) Complexes

A *P*-thiophenylphosphito substrate was synthesized using diethyl thiophenylphosphite as the trivalent phosphorus reagent. In general, organic phosphorothiolate esters (O=P–SR) are much more chemically reactive than the

corresponding phosphate esters (O=P–OR). A similar relationship holds for anti-AChE activity (thiolo effect).[31,37] Such high activity of phosphorothiolate esters, despite the low electronegativity of the sulfur atom, has been attributed both to the low bond strength of the P–S bond, owing to the small $d\pi$ - $p\pi$ contribution to P–S linkage resulting from poor overlap between the *3d* orbital of phopshorus and the *3p* orbital of sulfur,[37] and the polarizability of the sulfur atom. [31] Therefore, the thiophenyl function was introduced into the inorganometallic phosphorus moiety in order to provide another available leaving group.

2.2.3.1 Synthesis and Characterization

Treatment of starting material **1**, $(\eta^5\text{-}C_5H_5)Co(PPhMe_2)(C_3F_7)(I)$, with one equivalent of diethyl thiophenylphosphite, $P(OEt)_2(SPh)$, gave an orange mixture of the *P*-thiophenylphosphito Co(III) complexes (Figure 2.10). Prolonged heating is necessary for the transformation because of the inertness of the –OEt group in the

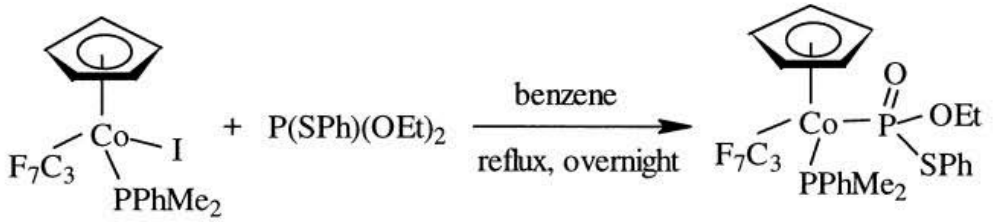

1 **2-4 a,b**

Figure 2.10 Synthesis of *P*-thiophenylphosphito Co(III) complexes

Arbuzov reaction as discussed above. The crude products were separated by chromatography to afford the diastereomers of *P*-thiophenylphosphito Co(III) complexes, **2-4a** and **2-4b** in the order of decreasing R_f values, with **2-4a** as the major diastereomer. The diastereomeric excess is 42.4% based upon isolated products. IR and ^{1}H, ^{13}C, ^{31}P and ^{19}F data are shown in Tables 2.4.1 – 2.4.3.

2.2.3.2 Solid-State Structure and Absolute Configuration

A single crystal X-ray structure of compound **2-4a** was determined using crystals grown by slow diffusion of pentane into a dichloromethane solution of the compound at room temperature. As shown in Figure 2.11, the coordination sphere of cobalt can be described as distorted octahedral. Consistent with its $18e^-$ configuration, the cyclopentadienyl ring is η^5-bonded, occupying three *fac* coordination sites, while perfluoroalkane, phosphine and phosphonate complete the remaining three coordination sites. The interligand angles are approximately 90° (P(1)–Co–P(2) = 99.26(7), P(2)–Co–C(22) = 90.5(2), P(1)–Co–C(22) = 95.3(2)). Thus, the coordination geometry of the cobalt atom is pseudo tetrahedral with a typical three-legged piano-stool structure. Atomic coordinates, selected bond lengths and bond angles are given in Tables 2.4.4 – 2.4.7.

The relative configuration of compound **2-4a** was unequivocally assigned from

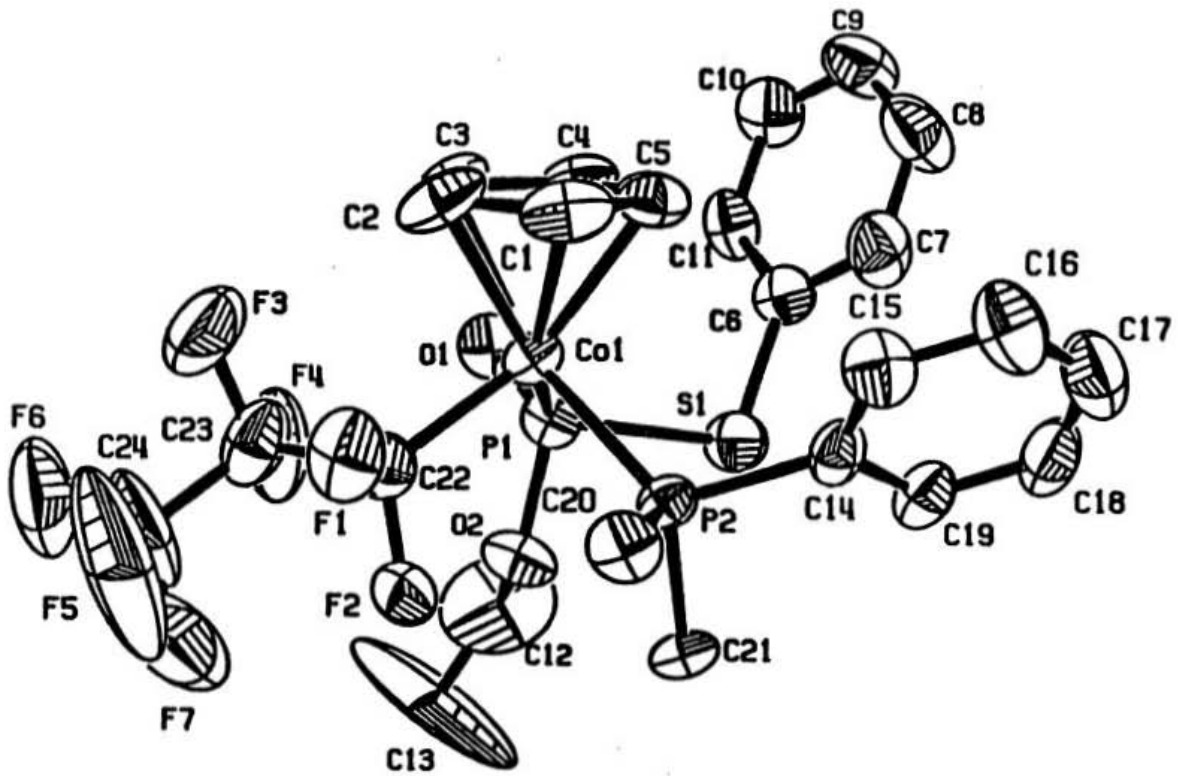

Figure 2.11 Molecular structure of P-thiophenylphosphito Co(III) complex **2-4a**

the X-ray analysis (Figure 2.12). Consideration of the compound as pseudotetrahedral with η^5–Cp occupying one coordination site and use of modified Cahn–Ingold–Prelog (CIP) rules[125,146-148] with the ligand priority series η^5–Cp > P(O)(OEt)(SPh) > $PPhMe_2$ > C_3F_7 for cobalt and Co > SPh > OEt > O for phosphorus specifies the relative configuration of **2-4a** as $R_{Co,}R_P$ / $S_{Co,}S_P$. The relative configuration of the diastereomers **2-4b** was therefore assigned $R_{Co,}S_P$ / $S_{Co,}R_P$.

Table 2.1.1 ^{1}H and ^{31}P NMR data for *P*-phosphito Co(III) complexes[a]: 2-1

compd	δ(OMe)	δ(Cp)	δ(PPhMe_2)	δ(Ph)	^{31}P
2-1a	3.44(d,12.0)	4.87(s)	2.08(d,11.5)	7.79(m), 7.73(m)	25.47(d,96.4) (P(III))
			1.98(d,11.4)	7.51(m), 7.43(m)	106.67(d,109.4) (P(V))
2-1b	3.45(d,12.4)	4.67(s)	2.02(d,12.2)	7.94(m), 7.85(m)	29.02[b] (P(III))
			1.92(d,11.6)	7.52(m), 7.47(m)	109.42[b] (P(V))
2-1c	3.83(d,10.8), 3.73(d,11.1)	5.09		7.73(m), 7.50(m)	104.67(d,122.96) (P(III)
	3.41(d,10.8)			7.33(m)	175.80(d,114.2) (P(V))
2-1d	3.87(d,11.1), 3.73(d,10.5)	4.98		7.75(m), 7.46(m)	111.11(d,117.73) (P(III))
	3.41(d,10.8)			7.37(m)	172.46(d,111.2) (P(V))

[a] ^{1}H (300.1 MHz) NMR chemical shifts are in ppm relative to internal TMS; ^{31}P (121.5 MHz) NMR chemical shifts are in ppm relative to external 85% H_3PO_4; *J* values in Hz are given in parentheses; solvent $CDCl_3$; abbreviations: m = multiplet, s = singlet, d = doublet; [b] coupling not resolved

Table 2.1.2 ^{13}C NMR data for *P*-phosphito Co(III) complexes[a]: 2-1

compd	δ(Cp)	δ(OMe)	δ(Me)	δ(Ph): ipso, ortho, meta, para
2-1a	89.32(d,2.7)	50.66(s)	17.13(d,13.4)	nf, 145.24(d,49.1)
			16.70(d,17.5)	127.64(d,9.8), 130.99(d,12.2), 130.46(d,9.7), 128.93(d,7.9)
				129.72(d,4.7), 130.17(d,2.4)
2-1b	90.06(d,2.3)	49.85(s)	17.89(d,19.4)	144.26(d,50.8), 140.22(d,43.7)
			17.45(d,21.3)	130.69(d,11.5), 130.42(d,7.2), 128.83(d,9.3), 128.12(d,11.3)
				129.99(d,2.3), 129.65(d,3.8)
2-1c	90.28	55.00(d,10.9)		144.48(d,58.3), 136.57(d,58.7)
		54.74(d,10.0)		131.25(d,10.6), 130.58(d,10.0), 127.83(d,12.9), 126.67(d,11.5)
		49.96(d,11.8)		130.93, 129.29
2-1d	89.96	55.44(d,11.6)		143.73(d,58.3), 137.13(d,58.1)
		54.74(d,10.0)		131.25(d,10.6), 130.58(d,10.0), 127.83(d,12.9), 127.67(d,11.5)
		49.96(d,11.8)		131.00, 129.21

[a] ^{13}C (75.5 MHz) NMR chemical shifts are in ppm relative to $CDCl_3$; *J* values in Hz are given in parentheses; abbreviations: d = doublet, nf = not found; perfluoroalkyl carbons were observed at 105 - 140 ppm with very weak intensities.

Table 2.1.3 ^{19}F NMR, IR and physical data for *P*-phosphito Co(III) complexes[a]: 2-1

compd	$\delta(^{19}F)$: C_γ,C_β,C_α	$\gamma_{P=O}$, $\delta_{P\text{-}OC}$, $\delta_{PO\text{-}C}$ (cm^{-1})	mp(°C)	color	anal. calcd. (found) C, H (%)
2-1a	-79.23(s)	1188, 1010, 799	117 - 120	orange	47.12 (47.24), 4.13 (4.10)
	-113.64(s)				
	-65.13(d,266.2), -70.85(d,266.3)				
2-1b	-78.96(s)	1129, 1028, 770	110 - 115	orange	
	-113.08(t,293.3)				
	-67.05(d,246.5), -67.67(d,246.5)				
2-1c	-79.02(d,27.7)	1121, 1008, 745	131 - 138	yellow	44.68 (44.86), 3.91 (4.05)
	-113.39(t,275.8)				
	-64.04(d,267.5), -65.68(d,267.7)				
2-1d	-79.11(d,55.3)	1187, 1011, 749	149 - 151	yellow	
	-114.8(t,92.2)				
	-64.79(d,273.2), -70.17(d,273.2)				

[a] ^{19}F (282.4 MHz) NMR chemical shifts are in ppm relative to $CFCl_3$; solvent = $CDCl_3$; $^2J_{FaFb}$ and $^3J_{FF}$ values in the case of CF_3 in Hz are given in parentheses; all CF_2 peaks show further unsolved splitting by about 5 - 10 Hz due to J_{FF}.

Table 2.1.4 Summary of crystallographic data for *P*-phosphito Co(III) complex 2-1a

Empirical Formula	$C_{23}H_{24}F_7O_2CoP_2$
Formula Weight	586.31
Crystal Colour, Habit	orange, irregular
Crystal Dimensions	0.40 × 0.35 × 0.40 mm
Crystal System	monoclinic
Lattice Type	C-centred
No. of Reflections Used for Unit cell determination (2θ range)	21 (41.3 – 43.4°)
Omega Scan Peak Width at Half-height	0.31°
Lattice Parameters	a = 16.554(3) Å b = 22.694(3) Å c = 14.089(2) Å b = 103.58(2)° V = 5145(1) Å^3
Space Group	C2/c (#15)
Z value	8
D_{calc}	1.514 g/cm^3
F_{000}	2384.00
μ(MoKα)	8.61 cm^{-1}
Diffractometer	Rigaku AFC6S
Radiation	MoKa (l = 0.71069 Å) graphite monochromated
Take-off Angle	6.0°
Detector Aperture	4.5 mm horizontal 3.0 mm vertical
Crystal to Detector Distance	400 mm

Table 2.1.4 cont'd

Voltage, Current	50kV, 30mA
Temperature	26.0°C
Scan Type	ω-2θ
Scan Rate	8.0°/min (in ω) (up to 10 scans)
Scan Width	(1.42 + 0.35 tan θ)°
$2q_{max}$	55.1°
No. of Reflections Measured	Total: 6299
	Unique: 6094 (R_{int} = 0.014)
Corrections	Lorentz-polarization, Abs
	(trans. factors: 0.8285 – 1.0000)
	Secondary Extinction
	(coefficient: 3.26054e-007)
Structure Solution	Direct Methods (SHELXS86)
Refinement	Full-matrix least-squares
Function Minimized	Σ w (|Fo| - |Fc|)^2
Least Squares Weights	$1/\sigma^2(Fo) = 4Fo^2/\sigma^2(Fo^2)$
p-factor	0.0061
Anomalous Dispersion	All non-hydrogen atoms
No. Observations (I>3.00s(I))	4488
No. Variables	317
Reflection/Parameter Ratio	14.16
Residuals: R[a]; Rw[b]	0.034 ; 0.032
Goodness of Fit Indicator	2.01
Max Shift/Error in Final Cycle	0.00
Maximum peak in Final Diff. Map	0.23 $e^-/Å^3$
Minimum peak in Final Diff. Map	-0.22 $e^-/Å^3$

[a] $R = \Sigma \, ||Fo| - |Fc|| / \Sigma \, |Fo|$. [b] $R_w = [(\Sigma \, w \, (|Fo| - |Fc|)^2 / \Sigma \, w \, Fo^2)]^{1/2}$.

Table 2.1.5[a] Selected bond angles (°) for the *P*-phosphito Co(III) complex 2-1a

P(1)–Co(1)–P(2)	93.33(2)
P(1)–Co(1)–C(16)	94.02(6)
Co(1)–P(1)–O(1)	104.34(5)
Co(1)–P(1)–O(2)	118.88(5)
Co(1)–P(1)–C(1)	104.66(6)
O(1)–P(1)–O(2)	109.63(7)
O(1)–P(1)–C(1)	102.26(9)
P(2)–Co(1)–C(16)	91.52(6)
O(2)–P(1)–C(1)	105.78(9)

[a] Angles are in degrees. Estimated standard deviations in the least significant figure are given in parentheses.

Table 2.1.6[a] Selected bond distances (Å) for *P*-phosphito Co(III) complex 2-1a

atom	atom	distance	atom	atom	distance
Co(1)	P(1)	2.2259(6)	F(1)	C(16)	1.403(2)
Co(1)	P(2)	2.2207(6)	F(2)	C(16)	1.386(2)
Co(1)	C(16)	1.968(2)	F(3)	C(17)	1.346(3)
Co(1)	C(19)	2.106(2)	F(4)	C(17)	1.349(2)
Co(1)	C(21)	2.088(2)	Co(1)	C(20)	2.105(2)
Co(1)	C(23)	2.100(3)	Co(1)	C(22)	2.094(3)
C(19)	C(20)	1.388(3)	P(1)	O(1)	1.621(1)
C(19)	C(23)	1.407(3)	P(1)	O(2)	1.493(1)
C(20)	C(21)	1.388(3)	P(1)	C(1)	1.835(2)
C(21)	C(22)	1.384(4)	P(2)	C(8)	1.822(2)
C(22)	C(23)	1.383(3)	P(2)	C(14)	1.817(2)
C(16)	C(17)	1.549(3)	P(2)	C(15)	1.815(2)

[a] distances are in Angstroms. Estimated standard deviations in the least significant figure are given in parentheses.

Table 2.1.7 Atomic coordinates for the *P*-phosphito Co(III) complex 2-1a

atom	X	Y	Z	B(eq)
Co(1)	0.23547(1)	0.08405(1)	0.04827(2)	3.161(5)
P(1)	0.28506(3)	0.08890(2)	0.20923(3)	3.64(1)
P(2)	0.18861(3)	-0.00727(2)	0.05389(3)	3.21(1)
F(1)	0.06259(6)	0.09049(5)	-0.01700(8)	5.18(3)
F(2)	0.10270(6)	0.10725(5)	0.13923(8)	4.73(3)
F(3)	0.09950(8)	0.19561(5)	-0.06198(9)	0.64(4)
F(4)	0.17077(8)	0.21670(5)	0.08385(9)	5.92(3)
F(5)	0.0158(1)	0.26339(6)	0.0245(1)	9.51(5)
F(6)	0.0367(1)	0.21218(7)	0.1549(1)	9.72(6)
F(7)	-0.03751(9)	0.17782(7)	0.0213(1)	9.53(5)
O(1)	0.38197(8)	0.07050(7)	0.22554(9)	5.30(4)
O(2)	0.24513(7)	0.05248(5)	0.27377(8)	3.83(3)
C(1)	0.2922(1)	0.16369(9)	0.2600(1)	5.07(5)
C(2)	0.3558(2)	0.2021(1)	0.2552(2)	7.85(8)
C(3)	0.3582(3)	0.2589(2)	0.2976(2)	10.2(1)
C(4)	0.2974(3)	0.2745(2)	0.3417(3)	10.9(1)
C(5)	0.2352(2)	0.2376(1)	0.3469(2)	8.9(1)
C(6)	0.2311(2)	0.1822(1)	0.3052(2)	6.10(6)
C(7)	0.4270(1)	0.0578(1)	0.3238(2)	8.91(8)
C(8)	0.2725(1)	-0.06080(8)	0.0876(1)	3.56(4)
C(9)	0.3009(1)	-0.09314(8)	0.0185(1)	4.47(5)
C(10)	0.3657(1)	-0.1324(1)	0.0468(2)	5.53(6)
C(11)	0.4032(1)	-0.1401(1)	0.1432(2)	6.28(6)
C(12)	0.3757(2)	-0.1086(1)	0.2123(2)	6.86(7)
C(13)	0.3113(1)	-0.0694(1)	0.1849(1)	5.40(6)
C(14)	0.1263(1)	-0.03356(8)	-0.0622(1)	4.30(5)
C(15)	0.1214(1)	-0.02449(8)	0.1351(1)	4.19(5)
C(16)	0.1266(1)	0.11729(8)	0.0527(1)	3.81(4)
C(17)	0.1074(1)	0.18361(9)	0.0333(2)	4.88(5)
C(18)	0.0288(2)	0.2091(1)	0.0594(2)	6.88(8)
C(19)	0.2334(1)	0.1066(1)	-0.0972(1)	5.09(6)
C(20)	0.2796(1)	0.05551(9)	-0.0725(1)	4.46(5)
C(21)	0.3459(1)	0.0671(1)	0.0059(1)	4.70(5)
C(22)	0.3429(1)	0.1262(1)	0.0287(2)	5.79(6)
C(23)	0.2743(2)	0.15094(9)	-0.0340(2)	6.01(7)

Table 2.2.1 ^{1}H and ^{31}P NMR data for *P*-amidophosphito PNH Co(III) complexes[a]: 2-2

compd	δ(OMe)	δ(NCH_2Me)	δ(NCH_2*Me*)	δ(Cp)	δ(Ph)	δ(NH)[b]	δ(C*H)[c]	δ(OMe)	^{31}P
2-2a	3.44(d,	3.39(m)	1.25(t,7.1)	4.83(s)	7.93(m), 7.67(m)	6.65(dd,	3.65(m)	1.32(dd,	81.93(d,121.9) (P(III))
	11.2)	3.26(m)			7.42(m), 7.27(m)	6.6, 6.0)		6.75,1.1)[d]	89.86(d,121.9) (P(V))
					6.92(m), 6.82(m)				
2-2b	3.51(d,	3.40(m)	1.22(t,6.2)	4.83(s)	7.92(m), 7.45(m)	6.37(dd,	3.65(m)	1.26(d,	77.96(d,122.1) (P(III))
	11.2)	3.27(m)			7.23(m), 7.15(m)	10.6,7.5)		7.1)	87.19(d,122.1) (P(V))
					7.01(m), 6.97(m)				
2-2c	3.41(d,	3.54(m)	1.22(t,7.0)	4.84(s)	7.96(m), 7.84(m)	4.97(dd,	3.93(m)	1.15(d,	71.44(d,125.8) (P(III))
	11.2)	3.42(m)			7.48(m)	15.5,9.5)		6.7)	83.00(d,125.8) (P(V))
					7.26 - 6.9(m)				
2-2d	3.51(d,	3.59(m)	1.25(t,7.0)	4.86(s)	8.20(m), 7.69(m)	4.87[e]	4.22(m)	1.07(d,	72.02(d,117.6) (P(III))
	11.2)	3.43(m)			7.52(m), 7.14(m)			6.7)	82.09(d,117.6) (P(V))
					7.14(m), 7.07(m)				

[a] ^{1}H (300.1 MHz) NMR chemical shifts are in ppm relative to internal TMS; ^{31}P (121.5 MHz) NMR chemical shifts are in ppm relative to external 85% H_3PO_4; *J* values in Hz are given in parentheses; solvent $CDCl_3$; abbreviations: m = multiplet, s = singlet, d = doublet; [b] doublet of doublets ($^{2}J_{PH}$, $^{3}J_{C*HH}$); [c] multiplet ($^{3}J_{PH}$, $^{3}J_{NHH}$, $^{3}J_{HH}$); [d] doublet of doublet ($^{3}J_{C*HH}$, $^{4}J_{PH}$); [e] overlapping with Cp

Table 2.2.2 ^{13}C NMR data for *P*-amidophosphito PNH Co(III) complexes[a]: 2-2

compd	δ(PPh): ipso,ortho, meta,para	δ(C*-Ph): ipso,ortho, meta,para	δ(N*CH*$_2$ Me)	δ(NCH$_2$ *Me*)	δ(Cp)	δ(OMe)	δ(C*H)	δ(C*Me)
2-2a	132.70(d,55.93), nf 134.98(d,9.6), 131.52(d,10.0) 127.53(d,10.0),127.11(d,10.4) 130.93(d,2.8), 129.27(d,2.7)	47.51 128.30 126.04 125.47	41.70(d, 4.8)	14.57	87.82(ps, 2.5)[c]	54.62(d, 7.9)	49.90(d, 10.7)	26.62(d, 9.9)
2-2b	137.36(d,40.7),133.62(d,61.3) 133.81(d,9.4), 132.12(d,9.8) 127.84(d,9.3), 127.50(d,10.5) 130.52(d,2.7), 129.95(d,2.9)	146.45(d,3.5) 128.31 125.84 125.51	41.71(d, 4.9)[b]	14.41	87.97(ps, 2.5)[c]	53.69(d, 11.7)	50.16(d, 10.8)	27.09(d, 4.5)
2-2c	136.17(d,53.7), 135.39(d,53.6) 133.66(d,8.9), 133.30(d,10.6) 127.62(d,10.6), 127.45(d,11.4) 130.55(d,3.1), 130.15(d,2.9)	145.63(d,3.7) 128.04 126.14 125.77	40.73(d, 5.1)	14.61	89.44(ps, 2.5)	54.04(d, 10.9)	49.19(d, 12.3)	26.40(d, 4.2)

Table 2.2.2 cont'd

2-2d	nf, nf	nf	40.86(d,	14.69	89.34(ps,	53.68(d,	49.10(d,	27.18(d,
	133.39(d,9.5), 132.19(d,10.3)	128.79	4.6)		2.5)	10.9)	12.3)	4.3)
	128.25(d,10.2),127.10(d,9.9)	126.08						
	130.57(d,2.5), 130.24(d,2.7)	123.59						

[a] ^{13}C (75.5 MHz) NMR chemical shifts are in ppm relative to $CDCl_3$; *J* values in Hz are given in parentheses; [b] temperature independence to −90 °C; [c] abbreviations: d = doublet, nf = not found, ps = pesudo triplet.

Table 2.2.3 IR and physical data for *P*-amidophosphito PNH Co(III) complexes: 2-2

compd	$\gamma_{P=O}$, $\delta_{P\text{-}OC}$, $\delta_{PO\text{-}C}$ (cm^{-1})	mp(°C)	color	anal. calcd. (found) C, H, N (%)
2-2a	1130, 1022, 697	125.2 - 125.8	dark green	
2-2b	1132, 1020, 701	159.5 - 160.0	dark green	51.04 (49.99), 5.42 (5.36), 3.97(3.79)

Table 2.3.1 ^{1}H and ^{31}P NMR data for *P*-amidophosphito $PPhMe_2$ Co(III) complexes[a]: 2-3

compd	δ(OMe)	δ(NCH_2Me)	δ(NCH_2Me)	δ(Cp)	δ(Ph)	δ($PPhMe_2$)	^{31}P
2-3a	3.51(d, 11.9)	3.20(m) 2.95(m)	1.21(t, 7.4)	4.86(s)	7.80(m), 7.76(m) 7.74(m), 7.47(m) 7.45(m)	2.05(d,10.1) 1.88(d,12.1)	26.57(d,167.0) (P(III)) 88.39(d,100.0), (P(V))
2-3b	3.49(d, 10.1)	3.19(m) 2.93(m)	1.17(t, 7.3)	4.85(s)	7.79(m), 7.76(m) 7.73(m), 7.45(m) 7.43(m)	2.03(d,10.5) 1.87(d,8.4)	25.49(d,102.4) (P(III)) 101.75(d,98.9) (P(V))

[a] ^{1}H (300.1 MHz) NMR chemical shifts are in ppm relative to internal TMS; ^{31}P (121.5 MHz) NMR chemical shifts are in ppm relative to external 85% H_3PO_4; *J* values in Hz are given in parentheses; solvent $CDCl_3$; abbreviations: m = multiplet, s = singlet, d = doublet.

Table 2.3.2 ^{13}C NMR data for *P*-amidophosphito $PPhMe_2$ Co(III) complexes[a]: 2-3

compd	δ(OMe)	δ(NCH_2Me)	δ(Cp)	δ(NCH_2Me)	δ(Ph): ipso,ortho, meta,para	δ($PPhMe_2$)
2-3a	49.37(d,10.7)	41.46(d,4.2)	88.50(ps,2.4)	16.01	126.40(d,12.7) 128.82(d,9.0) 129.85(d,4.7) 130.58(d,9.6)	17.71(d,14.2) 17.18(d,17.0)
2-3b	39.48(d,7.9)	39.90(d,4.0)	90.42(ps,4.9)	17.75	126.42(d,10.3) 128.92(d,11.5) 131.82(d,5.0) 129.82(d,8.9)	15.12(d,14.8) 14.34(d.15.1)

[a] ^{13}C (75.5 MHz) NMR chemical shifts are in ppm relative to $CDCl_3$; *J* values in Hz are given in parentheses; abbreviations: d = doublet, ps = pesudo triplet; perfluoroalkyl carbons distributed in the chemical shift range of 105 - 140 ppm with very weak intensities.

Table 2.3.3 ^{19}F NMR, IR and physical data for *P*-amidophosphito $PPhMe_2$ Co(III) complexes[a]: 2-3

compd	$\delta(^{19}F)$: $C_\gamma, C_\beta, C_\alpha$	$\gamma_{P=O}$, $\delta_{P\text{-}OC}$, $\delta_{PO\text{-}C}$ (cm^{-1})	mp(°C)	color	anal. calcd. (found): C, H, N (%)
2-3a	-78.71(s)	1192, 1034, 724	99.6 - 101.2[c]	orange	43.41 (45.15)[b]
	-114.27(s)				5.03 (5.91)
	-66.66(d,274.3), -71.66(d,274.3)				2.41 (2.41)
2-3b	-78.81(s)	1186, 1025, 717	111.3 - 112.1	orange	
	-114.64(t,324)				
	-63.73(d,268.2), -70.92(d,279.4)				

[a] ^{19}F (282.4 MHz) NMR chemical shifts are in ppm relative to $CFCl_3$; solvent = $CDCl_3$; $^2J_{FaFb}$ and $^3J_{FF}$ values in the case of CF_3 in Hz are given in parentheses; all CF_2 peaks show further unsolved splitting by about 5 - 10 Hz due to J_{FF}; [b] viscous oil which solidified over time; [c] mp was obtained from the solid.

Table 2.4.1 ^{1}H and ^{31}P NMR data for *P*-thiophenylphosphito Co(III) complexes[a]: 2-4

compd	δ(SPh)	δ(OCH_2Me)	δ(OCH_2Me)	δ(Cp)	δ(P*Ph*Me_2)	δ(PPhMe_2)	^{31}P
2-4a	7.29(m)	3.92(m)	1.08(t,7.5)	4.89(s)	7.51(m)	1.95(t,11.3)[b]	23.54(d,101.5) (P(III))
	7.66(m)	4.02(m)			7.78(m)		108.50(d,109.5), (P(V))
	7.67(m)				7.80(m)		
	7.69(m)				7.83(m)		
2-4b	7.31(m)	4.01(m)	1.15(t,7.7)	4.89(s)	7.47(m)	1.97(d,2.7)	23.84(d,117.5) (P(III))
	7.33(m)	4.09(m)			7.83(m)	1.93(d,2.5)	110.00(d,105.9) (P(V))
	7.70(m)				7.86(m)		
	7.73(m)				7.89(m)		

[a] ^{1}H (300.1 MHz) NMR chemical shifts are in ppm relative to internal TMS; ^{31}P (121.5 MHz) NMR chemical shifts are in ppm relative to external 85% H_3PO_4; *J* values in Hz are given in parentheses; solvent $CDCl_3$; abbreviations: m = multiplet, s = singlet, d = doublet; [b]overlapped

Table 2.4.2 ^{13}C NMR data for *P*-thiophenylphosphito Co(III) complexes[a]: 2-4

compd	δ(SPh):ispo,ortho meta,para	δ(OCH_2Me)	δ(OCH_2Me)	δ(Cp)	δ(P*Ph*Me_2)	δ(PPhMe_2)
2-4a	139.95(d,46.1)	60.80(d,14.8)	16.41(d,8.1)	90.26(ps,2.8)	nf	18.44(d,29.2)
	127.76(d,1.6)				128.90(d,9.7)	16.78(d,30.3)
	128.82(d,1.6)				130.42(d,9.7)	
	135.28(d,1.0)				133.92(d,4.8)	
2-4b	140.07(d,50.7)	60.80(d,11.5)	16.48(t,9.0)	90.88(ps,2.1)	nf	17.91(d,27.8)
	129.02(d,2.1)				129.17(d,9.5)	17.03(d,31.2)
	127.70(d,1.5)				130.37(d,8.7)	
	135.04(d,1.5)				134.73(d,4.3)	

[a] ^{13}C (75.5 MHz) NMR chemical shifts are in ppm relative to $CDCl_3$; *J* values in Hz are given in parentheses; abbreviations: d = doublet, ps = pesudo triplet, nf = not found; perfluoroalkyl carbons distributed in the chemical shift range of 105 - 140 ppm with very weak intensities.

Table 2.4.3 ^{19}F NMR, IR and physical data for *P*-thiophenylphosphito Co(III) complexes[a]: 2-4

compd	$\delta(^{19}F)$: C_γ,C_β,C_α	$\gamma_{P=O}$, $\delta_{P\text{-}OC}$, $\delta_{PO\text{-}C}$ (cm^{-1})	mp(°C)	color	anal. calcd. (found): C, H (%)
2-4a	-79.12(s) -114.12(q,718.8) -57.34(d,255.0), -77.36(d,277.4)	1126, 1081, 750	125.6 - 126.1	orange	45.61 (44.49), 4.27 (4.15)
2-4b	-79.00(s) -114.12(q,273.9) -62.92(d,274.9), -72.63(d,267.2)	1132, 1086, 750	116.5 - 117.1	orange	

[a] ^{19}F (282.4 MHz) NMR chemical shifts are in ppm relative to $CFCl_3$; solvent = $CDCl_3$; $^2J_{FaFb}$ and $^3J_{FF}$ values in the case of CF_3 in Hz are given in parentheses; all CF_2 peaks show further unsolved splitting by about 5 - 10 Hz due to J_{FF}.

Table 2.4.4 Summary of crystallographic data for *P*-thiophenylphosphito Co(III) complex 2-4a

Empirical Formula	$C_{24}H_{26}O_2P_2SCoF_7$
Formula Weight	632.40
Crystal Color, Habit	orange, irregular
Crystal Dimensions	0.25 × 0.10 × 0.35 mm
Crystal System	monoclinic
Lattice Type	Primitive
No. of Reflections Used for Unit	
Cell Determination (2 θ range)	22 (20.6 – 29.7°)
Omega Scan Peak Width	
at Half-height	0.33°
Lattice Parameters	a = 12.701(3) Å
	b = 15.502(6) Å
	c = 14.339(4) Å
	b = 102.40(2)°
	V = 2757(1) Å^3
Space Group	$P2_1/n$ (#14)
Z value	4
D_{calc}	1.523 g/cm^3
F_{000}	1288.00
μ(MoKα)	8.82 cm^{-1}
Diffractometer	Rigaku AFC6S
Radiation	MoKα (l = 0.71069 Å)
	graphite monochromated
Take-off Angle	6.0°
Detector Aperture	4.5 mm horizontal
	3.0 mm vertical
Crystal to Detector Distance	400 mm
Voltage, Current	50kV, 30mA

Table 2.4.4 cont'd

Temperature	26.0 °C
Scan Type	$\omega-2\theta$
Scan Rate	4.0°/min (in ω) (up to 10 scans)
Scan Width	$(1.10 + 0.35 \tan \theta)°$
$2q_{max}$	55.1°
No. of Reflections Measured	Total: 6900
	Unique: 6612 (R_{int} = 0.063)
Corrections	Lorentz-polarization
	Secondary Extinction
	(coefficient: 6.66080e-008)
Structure Solution	Direct Methods
Refinement	Full-matrix least-squares
Function Minimized	Σ w (|Fo| - |Fc|)^2
Least Squares Weights	$1/\sigma^2(Fo) = 4Fo^2/\sigma^2(Fo^2)$
p-factor	0.0045
Anomalous Dispersion	All non-hydrogen atoms
No. Observations (I>2.00s(I))	3360
No. Variables	335
Reflection/Parameter Ratio	10.03
Residuals: R[a]; Rw[b]	0.059 ; 0.052
Goodness of Fit Indicator	1.91
Max Shift/Error in Final Cycle	0.00
Maximum peak in Final Diff. Map	0.70 e$^-$/Å^3
Minimum peak in Final Diff. Map	-0.54 e$^-$/Å3

[a,b] same as Table 2.1.4

Table 2.4.5[a] Selected bond angles (°) for the *P*-thiophenylphosphito Co(III) complex 2-4a

P(1)–Co(1)–P(2)	99.26(7)
P(2)–Co(1)–C(22)	90.5(2)
P(1)–Co(1)–C(22)	95.3(2)
Co(1)–P(1)–S(1)	112.56(9)
Co(1)–P(1)–O(1)	116.1(2)
Co(1)–P(1)–O(2)	110.4(2)
S(1)–P(1)–O(1)	108.0(2)
S(1)–P(1)–O(2)	94.9(2)
O(1)–P(1)–O(2)	112.9(3)

[a] Angles are in degrees. Estimated standard deviations in the least significant figure are given in parentheses.

Table 2.4.6[a] Selected bond distances (Å) for the *P*-thiophenylphosphtio Co(III) complex 2-4a

atom	atom	distance	atom	atom	distance
Co(1)	P(1)	2.212(2)	S(1)	P(1)	2.174(3)
Co(1)	P(2)	2.241(2)	S(1)	C(6)	1.773(7)
Co(1)	C(1)	2.133(6)	P(1)	O(1)	1.490(4)
Co(1)	C(2)	2.105(6)	P(1)	O(2)	1.604(4)
Co(1)	C(3)	2.069(6)	F(1)	C(22)	1.389(7)
Co(1)	C(4)	2.104(6)	F(2)	C(22)	1.382(7)
Co(1)	C(5)	2.119(7)	F(3)	C(23)	1.320(9)
Co(1)	C(22)	1.972(7)	C(22)	C(23)	1.558(9)

[a] Distances are in Angstroms. Estimated standard deviations in the least significant figure are given in parentheses.

Table 2.4.7 Atomic coordinates for the *P*-thiophenylphosphito Co(III) complex 2-4a

atom	X	Y	Z	B(eq)
Co(1)	1.24445(5)	0.26304(4)	0.70837(4)	2.72(1)
S(1)	1.0100(1)	0.13383(9)	0.60004(9)	3.87(3)
P(1)	1.1849(1)	0.13976(7)	0.63891(9)	2.91(2)
P(2)	1.1477(1)	0.35491(7)	0.60308(8)	2.82(2)
F(1)	1.4191(2)	0.3518(2)	0.6701(2)	5.19(8)
F(2)	1.3407(2)	0.2780(2)	0.5464(2)	4.45(7)
F(3)	1.5137(3)	0.2106(3)	0.7549(3)	8.5(1)
F(4)	1.4261(2)	0.1280(2)	0.6472(3)	7.0(1)
F(5)	1.5834(4)	0.2924(3)	0.6019(7)	17.9(3)
F(6)	1.6299(3)	0.1636(3)	0.6370(4)	10.1(1)
F(7)	1.5131(5)	0.1959(6)	0.5179(5)	17.2(3)
O(1)	1.2243(2)	0.0598(2)	0.6929(2)	3.68(8)
O(2)	1.2009(3)	0.1379(2)	0.5309(2)	3.98(7)
C(1)	1.2551(5)	0.3508(3)	0.8245(3)	4.3(1)
C(2)	1.3462(4)	0.2983(3)	0.8389(3)	4.7(1)
C(3)	1.3154(4)	0.2114(3)	0.8400(3)	4.30(9)
C(4)	1.2026(4)	0.2099(3)	0.8305(3)	3.76(9)
C(5)	1.1649(4)	0.2950(3)	0.8193(3)	3.9(1)
C(6)	0.9721(4)	0.1177(3)	0.7108(3)	3.5(1)
C(7)	0.9115(4)	0.1792(3)	0.7452(4)	4.9(1)
C(8)	0.8822(5)	0.1675(4)	0.8307(4)	6.1(2)
C(9)	0.9125(5)	0.0951(4)	0.8840(4)	5.3(2)
C(10)	0.9704(4)	0.0326(3)	0.8502(4)	4.7(1)
C(11)	1.0000(4)	0.0421(3)	0.7633(4)	3.9(1)
C(12)	1.1919(7)	0.0573(4)	0.4778(6)	9.5(2)
C(13)	1.244(1)	0.0593(8)	0.4042(8)	20.0(5)
C(14)	1.0192(4)	0.3907(3)	0.6286(3)	3.25(9)
C(15)	1.0175(4)	0.4547(3)	0.6962(4)	4.6(1)
C(16)	0.9208(5)	0.4806(4)	0.7168(5)	5.8(2)
C(17)	0.8261(5)	0.4437(4)	0.6679(5)	5.7(2)
C(18)	0.8267(4)	0.3823(4)	0.6004(4)	4.9(1)
C(19)	0.9230(4)	0.3550(3)	0.5804(3)	3.8(1)
C(20)	1.2157(4)	0.4573(3)	0.5955(4)	3.8(1)
C(21)	1.1086(4)	0.3240(3)	0.4776(3)	4.0(1)
C(22)	1.3671(4)	0.2737(3)	0.6449(3)	3.68(9)
C(23)	1.4624(4)	0.2083(4)	0.6646(4)	5.1(1)
C(24)	1.5508(7)	0.2188(6)	0.6129(8)	10.0(2)

2.4 Summary

Four trivalent phosphorus esters, $P(OEt)_2Cl$, $PPh(OMe)_2$, $P(NEt_2)(OMe)_2$ and $P(OEt)_2(SPh)$ have been used in the transition-metal-mediated (TMM) Arbuzov reaction for synthesis of chiral pentavalent phosphorus derivatives. $P(OEt)_2Cl$ does not undergo the Arbuzov reaction because low electron density on its phosphorus center prevents coordination to cobalt. The other three phosphonites react with Co(III) complexes to give *P*-phosphito Co(III) compounds containing phosphorus and cobalt chiral centers. Diastereomers have been separated via chromatography and characterized. The *P*-phosphito Co(III) diastereomers are configurationally stable in the solid state and in solution.

2.4 Experimental Section

2.4.1 Reagents and Methods

Unless specially noted, all manipulations were performed under a dry nitrogen atmosphere using standard Schlenk techniques. Nitrogen was purified through a series of columns containing DEOX (Alfa) catalyst heated to 120°C, granular P_4O_{10} and activated 4Å molecular sieves. Reactions were monitored by analytical thick-layer chromatography (precoated TLC plates, silica gel F-24, Merck). Chromatographic separations were carried out using a Chromatotron (Harrison Associates) with 1-, 2-mm or 4-mm thickness silica gel 60 PF-254 (Merck) adsorbent. NMR spectra were recorded on a General Electric GN300-NB spectrometer. Solution IR spectra were collected on a Mattson Polaris FTIR spectrometer. Mass spectra were determined under 70 ev on a V. G. Micromass 7070HS using monoisotopic masses. Melting points were determined in sealed capillaries using a Büchi SMP-20 apparatus and are uncorrected. Benzene, THF and diethyl ether were distilled from blue solutions of sodium benzophenone ketyl. Toluene was dried by distillation from potassium metal. Acetone and ethyl acetate were distilled from activated 4Å molecular sieves. Methylene chloride was distilled under nitrogen from CaH_2. Methanol was freshly distilled from *in situ* prepared sodium methoxide before use. Spectral grade

chloroform was used as received. Triethylamine was refluxed and distilled from solid KOH. Thiophenol was distilled before use. $PPhMe_2$ and $PPh(OMe)_2$ were purchased from Aldrich and were used as received.

2.4.2 Crystal Structure Determination

Single crystal data was collected at a temperature of 26±1 °C on a Rigaku AFC6S diffractometer with graphite-monochromated Mo Kα radiation (λ = 0.71069 Å) and a 2 kW sealed tube generator using the ω – 2θ scan technique to a maximum 2θ value of 50.1 °. Cell constants and an orientation matrix for data collections were obtained from a least-squares refinement using the setting of 21 (**2-1a**) or 22 (**2-4a**) carefully centered reflections in the range 41.27° < 2θ < 43.38° (**2-1a**) or 20.57° < 2θ < 29.71° (**2-4a**) and are given in Table 2.1.4 and Table 2.4.4. The space group C2/c (No. 15) (**2-1a**) or $P2_1/n$ (No. 14) (**2-4a**) was determined on the basis of systematic absences (hkl: h+k ≠ 2n and h0l: l ≠ 2n (**2-1a**) or h0l: h+l ≠ 2n and 0k0: k ≠ 2n) on a statistical analysis of intensity distribution and on the successful solution and refinement of the structure. ω scans of several intense reflections, made prior to data collection, had an average width at half-height of 0.31° (**2-1a**)or 0.33° (**2-4a**) with a takeoff angle of 6.0°. Scans of (1.42 + 0.35 tanθ)° (**2-1a**) or (1.10 + 0.35 tanθ)° (**2-4a**) were made at a speed of 8.0°/min (in ω) (**2-1a**) or 4.0°/min (in ω) (**2-**

4a). Weak reflections ($I < 10.0\ \sigma\ (I)$) were rescanned (maxima of 10 scans), and the counts were accumulated to ensure good counting statistics. Stationary background counts were recorded on each side of the reflection. The ratio of peak counting time to background counting time was 2:1. The diameter of the incident beam collimator was 1.0 mm, and the crystal to detector distance was 400 mm. The intensity of three representative reflections, which were measured after every 150 reflections, remained constant throughout data collection, indicating crystal and electronic stability, hence no decay correction was applied. The absorption coefficient for MoKα is 8.6 cm^{-1} (**2-1a**) or 8.8 cm^{-1} (**2-4a**). An empirical absorption correction, based on azimuthal scans of several reflections, was applied which resulted in transmission factors ranging from 0.83 to 1.00 (**2-1a**). The data were corrected for Lorentz and polarization effects. A correction for secondary extinction was applied (coefficient $= 3.26054 \times 10^{-7}$ (**2-1a**) or 6.66080×10^{-8} (**2-4a**)). The structure was solved by direct methods[157] and expanded using Fourier techniques.[158] The non-hydrogen atoms were refined anisotropically. Hydrogen atoms were included but not refined. All calculations were performed using the TEXSAN crystallographic software package of Molecular Structure Corporation.

2.4.3 Synthesis of Starting Materials 1, 9

2.4.3.1 Synthesis of Starting Material 1: $(\eta^5\text{-}C_5H_5)Co(C_3F_7)(PPhMe_2)(I)$

Starting material **1** was prepared from the reaction between $PPhMe_2$ and $(\eta^5\text{-}C_5H_5)Co(C_3F_7)(I)(CO)$ in benzene at ambient temperature in 92.9% yield by the literature route.[145]

2.4.3.2 Synthesis of Starting Material 9: $(\eta^5\text{-}C_5H_5)Co(PNH)(I)_2$

2.4.3.2.1. Synthesis of PNH (PNH = (S_C)-(−)-$PPh_2NHCH(Me)Ph$)

PNH was prepared from the reaction between (S_C)-(−)-$NH_2CH(Me)Ph$ and PPh_2Cl in 70.9% yield by the literature method.[125]

2.4.3.2.2 Synthesis of $(\eta^5\text{-}C_5H_5)Co(PNH)(I)_2$[125]

The purple starting material **9**, $(\eta^5\text{-}C_5H_5)Co(PNH)(I)_2$, was prepared from the reaction of $(\eta^5\text{-}C_5H_5)Co(I)_2(CO)$ with PNH at ambient temperature in 74.1% yield by the literature route.[125]

2.4.4 Synthesis of *P*, *Co*-chiral Co(III) Complexes

2.4.4.1 Synthesis of *P*-phosphito Co(III) Complexes: 2-1

A 0.2730 g (1.607 mmol) amount of $PPh(OMe)_2$ was added, with stirring, to

a deep brown solution of 0.9000 g of **1** (1.613 mmol) in 50 mL of acetone. The mixture was refluxed overnight and the color changed to red. Volatiles were moved at aspirator followed oil pump vacuum to leave a red residue, which was separated without protection from air by radial thick layer chromatography on 2-mm silica gel plates. Elution with 1:4 ethyl acetate / hexane separated, in the order of decreasing R_f values, greenish brown starting material (65.4 mg, 7.3%), orange compound **2-1a** (53.23 mg, 59.6%) and orange compound **2-1b** (20.85 mg, 23.8%). After **2-1a** and **2-1b** were collected, the eluent was changed to acetone and, in order of decreasing R_f values, yellow compound **2-1c** (7.1 mg, 7.7%) and yellow compound **2-1d** (4.2 mg, 4.5%) were eluted.

Compounds **2-1c** and **2-1d** were also similarly prepared from reaction of $(\eta^5\text{-}C_5H_5)Co(C_3F_7)(PPh(OMe)_2)(I)$, which was prepared in the same way as discussed in 2.4.2.1, with $PPh(OMe)_2$ at ambient temperature for 2 hours. Acetone was used as eluent for chromatographic separation.

2.4.4.2 Synthesis of *P*-amidophosphito Co(III) Complexes

2.4.4.2.1. Synthesis of $P(OMe)_2(NEt_2)$

The amidophosphite $Et_2NP(OMe)_2$, bp 29.1 - 31.3 °C (2.5×10^{-4} mmHg), was first prepared in low yield by reacting Et_2NPCl_2, prepared from PCl_3 and Et_2NH in

Et_2O, with MeOH in Et_3N according to the literature method for $(Me_2N)P(OMe)_2$.[151]

Better yields were obtained by reaction of Et_2NPCl_2 with MeONa in MeOH. The solution turned cloudy after stirring overnight at room temperature. After filtration, the MeOH was removed at aspirator pressure. Water was added and Et_2O was used to extract the amidophosphite. The ether extracts were washed with saturated NaCl solution and dried over $CaSO_4$. Removal of Et_2O afforded the product, which was used without further purification, in 63.0 % yield.

2.4.4.2.2. Synthesis of $(\eta^5\text{-}C_5H_5)Co(PNH)(I)(P(O)(OMe)(NEt_2))$: ***2-2***

Complexes **2-2a** - **2-2d** were prepared by reacting 0.3340 g (0.4889 mmol) starting material **9** with 0.0808 g $(NEt_2)P(OMe)_2$ (0.4891 mmol) in benzene at ambient temperature. Separation of the crude product via chromatography with 5:1 benzene / ethyl acetate as the eluent, according to the literature method, gave products **2-2a – 2-2d**.[125]

2.4.4.2.3. Synthesis of $(\eta^5\text{-}C_5H_5)Co(C_3F_7)(PPhMe_2)(P(O)(OMe)(NEt_2))$:***2-3***

A 88.8 mg (0.538 mmol) amount of $(NEt_2)P(OMe)_2$ was added to a greenish brown solution of 0.3000 g starting material **1** (0.5375 mmol) in benzene at ambient temperature. The mixture was refluxed for overnight to give a brown solution.

Volatiles were removed at aspirator and then oil pump vacuum to give a black residue which was subsequently purified by a 2-mm radial thick layer chromatography using 6:1 ethyl acetate / benzene as the eluent. In the order of decreasing R_f values, greenish brown starting material **1** (187.9 mg, 62.6%), orange compound **2-3a** (27.9 mg, 23.9%) and orange compound **2-3b** (8.4 mg, 7.2%) were respectively obtained. MS: $(\eta^5\text{-}C_5H_5)Co(C_3F_7)(PPhMe_2)(P(O)(OMe)(NEt_2))^{+\cdot}$ (M/Z = 581.97), $(\eta^5\text{-}C_5H_5)Co(C_3F_7)(PPhMe_2)^{+\cdot}$ (M/Z = 430.92), $(\eta^5\text{-}C_5H_5)Co(C_3F_7)^{+\cdot}$ (M/Z = 292.99), $C_3F_7^{+\cdot}$ (M/Z = 168.93), $P(O)(OMe)(NEt_2)^{+\cdot}$ (M/Z = 149.98), $PPhMe_2^{+\cdot}$ (M/Z = 138.04), $P(O)(NEt_2)^{+\cdot}$ (M/Z = 119.00), $P(O)(OMe)^{+\cdot}$ (M/Z = 78.01), $Cp^{+\cdot}$ (M/Z = 65.07).

2.4.5 Synthesis of *P*-thiophenylphosphito Co(III) Complexes

2.4.5.1. Synthesis of $P(SPh)(OEt)_2$

A 7.175 g (0.04583 mol) amount of $P(OEt)_2Cl$ was slowly added with vigorous stirring to a solution of 5.049 g PhSH (0.04583 mol) and 4.6376 g Et_3N (0.04583 mol) at ambient temperature. Stirring the mixture for 20 minutes resulted in a white cloudy solution. The precipitate was filtrated with N_2 protection giving a clear, colorless filtrate. The crude diethyl thiophenylphosphite was purified by distillation at 165 – 167 °C (5.0 mmHg) with 84.7 % yield. ^1H NMR ($CDCl_3$): 1.32 ppm (t, 6.1 Hz), 4.04 ppm (dq, 10.0 Hz), 7.32 ppm (m), 7.49 ppm (m), 7.52 ppm (m).

2.4.5.2. Synthesis of *P*-thiophenylphosphito Co(III) Complexes: 2-4

A 91.2 mg (0.3961 mmol) amount of $P(OEt)_2(SPh)$ was added slowly via syringe with stirring to a greenish brown solution of 0.1700 g **1** in 50 mL benzene at ambient temperature. Volatiles were removed at aspirator and then oil pump vacuum to give a brown residue after refluxing for 20 hours. The crude product was separated by 2 mm radial thick chromatography without protection from oxygen using acetone / hexane (1:4) as eluent. In the order of decreasing R_f values, brown starting material **1** (84.8 mg, 49.9%), orange compound **2-4a** (23.5 mg, 36.6%) and orange compound **2-4b** (10.7 mg, 14.8%) were obtained. MS: $(\eta^5\text{-}C_5H_5)Co(C_3F_7)(PPhMe_2)(P(O)(OEt))^{+\cdot}$ (M/Z = 523.08), $(\eta^5\text{-}C_5H_5)Co(C_3F_7)^{+\cdot}$ (M/Z = 293.16), $(\eta^5\text{-}C_5H_5)Co(PPhMe_2)^{+\cdot}$ (M/Z = 262.04), $P(O)(SPh)(OEt)^{+\cdot}$ (M/Z = 201.01), $C_3F_7^{+\cdot}$ (M/Z = 168.99), $P(O)(SPh)^{+\cdot}$ (M/Z = 156.03), $PPhMe_2^{+\cdot}$ (M/Z = 138.04), $SPh^{+\cdot}$ (M/Z = 108.98), $P(O)(OEt)^{+\cdot}$ (M/Z = 91.99), $Cp^{+\cdot}$ (M/Z = 65.09).

Chapter 3

Reactivity of *Co*- and *P*-Chiral Co(III) Complexes and Evidence for C–F Bond Activation

3.1 Introduction

Enantioselective synthesis of phosphorus-chiral compounds has attracted considerable research effort due both to the intrinsic interest in the preparation and stereochemistry of optical phosphorus-chiral systems, and to the rapidly growing utility of such compounds.[2,6,21] Substantial progress has been made in the preparation of homochiral organophosphorus compounds.[2,21,59] One successful approach is the transformation of the resolved phosphorus-chiral compounds into other forms via stereospecific reactions. Many substitutions of phosphorus compounds are known to be stereospecific or highly stereoselective under at least some conditions.[2,59] It is often possible to convert a readily available homochiral phosphorus compound into a desirable target molecule by a series of stereospecific steps.

A common method involves use of stereospecific alkylation of phosphinate alkoxy groups. Nudelmen and Mislow demonstrated that diastereomeric menthyl phenyl phosphinates could react with Grignard reagents to give phosphine oxides

R = C_3H_7, β–naphthyl, $C_6H_5CH_2$,

Figure 3.1 Substitution of alkoxy group in phosphinates via organometallic reagents

(Figure 3.1).[21,78-80] This work established that substitution of menthyl phosphinates with organometallic reagents occurs with inversion of configuration at phosphorus. Although, in general, reactions of this type must be carried out with an excess of a Grignard reagent under somewhat stringent conditions and are sensitive to variation of the phosphorus substituents, the method has become of general use due to its flexibility and the high level of stereospecificity.

It is also possible to exchange an alkoxy group via an electrophilic path (Figure 3.2).[2] Many chiral phosphinates are potentially available from menthylphosphinates and phosphinothiolates via the reaction shown in Figure 3.2.

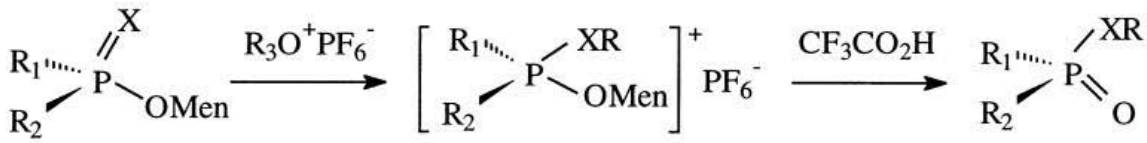

X = S, O
R = CH_3, C_2H_5

Figure 3.2 Exchange of alkoxy group via an ionic intermediate

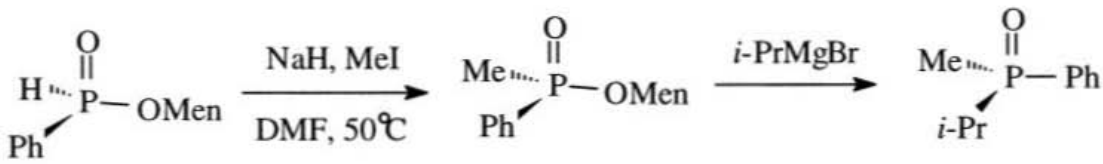

Figure 3.3 Multiple-step substitution of organophosphorus compounds

The preferred counterion is PF_6^-, and the configuration of the product is inverted compared to the starting material.[132,133]

Phosphinate substituents other than alkoxy were rarely tested. Mislow reported a stereospecific alkylation of a hydride with retention of the configuration of the phosphorus centre (Figure 3.3).[134,135] Although stereochemically reliable, the method has found little use probably because the separation of the diastereomerically pure precursors has proven difficult.[59] Moriyama and Bentrude[136] were able to convert enantiomerically pure thiophosphonates into phosphine oxides via their selective

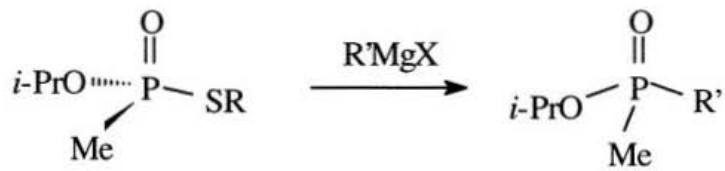

A. R = $C_2H_4OCH_2CH_2OEt$, R' = Ph, X = Br

B. R = Me, R' = $PhCH_2$, X = Cl

Figure 3.4 Substitution of a thioester in organophosphorus compounds

displacements of thiol ester (Figure 3.4 for R´≠H). The stereochemistry varies with the functionality of thiol ester. For example, the reaction of phosphorothiolate **A** in Figure 3.4, containing a chelating ester residue, with PhMgBr was found to occur with predominant inversion of configuration at phosphorus. However, the reaction of *S*-methyl ester **B** (Figure 3.4) with $PhCH_2MgCl$ yielded the pertinent phosphinate with predominant retention of configuration.

Multiple-step substitutions have also been used. Some examples used combinations of the substitutions discussed above (Figure 3.3). Mislow[134] also reported a transformation of the alkoxy function of an organophosphorus compound via chlorination by phosphorus pentachloride followed by subsequent replacement of the chloride by nucleophiles (Figure 1.19).

A report of a substitution on an inorganometallic phosphorus compound was published by Nakazawa.[111] Reaction of an iron *P*-amidophosphito complex with suitable nucleophiles, such as organometallic reagents, diethyl amine and methoxide

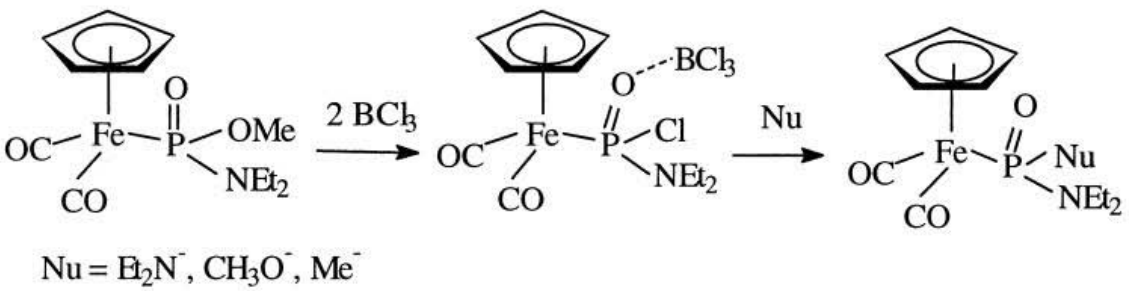

Figure 3.5 Substitution reaction of iron *P*-amidophosphito complex

in the presence of the electrophile BCl_3, led to substitution at phosphorus. The reaction was confirmed to proceed via a chloride-substituted phosphito intermediate. The molecular structure of the isolated intermediate established a bond between the oxygen atom of the phosphoryl group and the electrophile, BCl_3. Electron density was transferred from the phosphoryl group (Figure 3.5), hence, the Lewis acid, BCl_3, serves to both enhance electrophilicity and, by providing a good leaving group, to increase the susceptibility of the phosphorus centre towards nucleophiles.

This chapter describes attempts to derivitize chiral inorganometallic Co(III) pentavalent phosphorus moieties, using a modification of Nakazawa's method for the derivitization of amidophosphito moieties. Reactions of Co(III) phosphonates with the Lewis acid, BCl_3, followed by the nucleophiles were tested. Moreover, following the chemistry of analogous organophosphorus compounds, reactions with nucleophiles such as Grignard reagents, amines, alcohols, etc. were also tested.

3.2 Results and Discussion

3.2.1 Reactivity of *P*-amidophosphito Co(III) Complexes

3.2.1.1 Nucleophilic Substitution

Nucleophilic substitution of the methoxy group in organophosphonites is

generally a facile reaction. Extension of this chemistry to inorganometallic *P*-amidophosphito derivatives as in complex **2-2a**, (η^5–C_5H_5)Co(I)(PNH)(P(O)(OMe)(NEt_2)), was tested with a number of nucleophiles.

Complex **2-2a** was refluxed in the presence of an excess of aniline in benzene for 12 hours. ^{1}H NMR spectra and TLC indicated that no reaction had occurred. The starting material, **2-2a**, was recovered in quantitative yield via chromatographic separation. The more potent nucleophile, sodium methoxide-d_3, also failed to exchange the methoxy function of the phosphonate moiety under a variety of forcing conditions.

The inertness of complex **2-2a** toward nucleophilic attack was possibly due to insufficient electrophilicity of phosphorus centre of the phosphoryl group. It was hoped that complex **2-3a**, (η^5–C_5H_5)Co(C_3F_7)($PPhMe_2$)(P(O)(OMe)(NEt_2)), might increase the partial positive charge of the phosphorus centre as result of the strong electron-withdrawing supporting perfluoroalkane ligand. However, complex **2-3a** was also inert to sodium methoxide-d_3, aniline and methyllithium.

3.2.1.2. Nucleophilic Substitution in the Presence of BCl_3

The Lewis acid, BCl_3, was used in the reaction of the Co(III) *P*-amidophosphito complex **2-2a**, (η^5–C_5H_5)Co(I)(PNH)(P(O)(OMe)(NEt_2)), with

nucleophiles in order to modify the reactivity of the iron *P*-amidophosphito complex (Figure 3.5). Addition of two equivalents of BCl_3 turned the greenish brown solution of complex **2-2a** brown. Subsequent treatment with excess of sodium methoxide-d_6 gave a greenish brown solution which afforded a brown residue after removal of volatiles. Separation of the residue on a 1 mm thick-layer radial chromatographic plate gave a product, **3-1,** whose ^1H NMR (Table 3.1.1) contained signals for Cp, OMe, NEt_2 and Ph functions. The resonances belonging to functional groups on nitrogen and carbon of the PNH ligand were, however, missing. ^2H NMR indicated a peak at 3.65 ppm which is not same as OMe attached to phosphoryl group(3.44 ppm) but close to OMe of $PPh_2(OMe)$ (3.67 ppm). ^{31}P NMR (Table 3.1.3) showed both a P(III) and a P(V) site. This evidence collectively indicated that the reaction of compound **2-2a** with the BCl_3 / CD_3O^- occurred at the PNH ligand

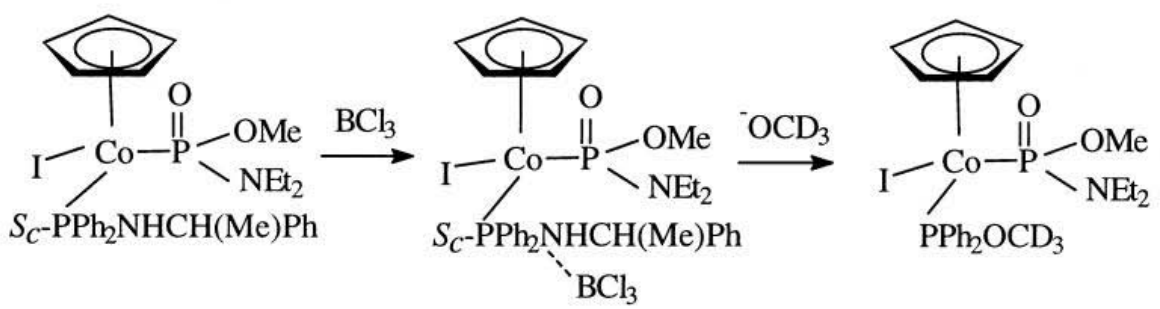

2-2a **10** **3-1**

Figure 3.6 Reaction of *P*-amidophosphito Co(III) complex **2-2a**

Table 3.1.1 ^{1}H and ^{2}H NMR data for compound 3-1[a]

cmpd	δ (Cp)	δ (OMe)	δ (NCH_2CH_3)	δ (NCH_2CH_3)	δ (Ph)	^{2}H
3-1	4.96 (s)	3.54 (d, 11.4)	3.25 (m)	1.86 (t,8.6)	7.42 (m)	3.65
			3.06 (m)		7.99 (m)	

[a] ^{1}H (300.1 MHz) NMR chemical shifts are in ppm relative to internal TMS; *J* values in Hz are given in parentheses; solvent $CDCl_3$; abbrevations m = mutiplet; s = singlet; d = doublet.

Table 3.1.2 ^{13}C NMR data for compound 3-1[a]

cmpd	δ (Cp)	δ (P(OMe))	δ ($P(OCD_3)$)	δ (NCH_2CH_3)	δ (NCH_2CH_3)	δ(Ph): ipso,ortho, meta,para
3-1	88.08(d,	54.91(d,	50.13(d,	41.97(d,	14.80(s)	nf, nf
	3.1)	7.2)	12.0)	4.8)		135.30(d,9.0) 131.77(d,9.1)
						127.50(d,10.8) 127.82(d,9.1)
						127.76(d,2.5), 129.53(d,2.6)

[a] ^{13}C (75.5 MHz) chemical shifts are in ppm relative to $CDCl_3$; *J* values in Hz are given in parentheses; abbreviations: d = doublet, nf = not found.

Table 3.1.3 ^{31}P NMR, IR and physical data for compound 3-1[a]

cmpd	^{31}P	$\gamma_{P=O}$, $\delta_{P\text{-}OC}$, $\delta_{PO\text{-}C}$ (cm^{-1})	mp(°C)	colour
3-1	89.92 (d,132.0)	1125, 1023, 697	108.7 – 109.4.3	brown
	86.07 (d,132.9)			

[a] ^{31}P (121.5 MHz) chemical shifts in ppm are relative to external 85% H_3PO_4, *J* values in Hz are given in parentheses; solvent = $CDCl_3$; abbreviations: d = doublet.

instead of the phosphonate ligand, giving the product (η^5–C_5H_5)CoI(PPh_2OCD_3)(P(O)(OMe)(NEt_2)) (Figure 3.6). The structure of the product was confirmed by the mass spectra. Critical fragments were observed corresponding to ICo(P(O)(OMe)(NEt_2))$^{+\cdot}$ (M/Z = 336.12), CpCoI$^{+\cdot}$ (M/Z = 250.88), $PPh_2(OCD_3)^{+\cdot}$ (M/Z = 219.05), Co(P(O)(OMe)(NEt_2))$^{+\cdot}$ (M/Z = 209.06), CoI$^{+\cdot}$ (M/Z = 185.85), P(O)(OMe)(NEt_2)$^{+\cdot}$ (M/Z = 150.02), I$^{+\cdot}$ (M/Z = 126.86), CpCo$^{+\cdot}$ (M/Z = 123.94), P(O)(OMe)$^{+\cdot}$ (M/Z = 77.98), $NEt_2^{+\cdot}$ (M/Z = 72.04) and Cp$^{+\cdot}$ (M/Z = 65.07). In addition, a peak at M/Z = 201.18 assigned to $[P(O)Ph_2]^{+\cdot}$ was found. This

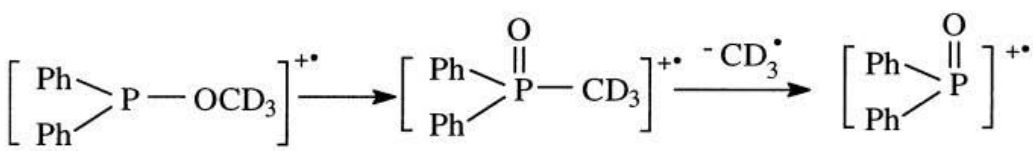

11 **12** **13**

Figure 3.7 Formation of P(O)Ph$^{+\cdot}$ fragment

fragment (**13** of Figure 3.7) can be explained by cleavage of CD_3 from **12**, which derives from the $PPh_2(OCD_3)$ ligand (**11** in Figure 3.7). Enhanced reactivity at the phosphine instead of the phosphonate ligand is consistent with a substantial contribution from resonance structure B (Figure 3.8), in which the nitrogen adopts sp^2 hybridization and donates the lone pair electrons to the phosphorus atom. The lone pair electrons on nitrogen of the phosphonate moiety is, therefore, less available for the reaction with the electrophile. The planarity of nitrogen was confirmed by the X-ray analysis of compound **2-2a**[125] with approximate 120° angles of P–N–C_1 (119.9) and P–N–C_2 (123.8).

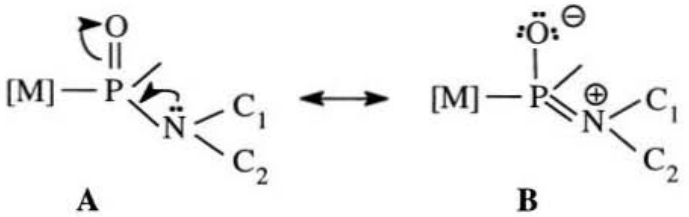

Figure 3.8 Lewis structure of amidophosphito moiety

3.2.2 Reactivity of *P*-phosphito Co(III) Complex

The perfluoropropyl group in the *P*-phosphito substrate **2-1a**, $(\eta^5\text{–}C_5H_5)Co(C_3F_7)(PPhMe_2)(P(O)(OMe)Ph)$, would be expected to decrease electron density at cobalt, owing to its strong electron-withdrawing ability, and hence activate the P(V) centre with respect to nucleophilic reactions. Moreover, compared to amidophosphonate substrate **2-2a,** the phenyl substituent on the phosphonate

eliminates the lone pair donation from the nitrogen, which serves to focus nucleophilic reactivity on the phosphorus centre.

3.2.2.1 Reaction with Nucleophiles

Nucleophiles, including organometallic reagents such as Grignard reagents, methyllithium, methanol, lithium aluminum hydride, diethyl sulfide, amines and alcohols were used as the nucleophiles to substitute the methoxy group of the Co(III) *P*-phosphito complex **2-1a**. ^{1}H NMR and TLC indicated that no reaction occurred even under forcing conditions with these reagents. The starting material, compound **2-1a**, was recovered in quantitative yields in each case.

3.2.2.2 Reaction with Phosphorus Pentachloride and Thionylchloride

The inertness of the *P*-phosphito moiety toward nucleophiles may be a result of either insufficient electron withdrawing capacity of the phenyl group or, alternatively, the poor leaving group ability of the methoxy. Introduction of chloride, which is a good leaving group, into the phosphonate moiety was tested as a means to facilitate nucleophilic substitution at the phosphonate.

As described in Chapter 2, introduction of chloride into the phosphonate moiety via the transition-metal-mediated (TMM) Arbuzov reaction using

chlorodiethyl phosphite failed. Therefore, phosphorus pentachloride, which was shown by Mislow[134] to substitute the methoxy function in pentavalent organophosphorus compounds, was examined. Thionyl chloride is also a common reagent for replacement of the alkoxy in organophosphorus compounds[156] and was tested as well. The reactions were carried out under conditions varying from mild to extreme.

3.2.2.2 i. Mild Conditions

Reaction between equimolar amounts of phosphorus pentachloride or thionylchloride and compound **2-1a** at 40°C produced an orange solid, compound **3-2**. The ^{1}H NMR contained signals for all functional groups in compound **2-1a** (–Cp, –OMe, –Me and Ph). However, the chemical shift of each peak was different from that in the starting material. For example, (cf. Table 3.2.1), the Cp singlet was shifted from 4.86 ppm in compound **2-1a** to 5.11 ppm in the product. The –OMe doublet moved from 3.44 ppm to 3.64 ppm and two –Me doublets shifted from 2.08 ppm and 1.98 ppm respectively to 2.14 ppm and 1.73 ppm. Surprisingly, attempted separation of the product on 2 mm thick-layer radial chromatographic plates afforded only the starting material. This behaviour seemed to indicate an ionic product present in equilibrium instead of a chloride-substituted phosphonate product (Figure 3.9).

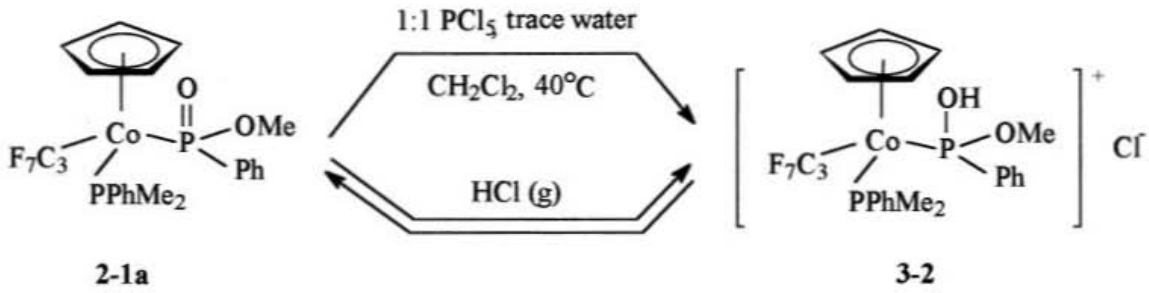

Figure 3.9 Reaction of *P*-phosphito moiety with PCl_5 under mild condition

The structure of the ionic product was confirmed by protonation of Co(III) *P*-phosphito compound **2-1a** with HCl(g). ^{1}H and ^{31}P NMR spectra indicated an identical product formed. It is hypothesized that PCl_5 reacts with adventitious water to afford HCl which subsequently protonates the phosphoryl group. Spectra data of the protonated product, compound **3-2**, is presented in Tables 3.2.1 – 3.2.3.

3.2.2.2 ii. Extreme Conditions

Prolonged heating was employed to promote reaction of compound **2-1a** with PCl_5 or $SOCl_2$. Refluxing equimolar amounts of compound **2-1a** and PCl_5 in toluene gave a brown cloudy solution with a green precipitate. The green precipitate did not dissolve in organic solvents such as benzene, acetone and chloroform and could not be identified. Removal of solvent from the brown solution afforded a brown solid, compound **3-3**. The ^{1}H NMR spectrum (Table 3.3.1) of the brown product **3-3**

Table 3.2.1 ^{1}H and ^{31}P NMR data for compound 3-2[a]

cmpd	δ (Cp)	δ (Me)	δ (OME)	δ (Ph)	^{31}P
3-2	5.10(s)	1.81(d,11.8)	3.58(d,11.5)	7.41(m)	25.80(d,109.2)(P(III))
		2.03(d,11.5)		7.51(m)	106.74(d,108.7)(P(V))
				7.60(m)	
				7.73(m)	

[a] ^{1}H (300.1 MHz) NMR chemical shifts are in ppm relative to internal TMS, ^{31}P (121.5 MHz) chemical shifts are in ppm relative to external 85% H_3PO_4; *J* values in Hz are given in parentheses; solvent $CDCl_3$; Abbrevations m = mutiplet; s = singlet; d = doublet.

Table 3.2.2 ^{13}C NMR data for compound 3-2[a]

cmpd	δ (Cp)	δ (Me)	δ (OMe)	δ(Ph): ipso,ortho,meta,para	
3-2	90.84(s)	17.84(d,8.6)	54.43(d,	138.39(d,47.5)	131.32(d,44.3)
		17.41(d,10.2)	12.2)	130.09(d,9.5)	129.24(d,9.4)
				128.52(d,9.4)	nf
				131.60(d,2.4)	130.88(d,2.8)

[a] ^{13}C (75.5 MHz) chemical shifts are in ppm relative to $CDCl_3$; *J* values in Hz are given in parentheses; abbreviations: d = doublet, nf = not found; perfluoroalkyl carbon resonances were observed in the chemical shift range of 105 – 140 ppm with very weak intensities.

Table 3.2.3 ^{19}F NMR, IR and physical data for compound 3-2[a]

cmpd	$\delta(^{19}F)$: C_γ, C_β, C_α	$\delta_{P\text{-}OH}$, $\delta_{P\text{-}OC}$, $\delta_{PO\text{-}C}$ (cm^{-1})	mp(°C)	colour
3-2	–78.93(s) –113.33(t,287.1) –61.58(d,251.2), –68.57(d,287.0)	1026, 1080, 749	113.2 – 113.5	orange

[a] ^{19}F (282.4 MHz) NMR chemical shifts are in ppm relative to $CFCl_3$; solvent = $CDCl_3$; $^2J_{FaFb}$ and $^3J_{FF}$ values in the case of CF_3 in Hz are given in parentheses; all CF_2 peaks show further unresolved splitting 5 – 10 Hz due to J_{FF} .

contained resonances assigned to –Cp, –Me and –Ph but no –OMe resonance was observed. ^{19}F NMR (Table 3.3.3) showed a typical C_3F_7 pattern. However, ^{31}P NMR (Table 3.3.3) revealed only one singlet assigned to P(III) at 21.33 ppm compared to two doublets of P(III) (25.74 ppm) and P(V) (106.67 ppm) of compound **2-1a**. The NMR data supported the assignment of the product **3-3** as $(\eta^5\text{–}C_5H_5)(C_3F_7)Co(PPhMe_2)Cl$ shown in Figure 3.10, the product of Co–P(V) bond cleavage.

Authentic $(\eta^5\text{–}C_5H_5)(C_3F_7)Co(PPhMe_2)Cl$ was synthesized via a rational synthetic route in order to confirm the nature of compound **3-3**. $AgBF_4$ was used to abstract the iodide of compound **1**, $(\eta^5\text{–}C_5H_5)(C_3F_7)Co(PPhMe_2)I$, in acetone solution

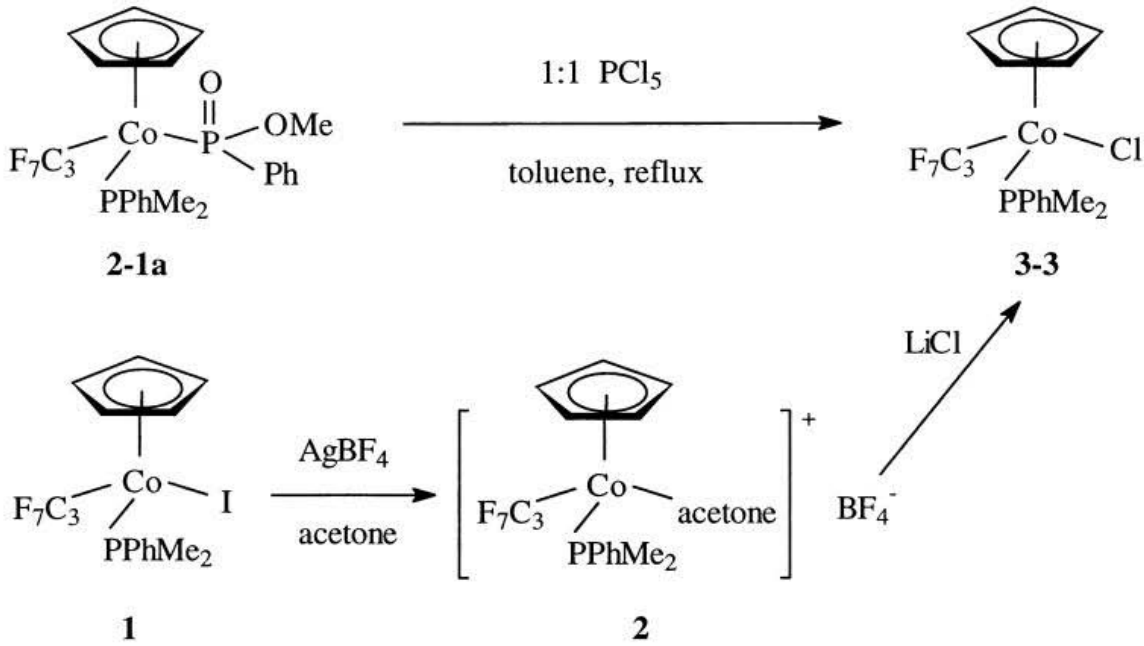

Figure 3.10 Reaction of *P*-phosphito moiety with PCl_5 at extreme condition

to give the solvent complex **2**. The coordination site resulting from the release of iodide was subsequently substituted with chloride through addition of lithium chloride, giving $(\eta^5\text{–}C_5H_5)(C_3F_7)Co(PPhMe_2)Cl$ (Figure 3.10). Comparison of ^1H, ^{19}F, ^{31}P NMR and TLC data confirmed that $(\eta^5\text{–}C_5H_5)(C_3F_7)Co(PPhMe_2)Cl$ is the product from the reaction of compound **2-1a** with one equivalent of PCl_5 at high temperature.

Table 3.3.1 ^{1}H and ^{31}P NMR data for compound 3-3[a]

cmpd	δ (Cp)	δ (Me)	δ (Ph)	^{31}P
3-3	4.90(s)	1.89(d,11.5)	7.37(m)	21.33(s)
		1.76(d,11.6)	7.54(m)	
			7.91(m)	

[a] ^{1}H (300.1 MHz) NMR chemical shifts are in ppm relative to internal TMS, ^{31}P (121.5 MHz) chemical shifts are in ppm relative to external 85% H_3PO_4; *J* values in Hz are given in parentheses; solvent = $CDCl_3$; Abbrevations m = multiplet; s = singlet; d = doublet.

Table 3.3.2 ^{13}C NMR data for compound 3-3[a]

cmpd	δ(Cp)	δ(Me)	δ(Ph): ipso,ortho,meta,para
3-3	88.86(s)	15.15(d,22.0)	nf
		14.50(d,22.0)	129.25(d,9.6)
			129.57(d,9.6)
			130.88(d,2.9)

[a] ^{13}C (75.5 MHz) chemical shifts are in ppm relative to $CDCl_3$; *J* values in Hz are given in parentheses; abbreviations: d = doublet, nf = not found; perfluoroalkyl carbons distributed in the chemical shift range of 105 – 140 ppm with very weak intensities.

Table 3.3.3 ^{19}F NMR and physical data for compound 3-3[a]

cmpd	δ(^{19}F): C_γ, C_β, C_α	mp(°C)	color
3-3	–79.24(s)	124.5 – 124.8	brown
	–115.14		
	–68.19(d,266.2), –77.82(d,266.2)		

[a] ^{17}F (282.4 MHz) NMR chemical shifts are in ppm relative to $CFCl_3$; solvent = $CDCl_3$; $^2J_{FaFb}$ and $^3J_{FF}$ values in the case of CF_3 in Hz given in parentheses; all CF_2 peaks show further unresolved splitting by about 5 – 10 Hz due to J_{FF}.

3.2.2.3 Reaction with Nucleophiles in the Presence of BCl_3

3.2.2.3.i Reaction with $NaOCD_3$ and $LiCH_3$ in the Presence of BCl_3

The Lewis acid, BCl_3, was used to modify the chemistry of the iron *P*-amidophosphito complex shown in Figure 3.5, in order to facilitate nucleophilic substitution of Co(III) *P*-phosphito complex **2-1a**. Addition of two equivalents of a BCl_3 solution in heptane into a solution of compound **2-1a** in methylene chloride at low temperature gave a rose red solution. ^{1}H NMR spectrum demonstrated that all functional groups were retained albeit with chemical shifts different from that of the starting material. The ^{31}P NMR spectrum showed two doublets corresponding to P(III) and P(V). Subsequently, excess $^-$OMe-d_3 or methyllithium were tested as nucleophiles for substitution. Surprisingly, the two nucleophiles gave the same

yellow product, **3-4**, as well as the unreacted starting material**, 2-1a.**

The ^{1}H NMR spectrum of compound **3-4** indicated that there was no –OMe group. The ^{19}F NMR spectrum showed three types of non-equivalent fluorine atoms, two of which were of the expected β,γ-perfluoroalkyl sites. However, the characteristic α-fluorine resonance was missing. A new doublet with J = 1057.8 Hz was observed. ^{31}P NMR spectrum at 121 MHz showed three apparent doublets. The doublet at 29.48 (J = 87.9 Hz) was assigned to P(III). The remaining two resonances at 124.66 ppm and 133.22 ppm were postulated as either signals corresponding to two different phosphorus atoms or splitting of the pentavalent phosphorus peak. The ^{31}P NMR spectrum at 40 MHz indicated that the difference in frequency between the two high field peaks did not change and hence are assigned to coupling of the P(V) atom. The coupling constant (1059.9 Hz) was tentatively assigned to $^{1}J_{PF}$, based upon the coupling constant of the P–F bond of compound PhP(O)(OMe)(F) which is 1035 Hz.[136] The assignment was confirmed successfully by the consistency of the coupling constant of 1057.8 Hz observed by ^{19}F NMR spectrum. Moreover, IR spectra also supported the presence of fluorine attached to the phosphoryl group. The P–O stretching frequency changed from 1154 cm^{-1} of the starting material **2-1a** to 1172 cm^{-1} for product **3-4**, due to the replacement of the methoxy group by the more electronegative fluorine group. The resulting decrease of electron density on the

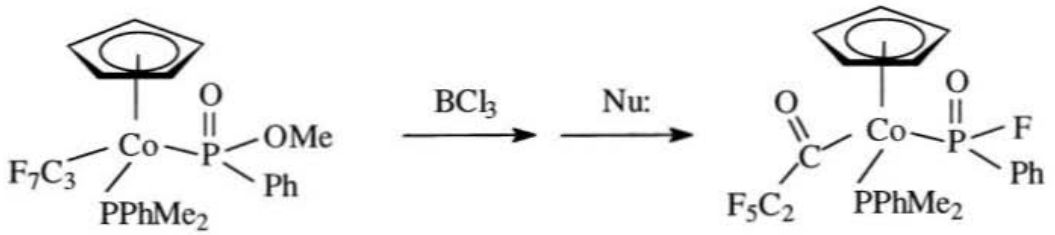

2-1a **3-4**

Nu: = $^{-}OCD_3$, $^{-}CH_3$

Figure 3.11 Reaction of *P*-phosphito moiety with nucleophiles in the presence of BCl_3

phosphorus atom depopulates the P–O anti-bonding orbital.[137,138] IR spectra also indicated the existence of a carbonyl group attached to metal centre. Collectively, the spectroscopic data shown in Tables 3.4.1 – 3.4.3 support a perfluoropropanyl cobalt *P*-fluorophosphito structure for product **3-4** (Figure 3.11). This structure was verified by its mass spectrum $CpCo(PPhMe_2)(C(O)C_2F_5)(P(O)(F)Ph)^{+\cdot}$ (M/Z = 552.06), $CpCo(PPhMe_2)^{+\cdot}$ (M/Z = 262.04), $C_2F_5C(O)^{+\cdot}$ (M/Z = 147.04), $P(O)(F)Ph^{+\cdot}$ (M/Z = 143.00), $PPhMe_2^{+\cdot}$ (M/Z = 138.06), $P(O)Ph^{+\cdot}$ (M/Z = 124.01), $C_2F_5^{+\cdot}$ (M/Z = 118.98), $P(O)F^{+\cdot}$ (M/Z = 66.07) and $Cp^{+\cdot}$ (M/Z = 65.10). High resolution mass spectra also proved the molecular formula $C_{22}H_{22}O_2CoP_2F_6$ (553.03314, obs. 553.03322).

Table 3.4.1 ^{1}H and ^{31}P NMR for compound 3-4[a]

cmpd	δ(Cp)	δ(Me)	δ(Ph)	^{31}P
3-4	4.88(s)	1.87(d,9.4)	7.46(m)	29.48(d,87.9)
		2.00(d,12.5)	7.52(m)	128.73(dd,90.2 1058.9)[b]
			7.78(m)	

[a] ^{1}H (300.1 MHz) NMR chemical shifts are in ppm relative to internal TMS, ^{31}P (121.5 MHz) chemical shifts are in ppm relative to external 85% H_3PO_4; *J* values in Hz are given in parentheses; solvent $CDCl_3$; abbreviations m = multiplet; s = singlet; d = doublet.

[b] $^{1}J_{PP'}$, $^{2}J_{PF}$

Table 3.4.2 ^{13}C NMR data for compound 3-4[a]

cmpd	δ(Cp)	δ(Me)	δ(Ph): ipso,ortho,meta,para
3-4	90.06(s)	16.54(d,31.5)	nf, nf
		15.56(d,32.8)	119.13(d,9.8), 128.13(d,11.4)
			129.52(d,9.8), 129.88(d,9.8)
			120.51(d,1.7), 128.13(d,11.4)

[a] ^{13}C (75.5 MHz) chemical shifts are in ppm relative to $CDCl_3$; *J* values in Hz are given in parentheses; abbreviations: s = singlet, d = doublet, nf = not found; perfluoroalkyl carbons distributed in the chemical shift range of 105 – 140 ppm with very weak intensities.

Table 3.4.3 ^{19}F NMR, IR and physical data of compound 3-4[a]

cmpd	δF: C_β,C_γ, (P)F	$\gamma_{P=O}$, γ_{CO}	MS(M^+)	mp(°C)	colour
3-4	– 79.78(s)	1173	553.03314 (calc.)	121.5 –	yellow
	– 110.26(d,48.6)	1656	553.03322 (obs)	121.9	
	– 15.32(d,1057.8)[b]				

[a] ^{19}F (282.4 MHz) NMR chemical shifts are in ppm relative to CF_3Cl; solvent = $CDCl_3$; $^2J_{FaFb}$ and $^3J_{FF}$ values in the case of CF_3 in Hz given in parentheses; all CF_2 peaks show further unresolved splitting by about 5 – 10 Hz due to J_{FF}; [b] J_{PF}

3.2.2.3.ii Proposed Mechanism

It is somewhat surprising that the reaction appears to occur at the perfluoroalkyl group since, in general, fluorine forms the strongest single bond with carbon.[139] C–F bonds in fluorocarbons are generally resistant to chemical attack and demonstrate high thermodynamic stability.[139,149,150] These properties of fluorocarbons have made them attractive to industry,[151] for example, as refrigerants. However, this chemical stability results in accumulation in the environment.[152-154]

Recently, it has been found that coordination to a transition metal can dramatically change the reactivity of fluoroalkyl groups. Upon coordination to a metal, the carbon-fluorine bonds α to the metal centre were found to have significantly longer bond lengths[140] and reduced infrared stretching

Figure 3.12 Transition metal activation of C–F bonds

frequencies.[141,142] It is postulated that the fluorine hyperconjugation from the perfluoroalkyl α-carbon causes contraction of the metal *d* orbital, resulting in a strengthened M–C bond and weakened C–F bond (Figure 3.12).[143] The weaked C–F bond is susceptible to electrophilic attack.[143] A wide variety of transition metals are reported to be capable of activating the C_α–F bond of σ-bonded perfluoroaromatics under extremely mild conditions. However, activation of the saturated perfluorocarbons remains a challenge.[139] The facile reaction of the compound **2-1a** with BCl_3 shown in Figure 3.11 suggests a novel model of C–F bond activation.

X-ray analysis of compound **2-1a** (Table 2.1.6) indicates that the bond length of the C_α–F bond (1.403 Å) in the σ-bonded C_3F_7 is longer than that of the C_β–F bond (1.347 Å). It suggests that coordination of perfluoroalkane with the cobalt also activates the C_α–F bond. In addition, the Lewis acid, BCl_3, was reported, by Roper,[144] to abstract a fluorine atom of the CF_3 ligand attached to transition metals such as ruthenium, palladium, osmium, manganese and iron. Therefore, a similar route is proposed for the reaction of compound **2-1a** with BCl_3 (Figure 3.13). The

subsequent nucleophilic reaction is proposed to go through a cobalt carbene intermediate **14**. Nucleophilic addition at the α-carbon site by deuterium methoxide or hydroxide from the solvent, followed by dissociation of methyl fluoride or

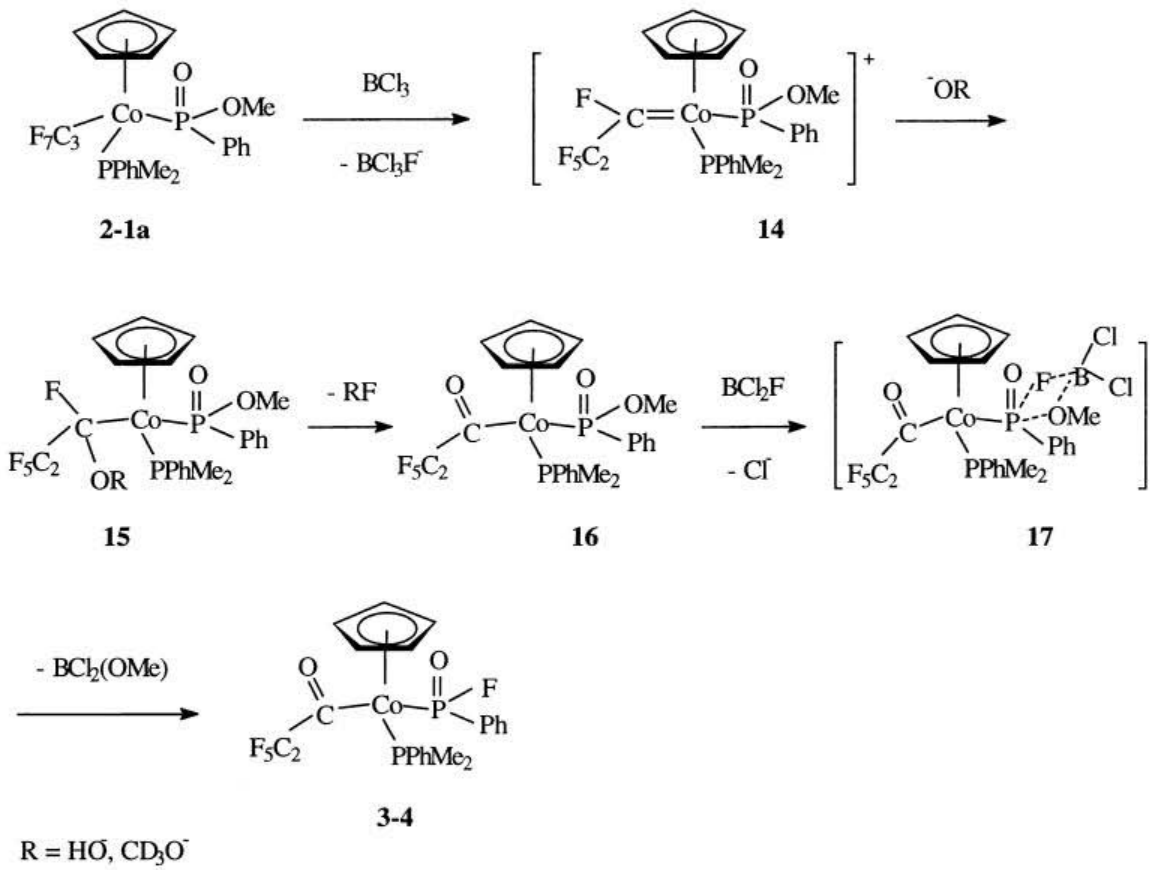

Figure 3.13 Proposed mechanism of reaction of Co(III) *P*-phosphito complex **2-1a** with nucleophiles in the presence of BCl_3

hydrogen fluoride, results in formation of the ketone complex **16**. Subsequent coordination of BCl_3 with the oxygen atom of the methoxy group and fluorine

migration (**17** in Figure 3.13) affords the *P*-fluorophosphito complex.

3.2.3 **Reactivity of the *P*-thiophenylphosphito Co(III) Complex**

The *P*-thiophenylphosphito Co(III) substrate, **2-4a**, includes two possible leaving groups, –OMe and –SPh. However, methoxide also failed to react with the pentavalent phosphorus moiety of compound **2-4a** and the starting material was recovered in near quantitative yields.

3.3 Summary

Reactivity of a number of *Co*- and *P*-chiral Co(III) complexes has been studied based upon current understanding of nucleophilic substitution in organo- and inorganometallic phosphorus chemistry.[156,111] Three Co(III) pentavalent phosphorus complexes were synthesized and found to be inert toward nucleophiles such as Grignard reagents, organolithiums, hydride, diethyl sulfides, alcohols and amines. The *P*-phosphito Co(III) complex, **2-1a**, reacted with nucleophiles only in the presence of BCl_3 to afford a perfluoropropanyl *P*-fluorophosphito Co(III) complex, which provides a new route to activate perfluoroalkyl C–F bonds. PCl_5 and $SOCl_2$ reacted with the *P*-phosphito Co(III) complex to afford an ionic product under mild conditions while cleavage of the Co–P(V) bond occurs to give a chloride-substituted cobalt product under extreme conditions.

3.4 Experimental Section

3.4.1 Reagents and Methods

All manipulations were performed under conditions similar to those described in Chapter 2. Spectral grade chloroform was used as received. The equipments used were same as those in Chapter 2. In addition, phosphorus pentachloride was freshly sublimed. Ethanethiol was distilled before use. BCl_3 in *n*-heptane and HCl gas were purchased from Aldrich and were used as received.

3.4.2 Experiments

3.4.2.1 Reactions of *P*-Phosphito Co(III) Complexes, 2-1a – 2-4a, with Nucleophiles

To a solution of the pentavalent phosphorus substrates, **2-1a – 2-4a**, in CH_2Cl_2 (20 mL), 4 equivalents of MeONa were added at room temperature. After stirring overnight, the solvent and volatiles were taken off by aspirator followed by oil pump vacuum. The crude products were separated via 2 mm radial thick-layer chromatography with the same eluent as used in process preparation of each substrate. Reactions with other nucleophiles such as EtSNa, Et_2NH, PhNH, MeMgI and $LiCH_3$ were carried out in a similar fashion. The reactions, which were refluxed

in toluene overnight, were performed similarly.

3.4.2.2 Reaction of the *P*-amidophosphito Co(III) Complex, 2-2a, with Methoxide in the Presence of BCl_3

To a greenish brown solution of compound **2-2a** (20.1 mg, 0.0285 mmol) in CH_2Cl_2 (10 mL), 56.9 uL of BCl_3 solution (1.0 M in heptane, 0.0568 mmol) was added at room temperature. After stirring at room temperature for 5 minutes, the reaction mixture turned brown. A solution of $NaOCD_3$ (6.5 mg, 0.114 mmol) in CD_3OD (2 mL) was added dropwise until the pH value of the mixture rose from 3.0 to 6.0. After stirring for an additional 15 minutes at room temperature, deionized water was added to quench the dark brown reaction mixture. The organic layer was washed with water and dried with $CaSO_4$. Removal of solvent and volatiles by aspirator followed by oil pump vacuum gave a brown residue. Radial thick layer chromatography (1 mm, $CH_3C(O)OEt$ / CH_2Cl_2 (4:1) followed by $CH_3C(O)CH_3$ elution) separated a yellow band which gave a brown product $CpCo(I)(PPh_2OCD_3)(P(O)(OMe)(NEt_2))$ (8.9 mg, 0.0146 mmol) in 51.2% yield.

3.4.2.3 Reaction of the *P*-Phosphito Co(III) Complex, 2-1a, with Phosphorus Pentachloride / Thionyl Chloride

3.4.2.3.1. Mild Conditions

To a solution of compound **2-1a** (42.1 mg, 0.0718 mmol) in $CHCl_3$ (20 mL) was added PCl_5 (149.5 mg, 0.718 mmol) at room temperature. After stirring at room temperature for 6 hours, the orange solution turned brown. The solvent was removed by aspirator, affording a brown residue, which was dissolved in benzene and separated by 2 mm radial thick-layer chromatography with $CH_3C(O)CH_3$ / C_6H_6 (3:1) as the eluent. The second band was collected. Removal of the solvent gave **2-1a** (34.9 mg, 0.0596 mmol).

The reaction of compound **2-1a** with $SOCl_2$ was performed analogously.

3.4.2.3.2. Extreme Conditions

To an orange solution of compound **2-1a** (88.4 mg, 0.151 mmol) in toluene (25 mL) was added PCl_5 (62.8 mg, 0.302 mmol). The reaction mixture was refluxed for 24 hours, giving a cloudy, dark-brown solution. After filtration to remove some insoluble material, the filtrate was concentrated by aspirator and purified by 2 mm radial thick-layer chromatography with $CH_3C(O)CH_3$ / C_6H_6 (1:6) as the eluent. The first brown band was collected. The solvent was removed at oil pump vacuum, affording brown solid $CpCo(PPhMe_2)(Cl)$ (46.3 mg, 0.0992 mmol) in 65.7 % yield.

The reaction of compound **2-1a** with $SOCl_2$ was performed similarly.

3.4.2.4 Preparation of Compound 3-2:

$[(\eta^5\text{–}C_5H_5)Co(C_3F_7)(PPhMe_2)(P(OH)(OMe)Ph)]^+Cl^-$

To a yellow solution in benzene (20 mL) of compound **2-1a** (138.1 mg, 0.2355 mmol) in a Schlenk tube protected with nitrogen was added HCl gas (12.9 mL, 0.3533 mmol). The solution turned pale yellow. After stirring for 10 min at room temperature, the solvent was taken off at oil pump vacuum, affording yellow solid which was washed with benzene to give $[CpCo(C_3F_7)(P(OH)(OMe)Ph)]^+Cl^-$ (145.7 mg, 0.2340 mmol) in 99.4% yield.

3.4.2.5 Preparation of Compound 3-3: $(\eta^5\text{–}C_5H_5)Co(C_3F_7)(PPhMe_2)Cl$

To a solution of $CpCo(C_3F_7)(PPhMe_2)I$ (56.2 mg, 0.101 mmol) in acetone (15 mL) was added the solution of $AgBF_4$ (19.6 mL, 0.101 mmol) in acetone (3 mL) at room temperature under protection of nitrogen. After stirring for 30 minutes, a brown solution containing a yellow precipitate was obtained. A solution of LiCl (12.8 mg, 0.303 mmol) in THF (10 mL) was added into the filtrate. The reaction mixture was refluxed for 1 hour to give a dark brown solution with a pale yellow precipitate. After filtration and removal of solvent at aspirator pressure, 5 mL of benzene was added to dissolve the cobalt complex. Removal of solvent from the filtrate at oil pump vacuum afforded a brown solid $CpCo(C_3F_7)(PPhMe_2)Cl$ (38.9 mg, 0.0834 mmol)

with yield of 82.6%.

3.4.2.6 Reaction of the *P*-phosphito Co(III) Complex, 2-1a, with Nucleophiles in the Presence of Lewis Acid

To a yellow solution of compound **2-1a** (126.0 mg, 0.215 mmol) in ethyl ether (15 mL) was added 0.43 mL of BCl_3 (1.0 M solution in heptane) at room temperature. Stirring for 30 minutes resulted in an orange reaction mixture. $NaOCD_3$ (24.5 mg, 0.43 mmol) in CD_3OD (5 mL) was added dropwise at room temperature. After the mixture was stirred for 3 hours, the reaction was quenched with water (5 mL). The organic layer was separated and dried over $CaSO_4$. Solvent and volatiles were removed at oil pump vacuum to afford a brown residue. The residue was dissolved in benzene and separated by 1 mm radial thick-layer chromatography, eluting with $CH_3C(O)OC_2H_5$ / C_6H_6 (1:6). The second yellow and the third yellow bands were collected. Removal of the solvent of both collections afforded $CpCo(C(O)C_2F_5)(PPhMe_2)(P(O)FPh)$ (10.8 mg, 0.0196 mmol, 9.1%) and compound **2-1a** (81.1 mg, 0.138 mmol, 64.2%).

The reaction of **2-1a** with $LiCH_3$ in the presence of BCl_3 was performed analogously.

Chapter 4

Molecular Orbital Analysis of Inorganometallic Phosphonate Reactivity

4.1 Introduction

Molecular orbital theory can lead to an understanding of chemical reactivity. The inorganometallic phosphonate moieties studied, unlike their organic analogues, are inert to reaction with nucleophiles. This chapter compares the molecular orbitals of inorganometallic vs. organic phosphonate compounds.

In general, reactions between neutral molecules or charged species having large overlaps are under orbital control, which means the interaction between the frontier orbitals of the reactants governs the course of the reaction. The dominant interactions are those between the highest occupied molecular orbital (HOMO) of one reagent and the lowest unoccupied molecular orbital (LUMO) of the other reagent.[160] For nucleophilic

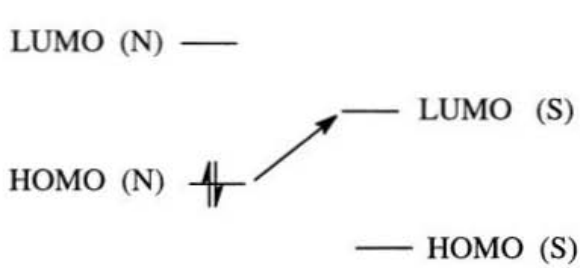

Figure 4.1 Frontier orbital interactions in nucleophilic reactions

reactions, electrons transfer from the nucleophile HOMO to the substrate LUMO and result in a two-electron interaction (Figure 4.1). Since orbital interaction depends on the difference in energy of the interacting fragment orbitals, a low energy LUMO facilitates nucleophilic reactions. Therefore, the difference between the LUMO energy of the inorganometallic phosphonate moieties and those of their organic analogs are related to their different reactivity toward nucleophiles.

Since the molecular orbitals of the target molecules of this study are complicated, containing interaction between many atoms, the fragment molecular orbital (FMO) method is adopted. The FMO analysis consists of imagining a complex molecule, whose electronic structure is not known, as an interaction of two smaller, chemically relevant fragments whose molecular orbitals are known. The orbitals of the complete molecule are then derived via the interaction of the orbitals of these two sub-systems. In this chapter, the cobalt phosphonate complexes were split into two fragments as shown in Figure 4.2. One fragment is the cobalt center with the supporting ligands

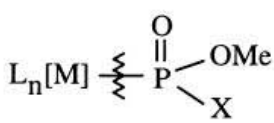

model **4-1a**: L_n = Cp, PH_3, I
model **4-2a**: L_n = Cp, PH_3,CF_3; X = NH_2
model **4-3a**: L_n = Cp, PH_3,CF_3; X = Me
model **4-4a**: L_n = Cp, PH_3,CF_3; X = SH

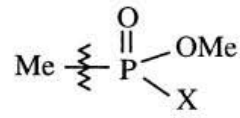

model **4-1b**: X = NH_2
model **4-2b**: X = Me
model **4-3b**: X = SH

Figure 4.2 Fragments of inorganometallic and organophosphonate compounds

while the other fragment is the phosphorus moiety with tetrahedral geometry.

Simplified models representing the cobalt phosphonate complexes were designed. For example, the phosphine ligand and perfluoroalkane ligand were replaced respectively with PH_3 and CF_3. Further, the functional groups attached to the pentavalent phosphorus center such as diethyl amine, phenyl and thiophenyl were replaced with NH_2, CH_3 and SH respectively. All of the models are constructed using the standard bond distances and bond angles collected from the X-ray data.[125,145]

The composition of the LUMOs in these models was analyzed using EHMO (Extended Hückel Molecular Orbital) formalism.[161] Two programs, EHC (Extended Hückel Caculation), and CACAO (Computer Aided Composition of Atomic Orbitals) are adopted. The EHC program focuses on outputting the information of MO calculation, such as energy levels, Wavefunction coefficients, Mulliken population analysis, etc. By specifying in the inpute file two fragments, in which the molecules ideally separated, the program performs a Fragment Molecular Orbital (FMO) analysis to provide the information of specific chemical bond(s) within the molecules. The CACAO program, based upon the data from the EHC program, concerns to produce diagrams including interaction diagrams, three-dimensional drawings of each MOs and its FMOs, etc. The combination of these two programs provides information of M–P(O) bonds in inorganometallic phosphonate moieties.

For comparison, organophosphorus analogs of the inorganometallic phosphonate models were also analyzed using the fragments shown in Figure 4.2.

4.2 EHMO Analysis of Inorganomtallic Phosphonate Moieties

4.2.1 *P*-amidophosphito Co(III) Complexes

4.2.1.1 *P*-amidophosphito Co(III) Complex with Iodide as the Supporting Ligand

The *P*-amidophosphito Co(III) complex with iodide as the supporting ligand (compound **2-2a**) was simplified as $CpCo(I)(PH_3)(P(O)(OMe)(NH_2))$ (model **4-1a**). The Co–P bond was cleaved to produce two fragments. FG1, the Co(III) fragment, has a positive charge while a negative charge was assumed on the formally P(III) center. The input file for the EHMO analysis in internal coordinates is listed in Schedule 4.1.

The interaction diagram between FG1 and FG2 of model **4-1a** is shown in Figure 4.3. Orbitals corresponding to each part are labeled. In the interaction diagram, the lines linking the molecular orbitals and the fragment orbitals represent the composition of the molecular orbitals. The color of the lines reflects the relative contributions of the fragment orbitals. Figure 4.3 indicates that the LUMO (MO 30)

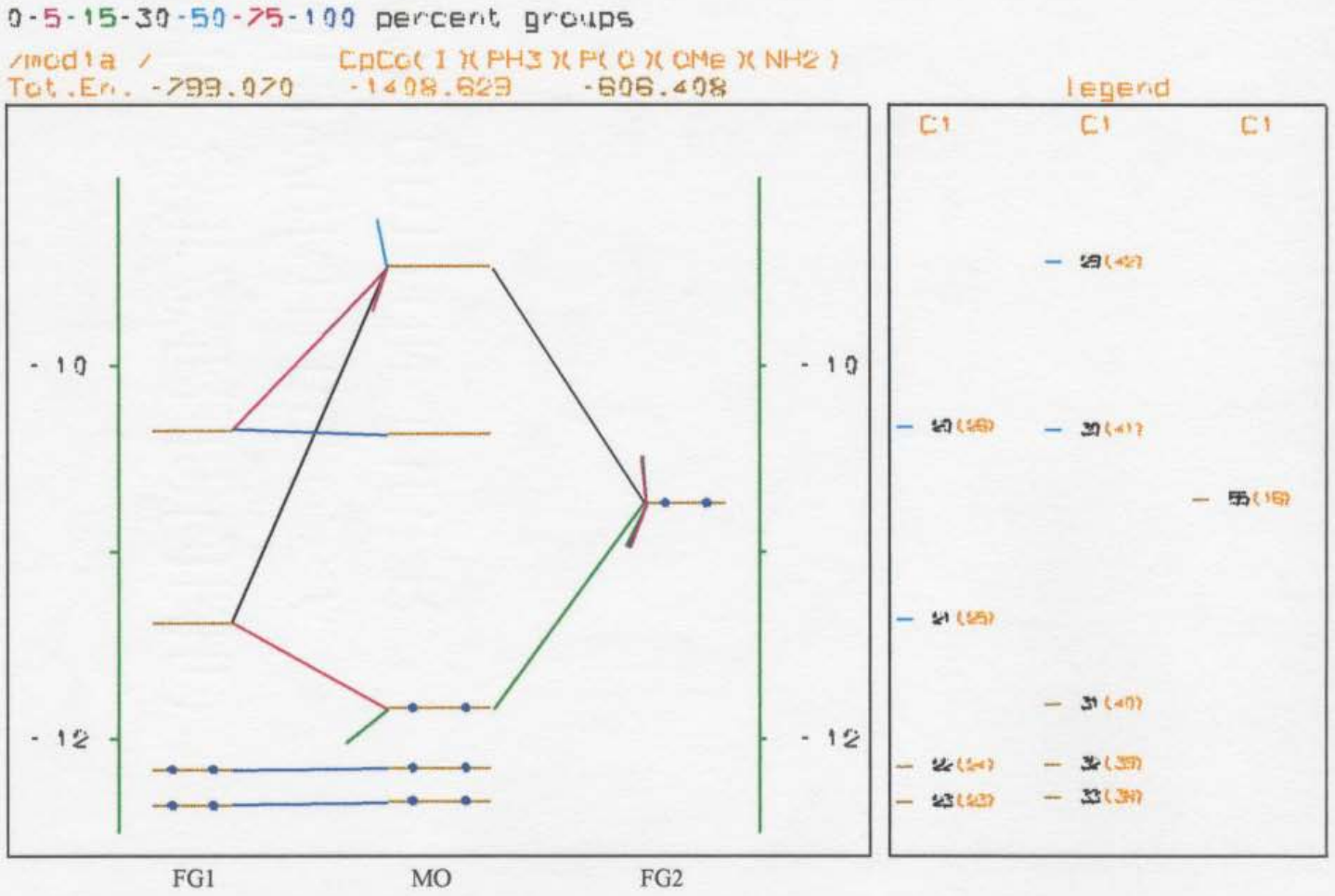

Figure 4.3 Interaction diagram between $Cp(I)(PH_3)Co^+$ (FG1) and $P(O)(OMe)(NH_2)^-$ (FG2) of model **4-1a**

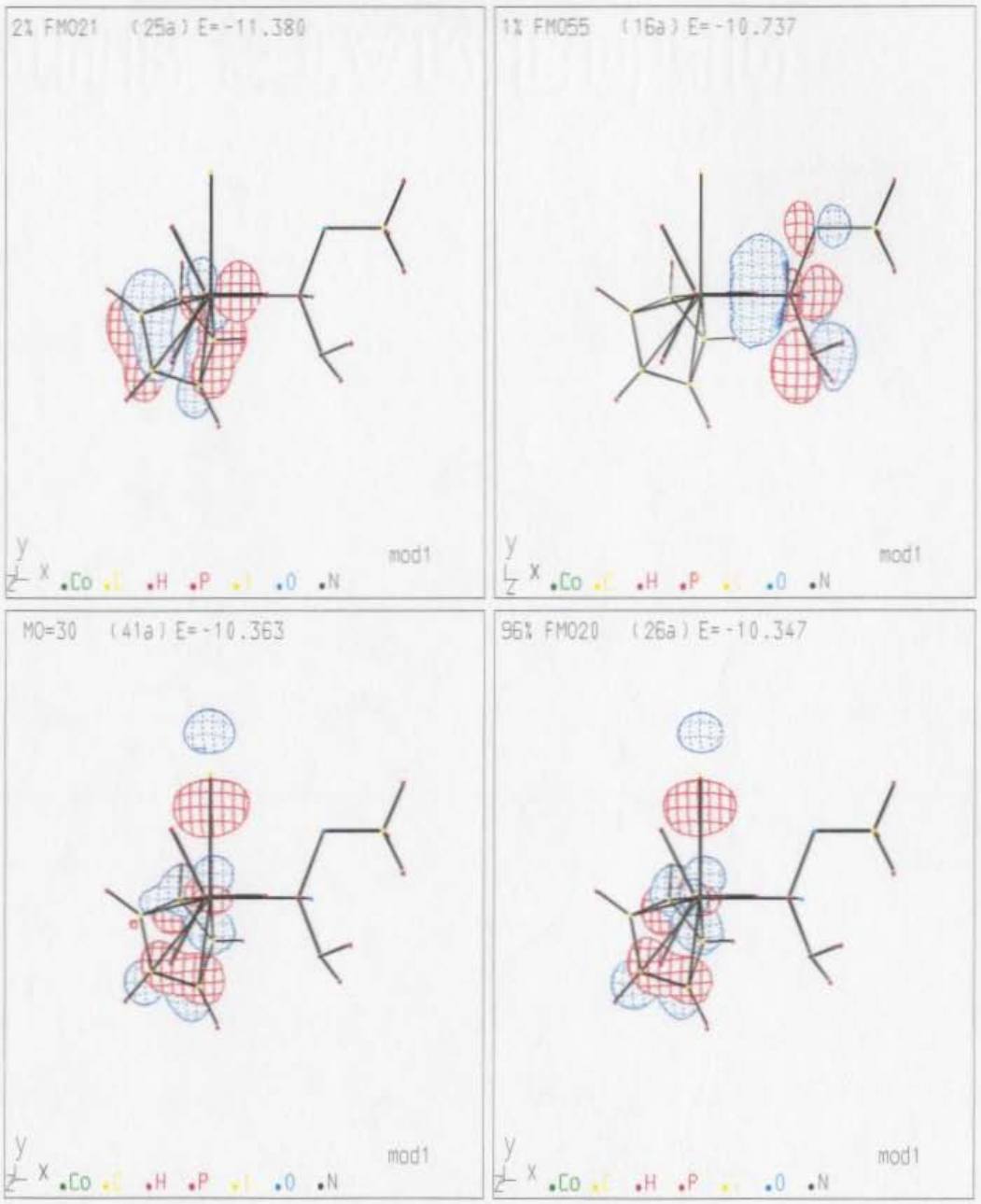

Figure 4.4 Plot of LUMO (MO30) and its component fragment orbitals for model **4-1a**

is almost entirely composed of orbitals from the metal fragment with less than 1% contribution from the phosphorus fragment. In the second empty molecular orbital (MO 29), a 25% contribution derives from the phosphorus fragment, in which less than 14% originates from the phosphorus atom. A plot of the LUMO of **4-1a** (MO 30) and its fragment orbitals are shown in Figure 4.4, which shows that the LUMO (MO 30) is essentially an empty, non-bonding metal centered orbital.

4.2.1.2 *P*-amidophosphito Co(III) Complex with Perfluoroalkane as the Supporting Ligand

A model of the perfluoroalkane *P*-amidophosphito Co(III) complex, **2-3a**, was constructed as $CpCo(CF_3)(PH_3)(P(O)(OMe)(NH_2))$ (model **4-2a**). The change of supporting ligand from iodide to the perfluoroalkane results in a decrease of electron density on cobalt center. The fragments used for this model (input file shown in Schedule 4.2) are similar to that of model **4-1a**.

The interaction diagram between the cobalt fragment (FG1) and the phosphorus fragment (FG2) is shown in Figure 4.5. The LUMO (MO 33) is also essentially a metal based non-bonding orbital. The contribution from the phosphorus fragment is 5%, of which only 3% originates from the pentavalent phosphorus *px* orbital. To the extent that phosphorus participates, it is slightly antibonding (Figure

4.6). The second empty molecular orbital (MO 32) contains 21% contribution from FG2 and 14% contribution is from the phosphorus orbitals. A diagram of the LUMO (Figure 4.6) showed that FMO 23 from FG1 dominates.

4.2.2 *P*-phosphito Co(III) Complex

The *P*-phosphito Co(III) complex (**2-1a**) was represented as $CpCo(CF_3)(PH_3)(P(O)(OMe)Me)$ (model **4-3a**). Fragments were developed through cleavage of Co–P bond as shown in Figure 4.2.

The interaction diagram (Figure 4.7) was calculated by using the input file listed in Schedule 4.3. The LUMO (MO 34) is again a non-bonding molecular orbital dominated by the orbitals from the cobalt fragment. The phosphorus fragment contributes 7% to the LUMO. The pentavalent phosphorus center contributes its *px* orbital to a total of less than 4% of the composition of the LUMO (MO 34 of Figure 4.8). The second empty orbital is also predominately metal based with 19% contribution of the phosphorus fragment, in which 11% contribution originates from the pentavalent phosphorus *px* orbital.

4.2.3 *P*-thiophosphito Co(III) Complex

Model **4-4a**, $(\eta^5\text{–Cp})Co(CF_3)(PH_3)(P(O)(OMe)(SH))$, was used to represent

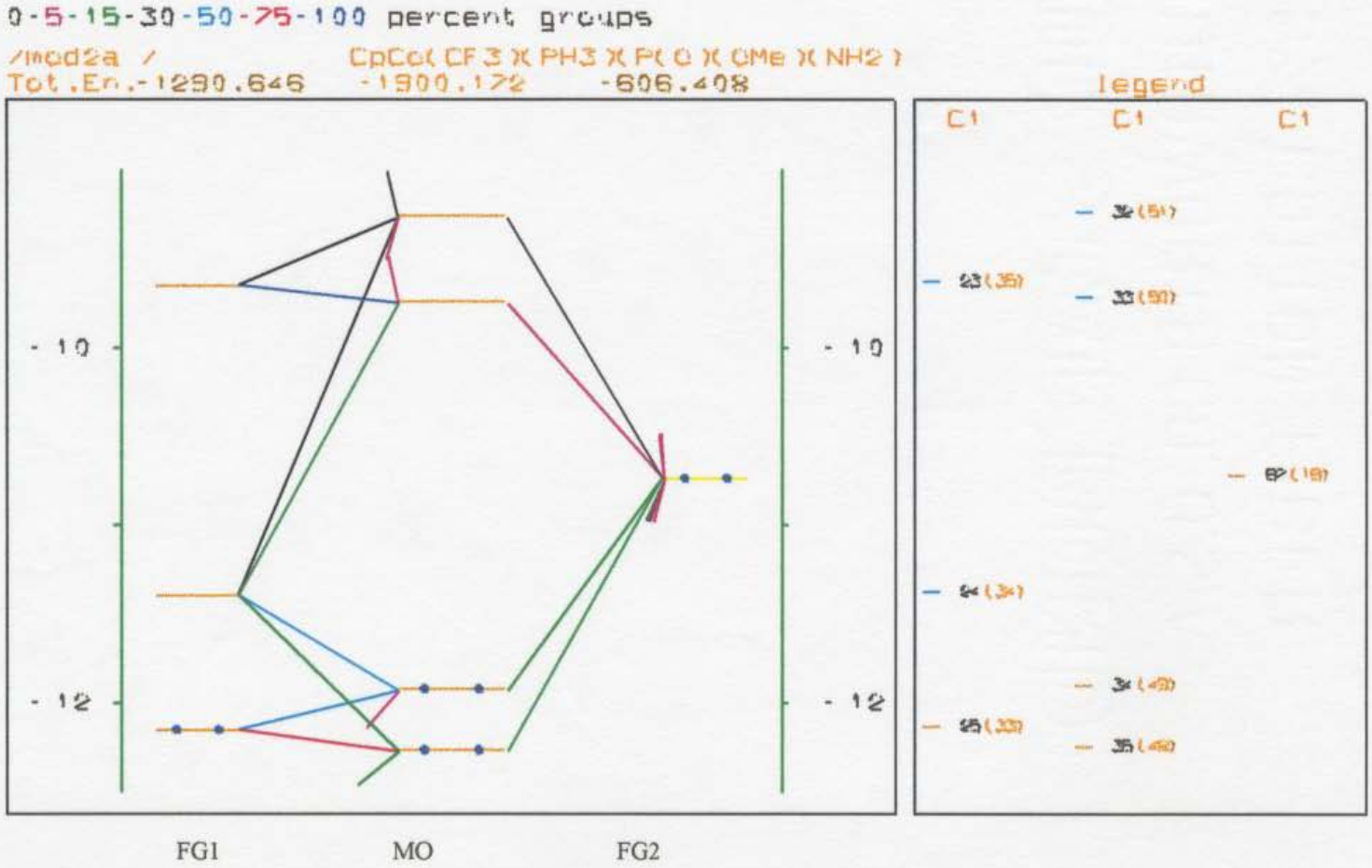

Figure 4.5 Interaction diagram between $Cp(CF_3)(PH_3)Co^+$ (FG1) and $P(O)(OMe)(NH_2)^-$ (FG2) of model **4-2a**

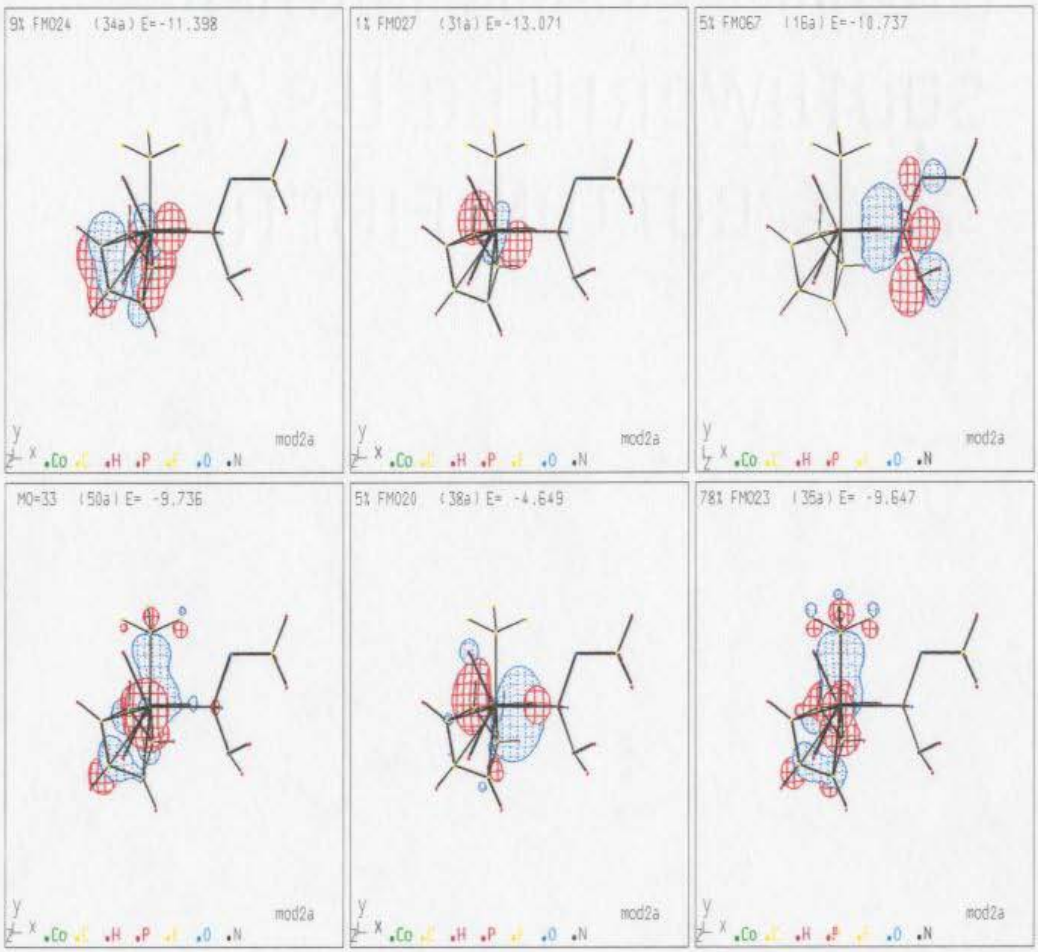

Figure 4.6 Plot of LUMO (MO 33) and its component fragment orbitals for model **4-2a**

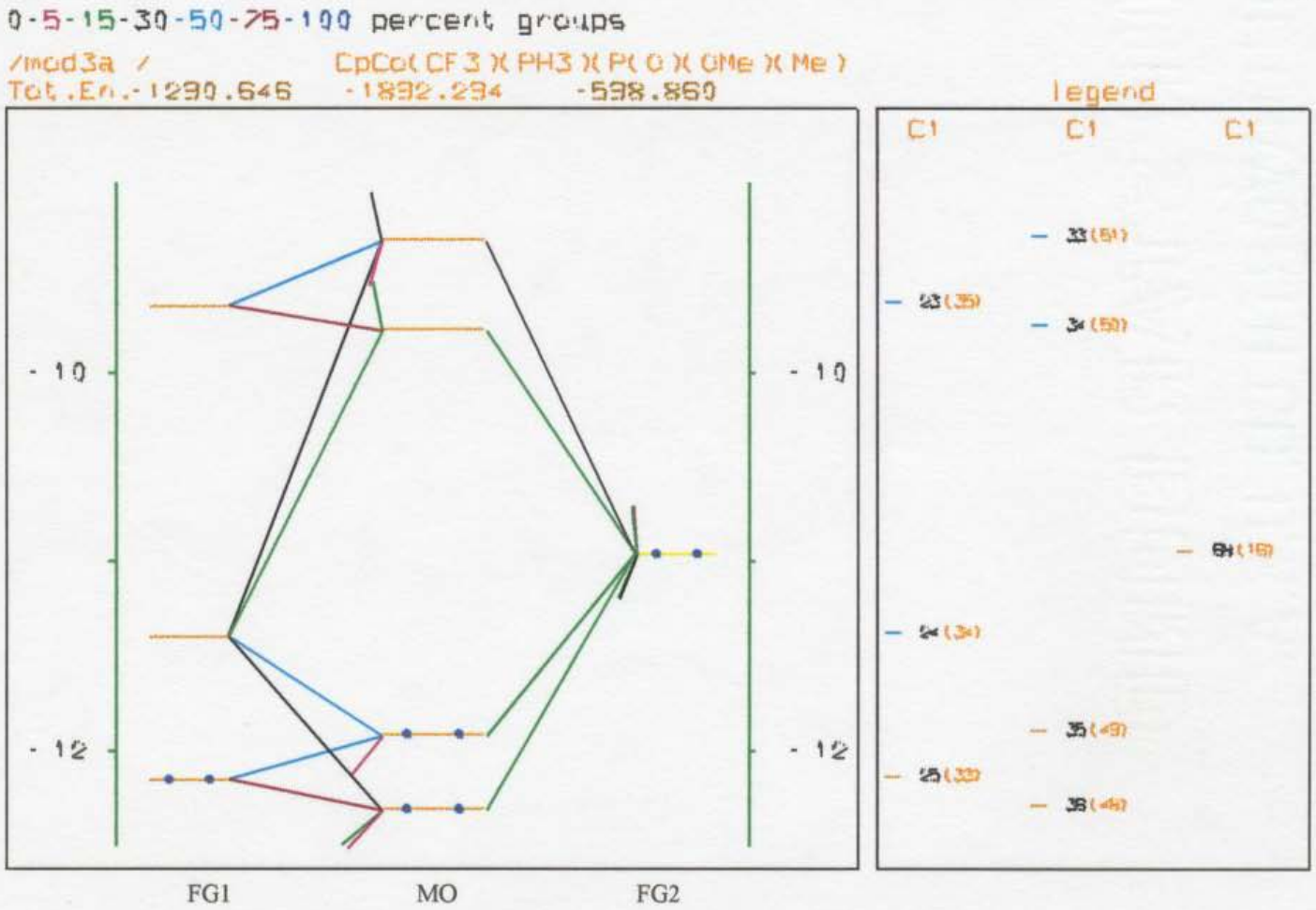

Figure 4.7 Interaction diagram between $Cp(CF_3)(PH_3)Co^+$ (FG1) and $P(O)(OMe)Me^-$ (FG2) of model **4-3a**

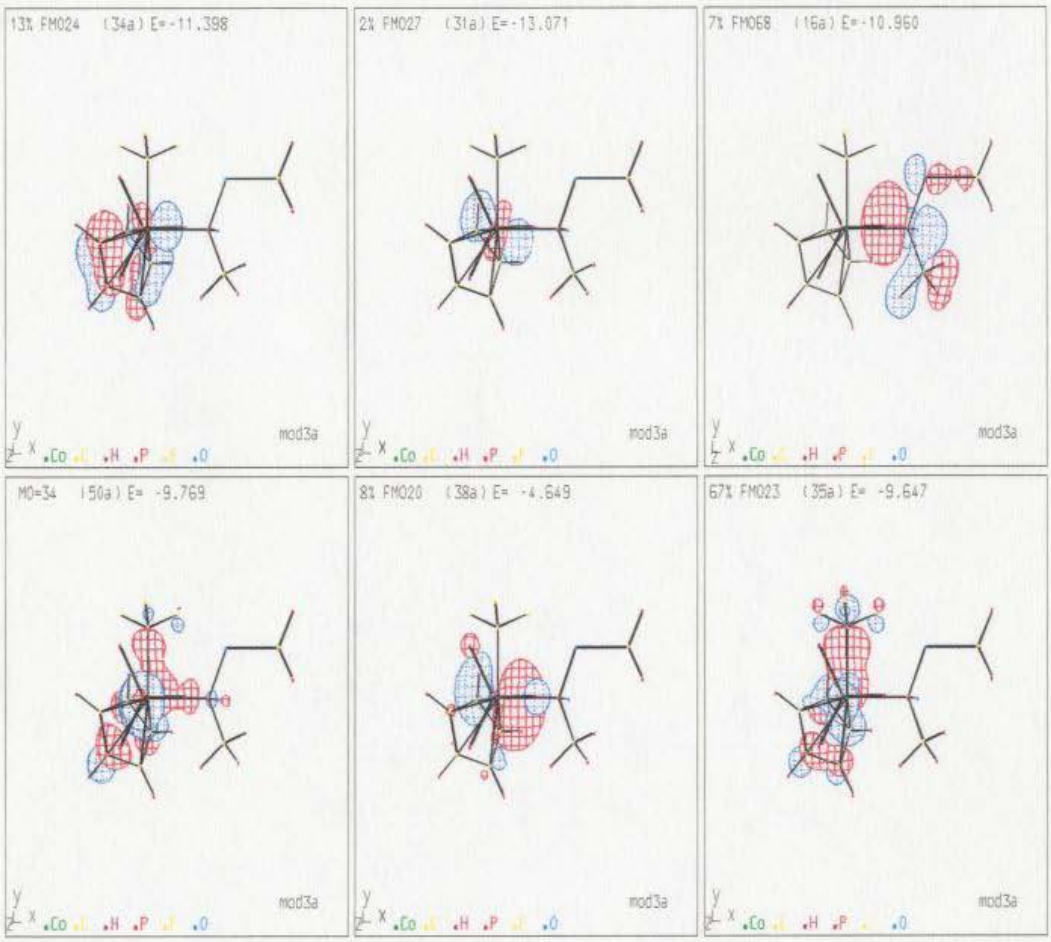

Figure 4.8 Plot of LUMO (MO 34) and its component fragment orbitals for model **4-3a**

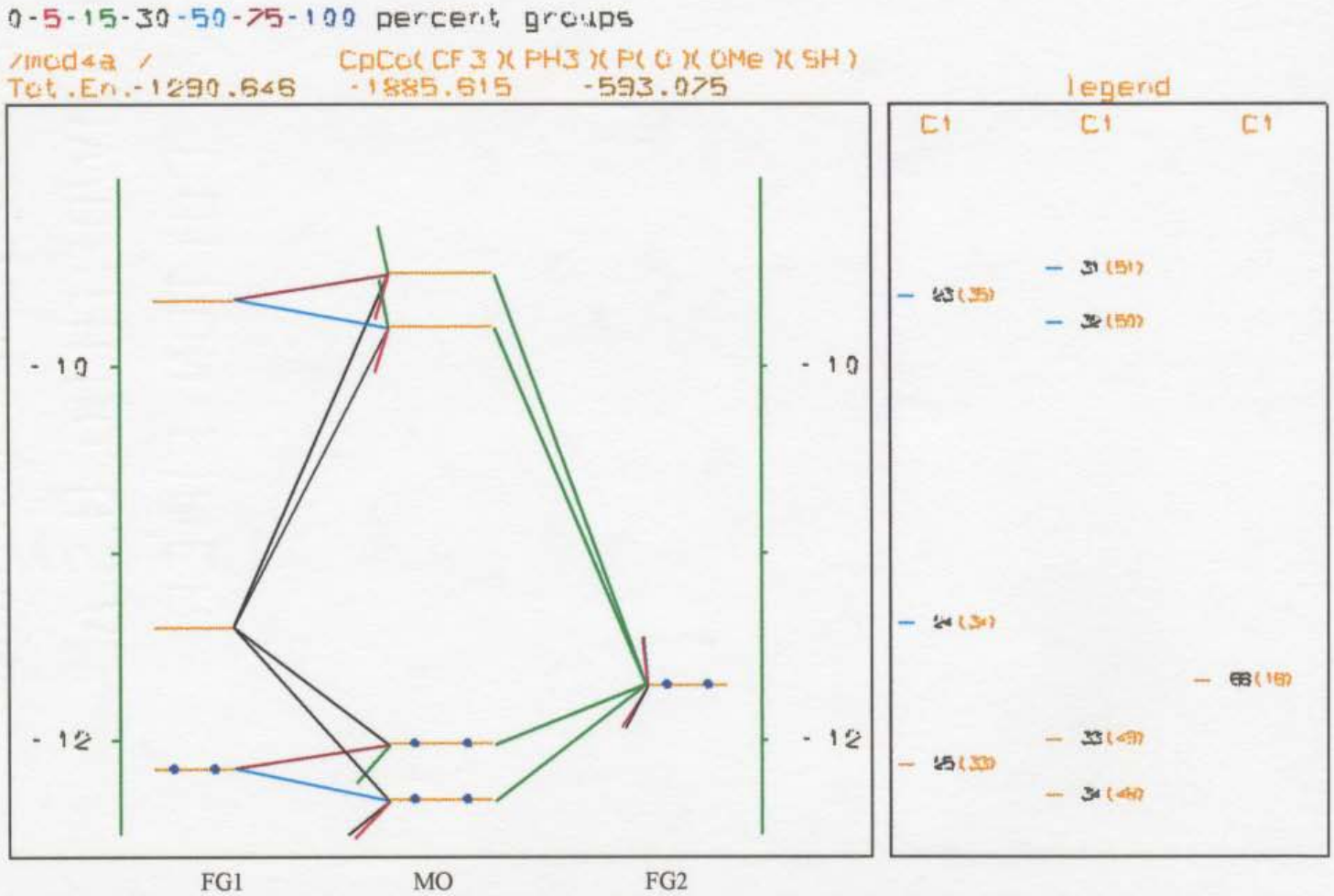

Figure 4.9 Interaction diagram between $Cp(CF_3)(PH_3)Co^+$ (FG1) and $P(O)(OMe)(SH)^-$ (FG2) of model **4-4a**

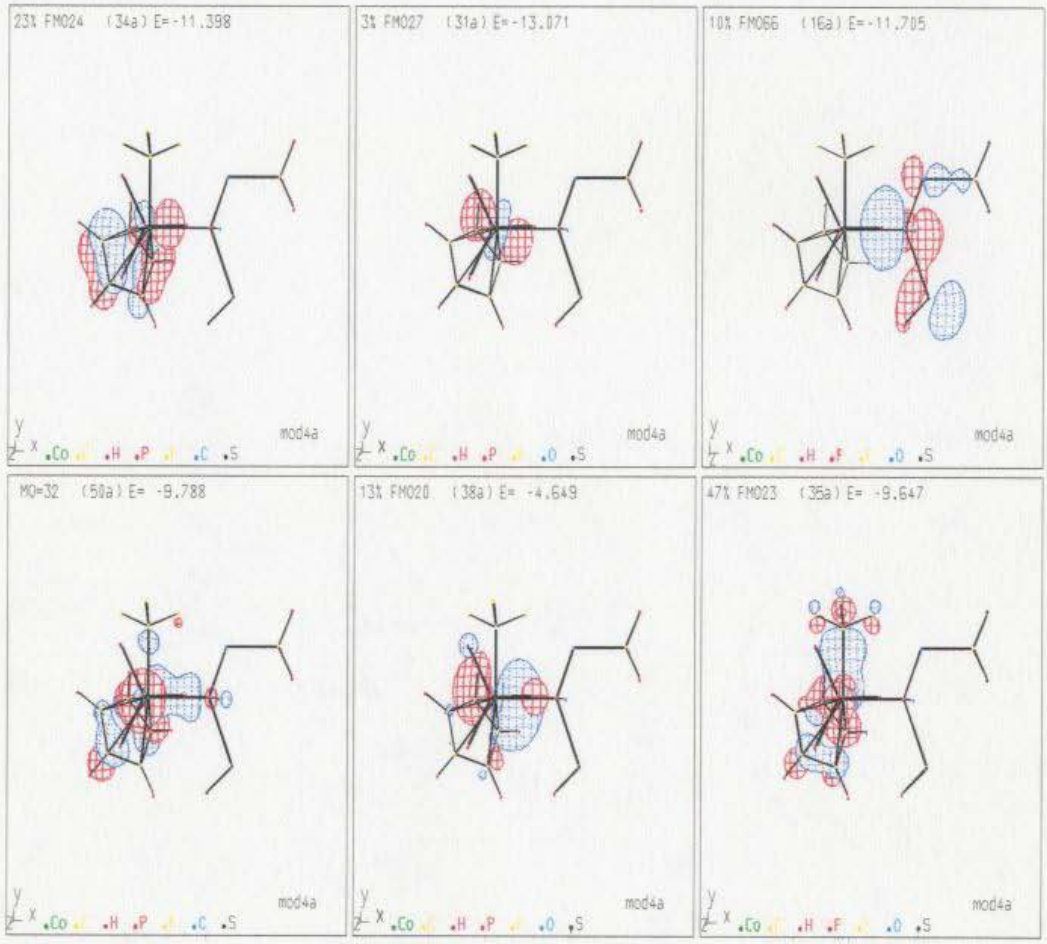

Figure 4.10 Plot of LUMO (MO32) and its major component fragment orbitals for model **4-4a**

the *P*-thiophosphito Co(III) compound **2-4a**. The fragments are developed as shown in Figure 4.2 with $P(O)(OMe)(SH)^-$ as the FG 2.

The input file for analysis is listed in Schedule 4.4. The interaction diagram (Figure 4.9) shows that orbitals from FG1 dominate the LUMO (MO 32), in which FMO 23 and FMO 26 are the major componential fragmental orbitals (Figure 4.10). Although the phosphorus fragment occupies up to 11% of the LUMO (MO 32), the pentavalent phosphorus center contributes less than 7% to the LUMO with its *px* orbital. As shown in Figure 4.10, the LUMO (MO 32) is essentially a metal-based nonbonding orbital with a slightly antibonding contribution from phosphorus. The second empty molecular orbital also contains less than 10% of the orbitals from the phosphorus fragment, in which 7% originates from the phosphorus center.

4.3 EHMO Analysis of Organophosphorus Compounds

The LUMOs of the inorganometallic phosphonate model were compared with those of the corresponding organophosphorus compounds in order to better understanding the vast difference in reactivity. The cobalt fragment in the inorganometallic phosphonate complexes was replaced with a methyl group, while the other functional groups on the pentavalent phosphorus center were left

unchanged so that the effect of the coordination of phosphorus to the cobalt center could be determined. The phosphorus-carbon bond was cleaved to construct the necessary, isostructural fragments (Figure 4.2). Moreover, the phosphorus part was assumed to be P(III) with a formal negative charge while a positive charge was placed on the methyl group in order to be consistent with the inorganometallic phosphonte systems.

Parallel models for **4-1a** and **4-2a**, model **4-1b** was constructed as P(O)(OMe)(NH_2)(Me) (input file listed in Schedule 4.5). The interaction diagram between P(O)(OMe)(NH_2)$^-$ (FG1) and Me^+ (FG2) of **4-1b** (Figure 4.11) demonstrates 91% of the LUMO (MO 13 in Figure 4.12) derives from the phosphorus fragment, in which the phosphorus atom contributes 72%. FG2 contributes 4% to the LUMO. The second empty molecular orbital (MO 12) is entirely composed of the orbitals from the phosphorus fragment.

The phosphinite P(O)(OMe)(Me)(Me) (model **4-2b**), analogous to model **4-3a**, was analyzed using the input file listed in Schedule 4.6. Fragments were developed similar to **4-1b** (Figure 4.2). The EHMO analysis (Figure 4.13 and Figure 4.14) indicated that the LUMO (MO 14) was dominated by the phosphorus fragment (95%). Surprisingly, FG2 contributes 30% to the second unoccupied molecular orbital (MO 13), in which 18% and 4% respectively originate from *px* and *py* orbitals

of the carbon center. However, the energy gap between the LUMO (−0.774 eV) and the second unoccupied molecular orbital (3.955 eV) is so large that nucleophilic reaction is reasonable only on the LUMO (MO 14).

The last organophosphorus model, **4-3b**, was constructed as P(O)(OMe)(SH)(Me) with model **4-4a** as the reference (input file listed in Schedule 4.7). Similar to model **4-1b** and **4-2b**, the LUMO (MO 12 shown in Figure 4.15 and 4.16) is dominated by the orbitals from the phosphorus fragment. In the second unoccupied molecular orbital (MO 11), the contribution from the carbon fragment is up to 67%, which is the largest in the three organophosphorus models. However, the energy gap between the LUMO (0.030 eV) and the second unoccupied molecular orbital (6.070 eV) is very large and is not expected to play a significant role in determining reactivity.

In each inorganometallic phosphonate model, the LUMO is essentially a metal-based, non-bonding orbital (Figure 4.4, 4.6, 4.8, 4.10). It appears likely that orbitally controlled nucleophilic reactions will therefore not occur at phosphorus. The situation is reversed for the organophosphorus compounds. Orbital controlled nucleophilic reactions are directed to the phosphorus center. The coordination of phosphorus to a transition metal protects it against reaction with nucleophiles.

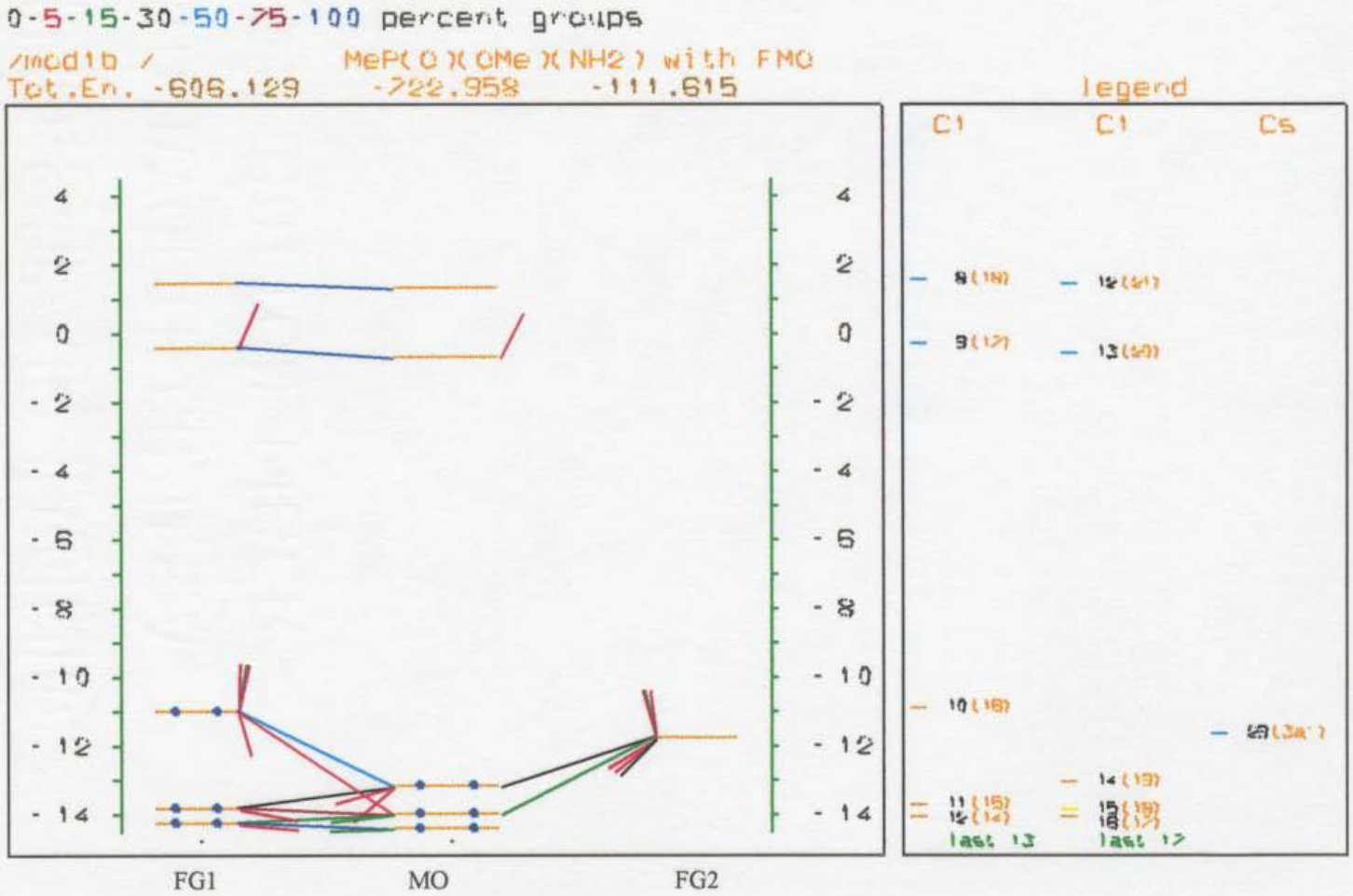

Figure 4.11 Interaction diagram between $P(O)(OMe)(NH_2)^{\cdot}$ (FG1) and Me^{+} (FG2) of model **4-1b**

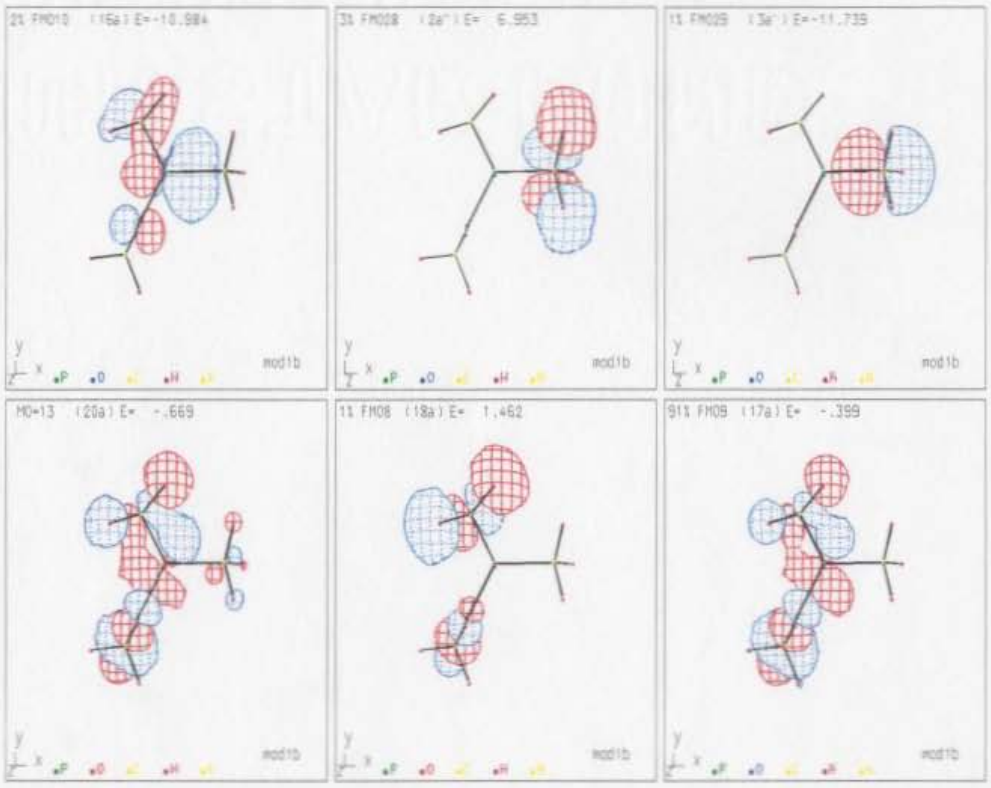

Figure 4.12 Plot of LUMO (MO 13) and its component fragment orbitals for model **4-1b**

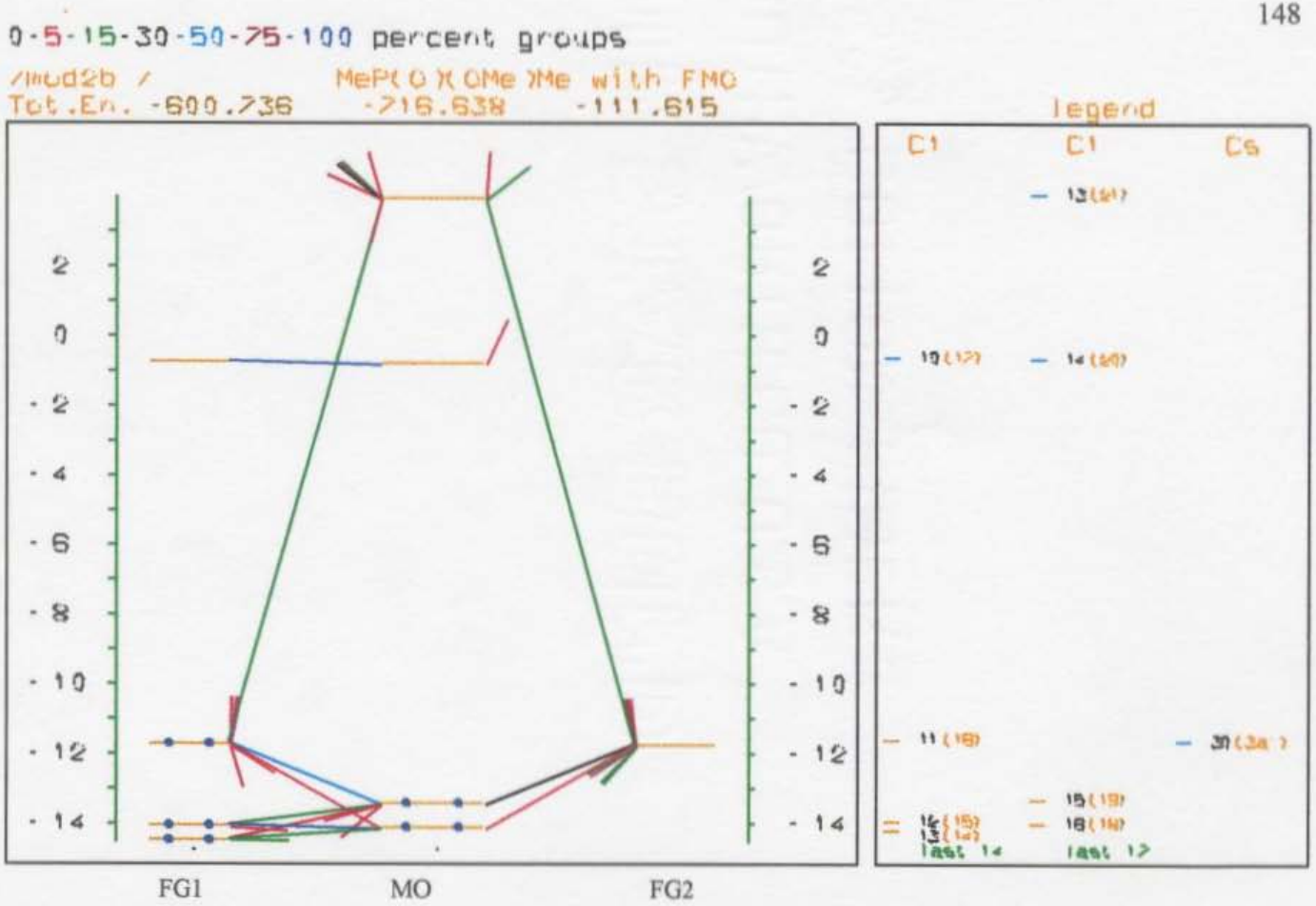

Figure 4.13 Interaction diagram between P(O)(OMe)Me$^-$ (FG1) and Me$^+$ (FG2) of model **4-2b**

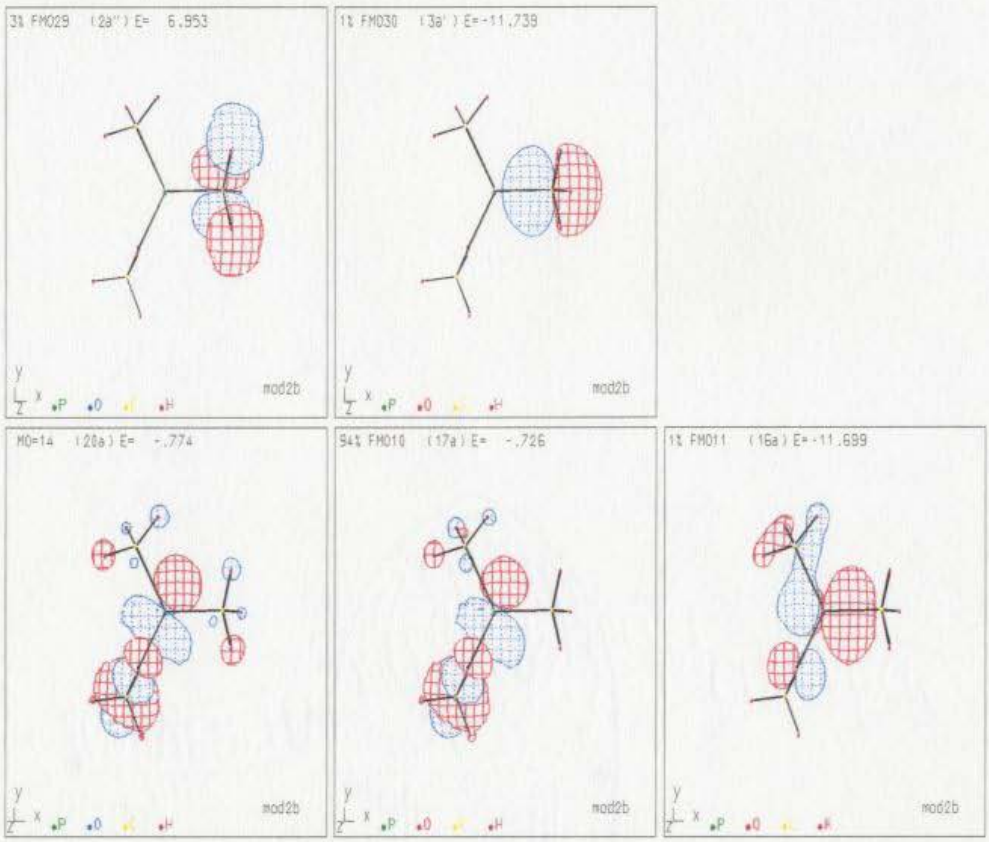

Figure 4.14 Plot of LUMO (MO 14) and its component fragment orbitals for model **4-2b**

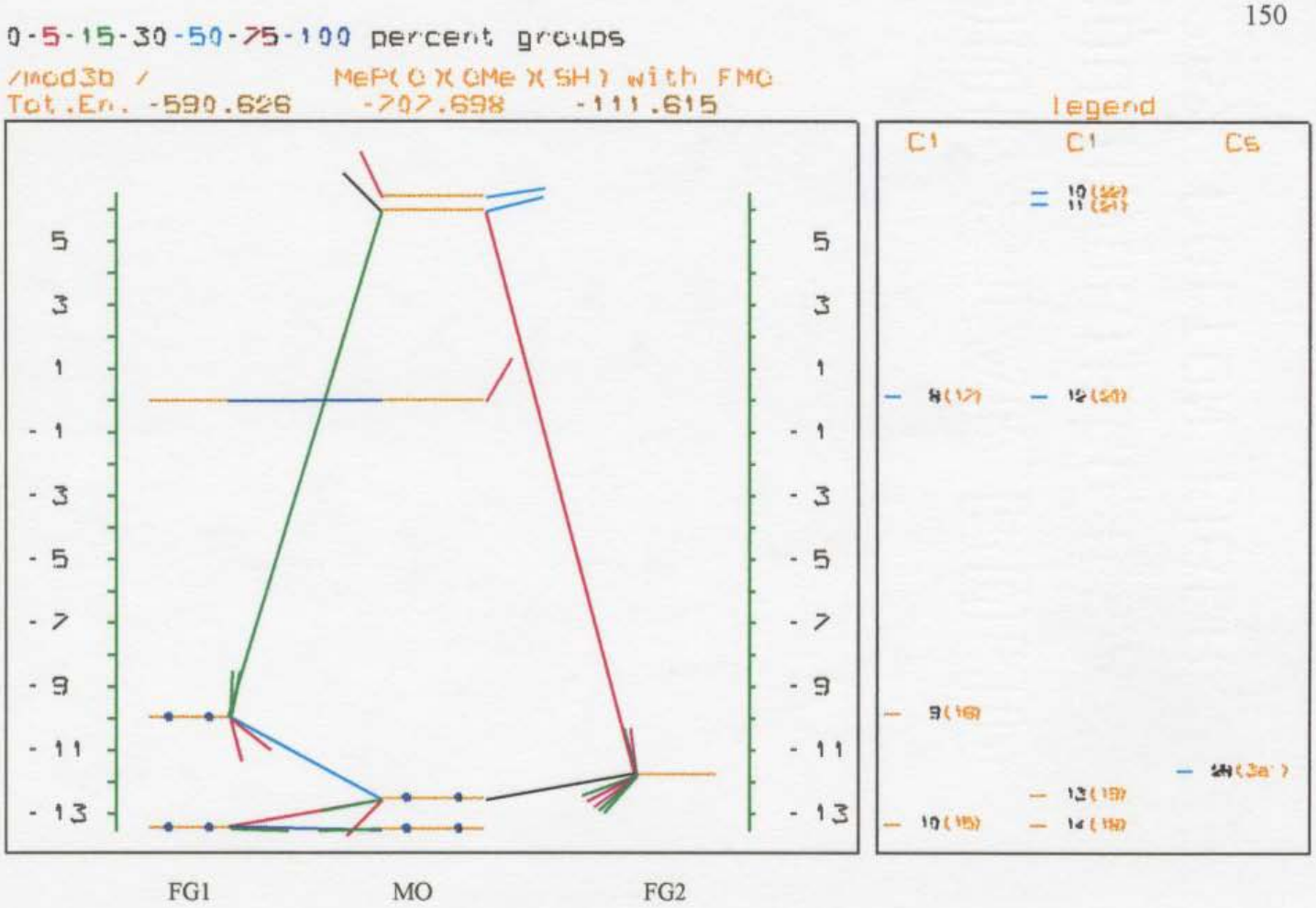

Figure 4.15 Interaction diagram between $P(O)(OMe)(SH)^-$ (FG1) and Me^+ (FG2) of model **4-3b**

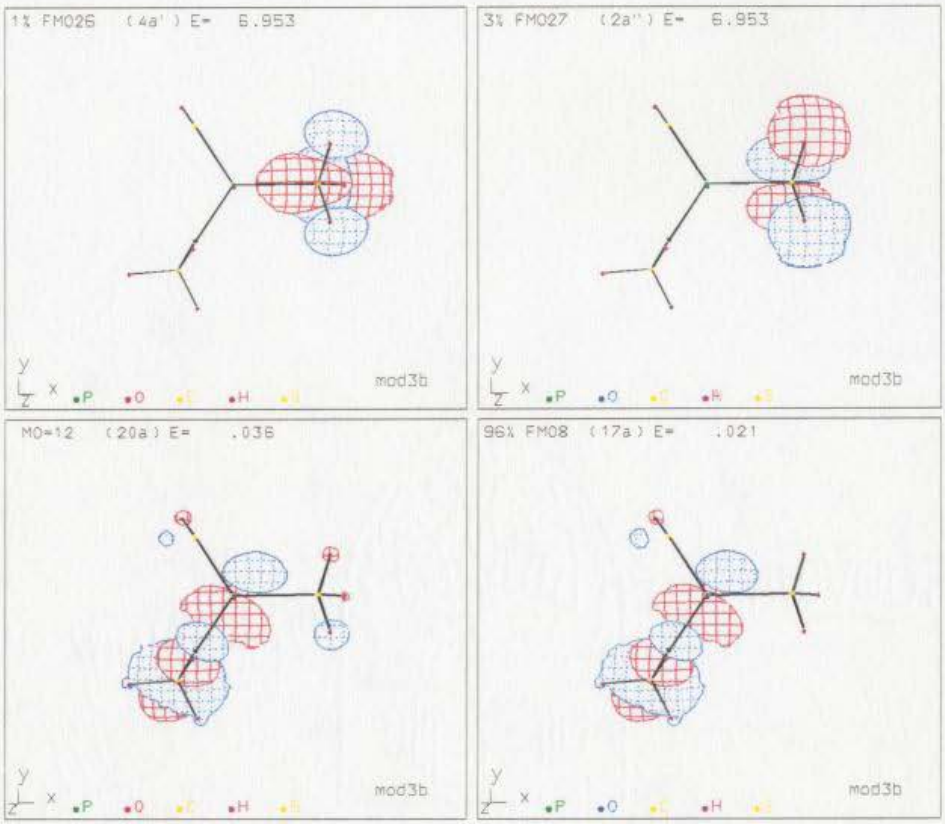

Figure 4.16 Plot of LUMO (MO 12) and its component fragment orbitals for model **4-3b**

4.4 Summary

Simplified models **4-1a** – **4-4a** and **4-1b** – **4-3b,** corresponding to the cobalt phosphonate complexes **2-1a** – **2-4a** and their organophosphorus analogs, were developed based upon the standard bond distances and bond angles. The compositions of LUMOs were analyzed using the EHMO formalism.

The LUMOs of the cobalt phosphonate complexes are dominated by the orbitals from the metal fragment. The influence of the pentavalent phosphorus fragment on the LUMO is very weak. The second empty molecular orbitals of these complexes also contain a very small contribution from the phosphorus fragments. In contrast, the LUMOs of the organic pentavalent phosphorus analogs are dominated by orbitals from the phosphorus fragments. Coordination of the phosphorus atom to the cobalt center shifts the LUMO from the phosphorus to the transition metal, which accounts for the reactivity difference between the inorganometallic and organic phosphonates toward nucleophiles.

Schedule 4.1 EHMO input file for model **4-1a**

```
CpCo(I)(PH3)(P(O)(OMe)(NH2))
 26  0DIST
0,0,0,CO
1,2,CP 2.0,-45.0,45.0
1,12,FO 2.18,180.0,0.0
1,16, I 2.57,90.,90.
1,17, P 2.25,90,0
17,18, O 1.48,109.5,0
17,19, O 1.61,109.5,120.
17,20, N 1.44,109.5,-120.
20,21, H 1.04,109.5,120.
20,22, H 1.04,109.5,-120.
19,23,ME 1.44,-109.5, 0.
FMO
  2 16 10  1 -1
```

Schedule 4.2 EHMO input file for model **4-2a**

```
CpCo(CF3)(PH3)(P(O)(OMe)(NH2))
 29  0DIST
0,0,0,CO
1,2,CP 2.0,-45.0,45.0
1,12,FO 2.18,180.0,0.0
1,16, C 1.95,90.,90.
16,17, F 1.36,-109.5,0.
16,18, F 1.36,-109.5,120.
16,19, F 1.36,-109.5,-120
1,20, P 2.25,90,0
20,21, O 1.48,109.5,0
20,22, O 1.61,109.5,120.
20,23, N 1.44,109.5,-120.
23,24, H 1.04,109.5,120.
23,25, H 1.04,109.5,-120.
22,26,ME 1.44,-109.5, 0.
FMO
  2 19 10  1 -1
```

Schedule 4.3 EHMO input file for model **4-3a**

```
CpCo(CF3)(PH3)(P(O)(OMe)(Me))
 30  0DIST
0,0,0,CO
1,2,CP 2.0,-45.0,45.0
1,12,FO 2.18,180.0,0.0
1,16, C 1.95,90.,90.
16,17, F 1.36,-109.5,0
16,18, F 1.36,-109.5,120.
16,19, F 1.36,-109.5,-120.
1,20, P 2.25,90,0
20,21, O 1.48,109.5,0
20,22, O 1.61,109.5,120.
22,23,ME 1.84,-109.5,0.
20,27,ME 1.44,109.5, -120.
FMO
  2 19 11  1 -1
```

Schedule 4.4 EHMO input file for model **4-4a**

```
CpCo(CF3)(PH3)(P(O)(OMe)(SH))
 28  0DIST
0,0,0,CO
1,2,CP 2.0,-45.0,45.0
1,12,FO 2.18,180.0,0.0
1,16, C 1.95,90.,90.
16,17, F 1.36,-109.5,0
16,18, F 1.36,-109.5,120.
16,19, F 1.36,-109.5,-120.
1,20, P 2.25,90,0
20,21, O 1.48,109.5,0
20,22, O 1.61,109.5,120.
22,23,ME 1.84,-109.5,0.
20,27, S 2.17,109.5, -120.
27,28, H 1.14,109.5,0.
FMO
  2 19  9  1 -1
```

Schedule 4.5 EHMO input file for model **4-1b**

```
MeP(O)(OMe)(NH2) with FMO
 14  0DIST
0.,0.,0., P
1,2, O 1.5,0.,0.
1,3, O 1.62,109.5,-120.
3,4,ME 1.44,109.5,0.
1,8, N 1.44,109.5,120.
8,9, H 1.04,109.5,120.
8,10, H 1.04,109.5,-120.
1,11,ME 1.80,109.5,0.
FMO
  2 10  4 -1  1
```

Schedule 4.6 EHMO input file for model **4-2b**

```
MeP(O)(OMe)Me with FMO
 15  0DIST
0.,0.,0., P
1,2, O 1.5,0.,0.
1,3, O 1.62,109.5,-120.
3,4,ME 1.44,109.5,0.
1,8,ME 1.80,109.5,120.
1,12,ME 1.80,109.5,0.
FMO
  2 11  4 -1  1
```

Schedule 4.7 EHMO input file for model **4-3b**

```
MeP(O)(OMe)(SH) with FMO
 13  0DIST
0.,0.,0., P
1,2, O 1.5,0.,0.
1,3, O 1.62,109.5,-120.
3,4,ME 1.44,109.5,0.
1,8, S 1.64,109.5,120.
8,9, H 1.04,109.5,0.
1,10,ME 1.80,109.5,0.
FMO
  2  9  4 -1  1
```

References

[1] Eardman, N. *Chem. & Engr. News* **1993**, Oct., 35

[2] Scott. J. W. In *Asymmetric Synthesis: Vol 5, Chiral Catalysis*; Morrison, J. D., Ed.; Academic Press: Orlando, 1985

[3] Brunner, H. In *The Chemistry of the Metal-Carbon Bonds: Vol. 5, Enantioselective Synthesis with Optically Active Transition Metal Catalysts*; Hartley, F. R., Ed.; John Wiley & Sons: Chichester, 1989

[4] Aitken, R. A.; Kilényi, S. N. In *Asymmetric Synthesis: Sources and Strategies for the Formation of Chiral Compounds*; Chapman & Hall: London, 1992

[5] Brunner, H.; Zettlmeier, W. In *Handbook of Enantioselective Catalysis*; VCH: New York, 1993

[6] Noyori, R. *Science* **1990,** *248*, 1194

[7] Coppola, G. M.; Schuster, H. F. In *Asymmetric Synthesis - Construction of Chiral Molecules Using Amino Acids*; John Wiley & Sons: New York, 1987

[8] Arnold, D.; Drover, J. C. G.; Vederas, J. C. *J. Am. Chem. Soc.* **1987**, *109*, 4649

[9] Kagon, H. B.; Fiaud, J. C. *Top. Stereochem.* **1988**, *18*, 249

[10] Seyden-Penne, J. In *Chiral Auxiliaries and Ligands in Asymmetric Synthesis*; John Wiley & Sons: New York, 1995

[11] Davies, S. G. In *Organotransition Metal Chemistry: Application To Organic Synthesis*;

Pergamon Press: New York, 1986

[12] Crabtree, R. H. In *The Orgaometallic Chemistry of the Transition Metals,* 3rd; John Wiley & Sons: New York, 1994

[13] Nozaki, H.; Moriuti, S.; Takaya, R.; Noyori, R. *Tetrahedron Lett.* **1966**, 5239

[14] Knowles, W. S.; Sabacky, M. J. *Chem. Commun.* **1968**, 1445

[15] Halpern, J. *Science* **1982**, *217*, 401

[16] Shriver, D. F.; Atkins, P.; Langford, C. H. In *Inorganic Chemistry*; Freeman: New York, 1994

[17] Kagan, H. B.; Dang, T.-P. *J. Am. Chem. Soc.* **1972**, *94*, 6429

[18] Vineyard, B. D.; Knowles, W. S.; Sabacky, M. J.; Bachman, G. L.; Weikauff, D. J. *J. Am. Chem. Soc.* **1977**, *99*, 5946

[19] Knowles, W. S.; Sabacky, M. J.; Vineyard, B. D. *J. Chem. Soc., Chem. Commun.* **1972**, 10

[20] Landis, C. R.; Halpern, J. *J. Am. Chem. Soc.* **1987**, *109*, 1746

[21] Brunner, H.; Nishiyama, H.; Itoh, K. In *Catalytic Asymmetric Synthesis*; Ojima, I., Ed.; VCH: New York, 1993

[22] Nugent, W. A.; RajanBabu, T. V.; Burk, M. J. *Science* **1993**, *259*, 479

[23] Blystone, S. I. *Chem. Rev.* **1989**, *89*, 1663

[24](a) Fernandez, J. M.; Emerson, K.; Larsen, R. D.; Gladysz, J. A. *J. Chem. Soc., Chem. Commun.* **1988**, 37; (b) Fernandez, J. M.; Larsen, R. H.; Gladysz, J. A. *J. Am. Chem. Soc.*

1986, *108*, 8268

[25] Davies, S. G.; Dordor, I. M.; Warner, P. *J. Chem. Soc., Chem. Commun.* **1984**, 956

[26](a) Liebeskind, L. S; Welker, M. E. *Tetrahedron Lett.* **1984**, *25*, 4314; (b) Liebeskind, L. S.; Welker, M. E.; Fengl, R. W. *J. Am. Chem. Soc.* **1986**, *108*, 6328

[27] Kosolapoff, G. M. In *Organic phosphorus Compounds*; John Wiley & Sons: New York, 1972

[28] Borman, S. *Chem. & Engr. News* **1990**, July 7, 9

[29] Fisher, E. B.; Van Wazer, J. R. In *Phosphorus and Its Compounds: Uses of Organic Phosphorus Compounds*, Vol II; Van Wazer, J. R., Ed.; Interscience: New York, 1961

[30] Bücher, J. W.; Shliebs, R.; Winter, G.; Büchel, K. H. In *Indurstrial Inorganic Chemistry*; VCH: New York, 1989

[31] Morifusa, E. In *Organophosphorus Pesticides: Organic and Biological Chemistry,* CRC Press, 1974

[32] Lange, W.; Krueger, B. *Chem. Ber.* **1932**, *65*, 1598

[33] Saunder, B. C. In *Some Aspects of the Chemistry and Toxic Action of Organic Compounds Containing Phosphorus and Fluorine;* Cambridge University Press: London, 1957

[34] Stinson, S. *Chem. & Eng. News* **1993**, 38

[35] Cramer, F. *Angew. Chem.* **1960**, *72*, 236

[36] Holmstedt, B. In *Cholinesterases and Anticholinesterase Agents: Structure-Activity*

Relationship of the Organophosphorus Antiocholinesterase Agents; Koeue, G. B., Ed.; Spring-Verlag: Berlin, 1963

[37] Eto, M. *Biosci. Biotechnol. Biochem.* **1997**, *61*, 1

[38] Grothusen, J. R.; Brown, T. M. *Pestic. Biochem. Physiol.* **1986**, *26*, 100

[39] Palmer, C. J.; Smith, I. H.; Moss, M. D. V.; Cadisa, J. E. *J. Agric. Food Chem.* **1990**, *38*, 1091

[40] Abell, L. M.; Hanna, W. S.; Kunitsky, K. J.; Kerscher, J. A. *Pestic. Sci.* **1995**, *44*, 89

[41] Baillie, A. C.; Wright, K.;Wright, B. J.; Earnshaw, C. G. *Pestic. Biochem. Physiol.* **1988**, *30,* 103

[42] Allen, J. G.; Atherton, F. R.; Hall, J. J.; Hassall, C. H.; Holmes, S. W.; Lambert, R. W.; Ringrose, P. S. *Nature* **1978**, *272*, 56

[43] Bachietto, T.; Saidrenau, P.; Bompeix, G. *Pestic. Biochem. Physiol.* **1983**, *19*, 122

[44] Shiguya, S.; Shimazai, I. In *Shibuya Index,* 7th; Zen-Noh, Kumiai Chem. Inc.: Tokyo, 1996

[45] Ember, L. *Chem & Eng. News* **1995**, March, 6

[46] Krise, J. P.; Stella, V. J. *Advanced Drug Delivery Reviews* **1996**, *19,* 287

[47] (a) Patel, D. V.; Rielly-Gauvin, K.; Ryono, D. E. *Tetrahedron. Lett.* **1990**, *31*, 5587; (b) Patel, D. V.; Rielly-Gauvin, K.; Ryono, D. E. *Tetrahedron. Lett.* **1990**, *31*, 5591

[48] Sikorski, J. A.; Miller, M. J.; Braccolino, D. S.; Cleary, D. G.; Corey, S. D.; Font, J. L.; Gruys, K. J.; Han, C. Y.; Lin, K. C.; Pansegrau, P. D.; Ream, J. E.; Schnur, D.; Shah, A.;

Walker, M. C. *Phosphorus, Sulfur, and Silicon* **1993**, *76,* 115

[49] Stowasser, B.; Budt, K.-H.; Li, J. Q.; Peyman, A.; Ruppert, D. *Tetrahedron Lett.* **1992**, *33*, 6625

[50] Wieczorek, P.; Lejczak, B.; Kaczanowska, M.; Kafarski, P. *Pestic. Sci.* **1990**, *30*, 43

[51] Hassan, A.; Dauterman, W. C. *Biochem. Pharmacol.* **1968**, *17*, 1431

[52] Meisenheimer, J.; Lichtenstadt, L. *Chem. Ber.* **1911,** *44*, 356

[53] Michel, H. O. *Fed. Proc.* **1955,** *14*, 255

[54] Ohkawa, H. In *Insecticide Mode of Action*; Coats, J. R., Ed.; Academic Press: New York, 1982

[55] Fukuto, T. R. *Bull. E. H. O.* **1977**, *44*, 31

[56] Berman, H. A.; Leonard, K. *J. Biol. Chem.* **1989**, *264*, 3942

[57] Miyazaki, A.; Nakamura, T.; Kawaradani, M.; Marumo, S. *J. Agric. Food Chem.* **1988**, *36*, 835

[58] Sussman, J. L.; Harel, M.; Frolow, F.; Oefner, C.; Goldman, A.; Toker, L.; Silman, I. *Science* **1991**, *253*, 872

[59] Pietrusiewiza, K. M.; Zablocka, M. *Chem. Rev.* **1994**, *94*, 1375

[60] Field, M.; Schmutzler, R. In *Organic Phosphorus Compounds, Vol.4*; Kosolapoff, G. M.; Maier, L., Eds.; Wiley Interscience: New York, 1972

[61] Meisenheimer, J.; Cooper, J.; Horing, M.; Lauter, W.; Lichtenstadt, L.; Samuel, M. *Justus Leibigs Ann. Chem.* **1926**, *449*, 213

[62] Cerivinka, O.; Kriz, O. *Collect Czech. Chem. Commun.* **1966**, *31*, 1910

[63] Ostrogovich, G.; Kerek, F. *Angew. Chem.* **1971**, *13*, 496

[64] Davies, W. C.; Mann, F. G. *J. Chem. Soc.* **1944,** 276

[65] Tani, K.; Brown, L. D.; Ahmed, J.; Ibers, J. A.; Yokota, M.; Nakamura, A.; Otsuka, S. *J. Am. Chem. Soc.* **1977**, *99*, 7876

[66] Otsuka, S.; Nakamura, A.; Kano, T.; Tani, K. *J. Am. Chem. Soc.* **1971**, *93*, 4301

[67] Roberts, N. K.; Wild, S. B. *J. Am. Chem. Soc.* **1979**, *101*, 6254

[68] Salem, G.; Wild, S. B. *Inorg. Chem.* **1983**, *22*, 4049

[69] Martin, J. W. L.; Palmer, J. A. L.; Wild, S. B. *Inorg. Chem.* **1984**, *23*, 2664

[70] Leung, P. H.; Willis, A. C.; Wild, S. B. *Inorg. Chem.* **1992**, *31*, 1406

[71] Bogdanović, B.; Henc, B.; Lösler, A.; Meister, B.; Pauling, H.; Wilke, G. *Angew. Chem, Int. Ed. Engl.* **1973**, *12*, 954

[72] Crisp, G. T.; Salem, G.; Wild, S. B. *Organometallics* **1989**, *8*, 2360

[73] Bader, A.; Salem, G.; Willis, A. C.; Wild, S. B. *Tetrahedron: Asymmetry* **1992**, *3*, 1227

[74] Yoshikuni, T.; Bailar, J. C., Jr. *Inorg. Chem.* **1982**, *21*, 2129

[75] Naylor, R. A.; Walker, B. J. *J. Chem. Soc., Chem. Commun.* **1975**, 45

[76] Stec, W. J. *Acc. Chem. Res.* **1983**, *16*, 411

[77] Harrison, J. M.; Inch, T. D.; Lewis, G. J. *J. Chem. Soc., Perkin Trans.* **1975**, *1*, 1892

[78] Nudelman, A.; Cram, D. J. *J. Am. Chem. Soc.* **1968**, *90*, 3869

[79] Korpiun, O.; Mislow, K. *J. Am. Chem. Soc.* **1967**, *89*, 4784

[80] Korpiun, O.; Lewis, R. A.; Chickos, J.; Mislow, K. *J. Am. Chem. Soc.* **1968**, *90*, 4842

[81] Carey, J. V.; Barker, M. D.; Brown, J. M.; Russel, M. J. H. *J. Chem. Soc., Perkin Trans.* **1993**, *1*, 831

[82] Blazis, V. J.; Cruz, A. D. L.; Koeller, K. *Phosphorus, Sulfur and Silicon* **1993**, *75*, 159

[83] Blazis, V. J.; Koeller, K. J.; Spilling, C. D. *Tetrahedron: Asymmetry* **1994**, *5*, 499

[84] Masci, B. *Tetrahedron* **1995**, *51*, 5459

[85] Masters, C. In *Homogeneous Transition-Metal Catalysis- A Gentle Art*; Chapman and Hall: New York, 1981

[86] Hitchcock, P. B.; Lappert, M. F.; Leung, W.-P. *J. Chem. Soc., Chem. Commun.* **1987**, 1282

[87] Cowley, A. H.; Pellerin, B.; Atwood, J. L.; Bott, S. G. *J. Am. Chem. Soc.* **1990**, *112*, 6734

[88] Mercier, F.; Mathey, F. *J. Chem. Soc., Chem. Commun.* **1984**, 782

[89] (a) Niecke, E.; Engelmann, M.; Zorn, H.; Krebs, B.; Henkel, G. *Angew. Chem.* **1980**, *92*, 738; (b) Niecke, E.; Engelmann, M.; Zorn, H.; Krebs, B.; Henkel, G. *Angew. Chem., Int. Ed. Engl.* **1980**, *19*, 710

[90] Marinetti, A.; Mathey, F. *J. Chem. Soc., Chem. Commun.* **1982**, 667

[91] Bauer, S.; Marinetti, A.; Ricard, L.; Mathey. F. *Angew. Chem.* **1990**, *102*, 1188

[92] Bauer, S.; Marinetti, A.; Ricard, L.; Mathey. F. *Angew. Chem., Int. Ed. Engl.* **1990**, *29*, 1161

[93] Mathey, F.; Marinetti, A.; Mercier, F. *Synlett* **1992**, (May) 363

[94] Stelzer, O.; Langhans, K.-P. In *The Chemistry of Organophosphorus Compounds,* Vol I; Hartley, F. R., Ed.; Wiley: New York, 1990

[95] Weber, L. *Angew.Chem., Int. Ed. Engl.* **1996**, *35*, 271

[96] Brown, T. L.; Lee, K. *Coord. Chem. Rev.* **1993**, *128*, 89

[97] Hall, C. R.; Williams, N. E. *Tetrahedron Lett.* **1980**, *21*, 4959

[98] Abell, A. M.; Hanna, W. S.; Kuntisky, K. J.; Herscher, J. A. *Pestic. Sci.* **1995**, *44*,89

[99] White, D.; Coville, N. J. *Advances in Organometallic Chemistry* **1994,** *36*, 95

[100] (a) Scherer, O. J.; Aitzmann, H.; Wolmershäuser, G. *Angew. Chem., Int. Ed. Engl.* **1985**, *24*, 351; (b) Scherer, O. J.; Schwalb, J.; Swarowsky, H.; Wolmershäuser, G; Kaim, W.; Gross, R. *Chem. Ber.* **1988**, *121*, 443

[101] (a) Scherer, O. J.; Schwalb, J.; Wolmershäuser, G; Kaim, W.; Gross, R. *Angew. Chem.* **1986**, *98*, 293; (b) Scherer, O. J.; Brück, H.; Wolmershäuser, G. *Chem. Ber.* **1989**, *122*, 2049

[102] Hitchcock, P. B.; Mahh, M. J.; Nixon, J. F. *J. Chem. Soc., Chem. Commun.* **1986**, 737

[103] Binger, P.; Milczarek, R.; Mynott, R.; Regitz, M.; Rosch, W. *Angew. Chem., Int. Ed. Engl.* **1986**, *25,* 644

[104] Gleiter, R.; Hyla-Kryspin, I.; Binger, P.; Regitz, M. *Organometallics,* **1992**, *11*, 177

[105] Binger, P.; Glaser, G.; Gabor, B.; Mynott, R. *Angew. Chem., Int. Ed. Engl.* **1995**, *34*, 81

[106] Fehlner, T. P. In *Inorganic Chemistry*; Plenum Press: New York, 1992

[107] Holah, D. G.; Hughes, A. N.; Kleemla, D. *J. Heterocycl. Chem.* **1978**, *15*, 1319

[108] Lacombe, S.; Gonbeau, D.; Cabioch, J.-L.; Pellerin, B.; Denis, J-M.; Pfister-Guillouzo, G. *J. Am. Chem. Soc.* **1988**, *110,* 6964

[109] (a) Hall, C. R.; Inch, T. D. *Phosphorus and Sulfur* **1979**, *7*, 171; (b) Hall, C. R.; Inch, T. D. *Tetrahedron Lett.* **1976**, 3645

[110] Van der Knap, Th. A.; Kebach, Th. C.; Lourens, R.; Vos, M.; Bickelhaupt, F. *J. Am. Chem. Soc.* **1983,** *105*, 4026

[111] Nakazawa, H.; Kadoi, Y.; Itoh, T.; Mizuta, T.; Miyoshi, K. *Organometallics* **1991**, *10*, 766

[112] Bhattacharya, A. K.; Thygarajan, G. *Chem. Rev.* **1981**, *81,* 415

[113] Landauer, S. R.; Rydon, H. N. *J. Chem. Soc.* **1953**, 2224

[114] Brill, T. B.; Landon, S. J. *Chem. Rev.* **1984**, *84*, 577

[115] Landon, S. J.; Brill, T. B. *J. Am. Chem. Soc.* **1982**, *104*, 6571

[116] Landon, S. J.; Brill, T. B. *Inorg. Chem.* **1984**, *23,* 1266

[117] Goh, L.-Y.; D'Aniello, M. J.; Slater, S.; Muetterties, E. L.; Tavanaiepour, I.; Chang, M. I.; Fredrich, M. F.; Day, V. W. *Inorg. Chem.* **1979**, *18,* 192

[118] Dessy, R. E.; Pohl, R. L.; King, R. B. *J. Am. Chem. Soc.* **1966**, *88*, 5121

[119] Howell, J. A. S.; Rowan, A. J. *J. Chem. Soc., Dalton Trans.* **1980**, 1845

[120] Howell, J. A. S.; Rowan, A. J.; Snell, M. S. *J. Chem. Soc., Dalton Trans.* **1981**, 325

[121] Nakazawa, H.; Yamaguchi, M.; Kubo, K.; Miyoshi, K. *J. Organomet. Chem.* **1992**,

428, 145

[122] Eliel, E. L.; Wilen, S. H. In *Stereochemistry of Organic Compounds*; John Wiley & Sons: New York, 1994

[123] (a) Brunner, H.; Schmidt, E. *J. Organomet. Chem.* **1970**, *21*, 53; (b) Brunner, H.; Schmidt, E. *J. Organomet. Chem.* **1972**, *36*, C18; (c) Brunner, H.; Schmidt, E. *J. Organomet. Chem.* **1973**, *50*, 219

[124] Brown, J. M.; Davies, S. G. *Nature* **1989**, *342*, 631

[125] Yu, Y.; Jablonski, C.; Bridson, J. *Organometallics* **1997**, *16*, 1270

[126] Brunner, H. *Angew. Chem., Int. Ed. Engl.* **1983**, *22*, 897

[127] Brunner, H. *J. Organomet. Chem.* **1986**, *300*, 39

[128] Brunner, H. *Top. Stereochem.* **1988**, *18*, 129

[129] Knowles, W. S.; Sabacky, M. J.; Vineyard, B. D.; Weinkauff, D. J. *J. Am. Chem. Soc.* **1975**, *97*, 2567

[130] Knowles, W. S.; Sabacky, M. J.; Vineyard, B. D. *Adv. Chem. Ser.* **1974**, *132*, 274

[131] Vinyard, B. D.; Knowls, W. S.; Bachman, G. L.; Weinkauff, D. J. *J. Am. Chem. Soc.* **1977**, *99*, 5946

[132] De Bruins, K. E.; Perrin, E. D. *J. Org. Chem.* **1975**, *40*, 1523

[133] Herriott, A. *J. Am. Chem. Soc.* **1971**, *93*, 3304

[134] Farnham, W. B.; Lewis, R. A.; Murray, R. K.; Mislow, K. *J. Am. Chem. Soc.* **1970**, *92*, 5809

[135] Farnham, W. B.; Murray, R. K.; Mislow, K. *J. Chem. Soc., Chem. Comm.* **1971**, 146

[136] Gorenstein, D. G. In *Phosphorus-31 NMR Principles and Applications*; Academic Press: Orlando, 1984

[137] Haines, R. J.; DuPreez, A. L.; Marais, L. L. *J. Organomet. Chem.* **1971**, *28*, 405

[138] Harder, V.; Werner, H. *Helv. Chim. Acta* **1973**, *56*, 1620

[139] Kiplinger, J. L.; Richmond, T. G.; Osterberg, C. E. *Chem. Rev.* **1994**, *94*, 373

[140] (a) Mason, R.; Russell, D. R. *J. Chem. Soc., Chem. Commun.* **1965**, 182; (b) Churchill, M. R. *Inorg. Chem.* **1965**, *4*, 1734; (c) Churchill, M. R. *Inorg. Chem.* **1967**, *6*, 185; (d) Churchill, M. R.; Fennessey, J. P. *Inorg. Chem.* **1967**, *6*, 1213

[141] (a) Cotton, F. A.; McClevery, J. A. *J. Organomet. Chem.* **1965**, *4*, 490; (b) Cotton, F. A.; Wing, R. M. *J. Organomet. Chem.* **1967**, *9*, 511-517; (c) Graham, W. A. G. *Inorg. Chem.* **1968**, *7*, 315; (d) Hall, M. B.; Fenske, R. F. *Inorg. Chem.* **1972**, *11*, 768

[142] King, R. B.; Bisnette, M. B. *J. Organomet. Chem.* **1964**, *2*, 15

[143] Gallop, M. A.; Roper, W. A. *Adv. Organomet. Chem.* **1986**, *25*, 121

[144] Brothers, P. J.; Roper, W. R. *Chem. Rev.* **1988**, *88*, 1293

[145] Zhou, Z. Ph.D dissertation, 1994, Memorial University of Newfoundland

[146] Zhou, Z.; Jablonski, C.; Bridson, J. *Organometallics* **1994**, *13*, 781

[147] Zhou, Z.; Jablonski, C.; Bridson, J. *Organometallics* **1993**, *461*, 215

[148] Stanley, K.; Baid, M. C. *J. Am. Chem. Soc.* **1975**, *97*, 6598

[149] Huheey, J. E. In *Inorganic Chemistry: Principles of Structure and Reactivity*, 3nd;

Harper and Row: New York, 1983

[150] Smart, B. E. In *Chemistry of Functional Groups, Supplement D*; Patai, S.; Rappoport, Z., Eds.; Wiley: New York, 1983

[151] Henri, C. D.; Silvester, M. J. *Alderichchim, Acta* **1988**, *21*, 3

[152] Risswall, T. *Environ. Sci, Technol.* **1991**, *25*, 567

[153] Schoeberl, M. R.; Hartmann, D. L. *Science* **1991**, *251,* 46

[154] Cicerone, R. J.; Eillotr, S.; Turco, R. P. *Science* **1991**, *254*, 1191

[155] Brunner, H.; Jablonski, C.; Johnes, P. *Organometallics*, **1988**, *7*, 1283

[156] Pietrusiewicz, K. M; Zablocka, M. *Chem. Rev.* **1994**, *94*, 1376

[157] Sheldrick, G. M. In *Crystallographic Computing 3*; Oxford University Press, 1985

[158] Beurskens, P. T.; Admiraal, G.; Bosman, W. P.; de Gelder, R; Israel, R.; Smits, J. M. M. The DIRDIF-94 program system, Technical Report of the Crystallography Laboratory, University of Nijmegen, The Netherlands

[159] Mitchell, M. C; Kee, T. P. *Coord. Chem. Rev.* **1997**, *158*, 359

[160] Jean, Y.; Volatron, F.; Burdett, J. In *An Introduction to Molecular Orbitals*; Oxford University Press: New York, 1993

[161] (a) Hoffman, R. J. *Chem. Phys.* **1963**, *39*, 1397; (b) Hoffman, R. J. *Chem. Phys.* **1962**, *39*, 1397

Appendices

The selected ^{1}H and ^{19}F NMR spectra are arranged according to the order in which they appear in the text. For the experimental details, see Experimental Section in the corresponding chapters.

Figure A1. ^{1}H NMR of ($R_{Co}R_P$) / ($S_{Co}S_P$) -(η^5-Cp)Co(C_3F_7)(PPhMe$_2$)(P(O)(OMe)Ph) **(2-1a)**

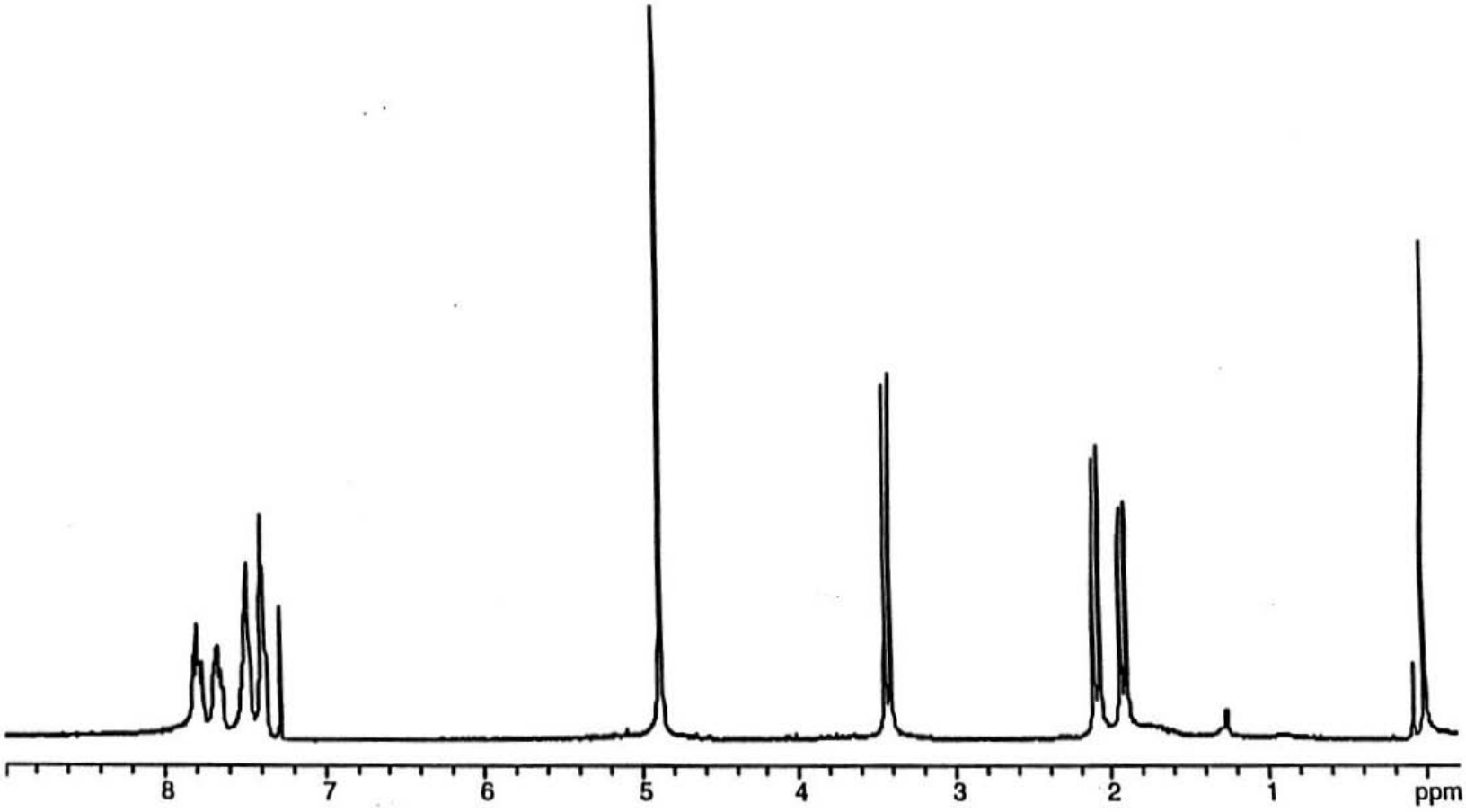

Figure A2 ^{1}H NMR of (S_{Co},R_P) / (R_{Co},S_P) -(η^5-Cp)Co(C_3F_7)($PPhMe_2$)(P(O)(OMe)Ph) **(2-1b)**

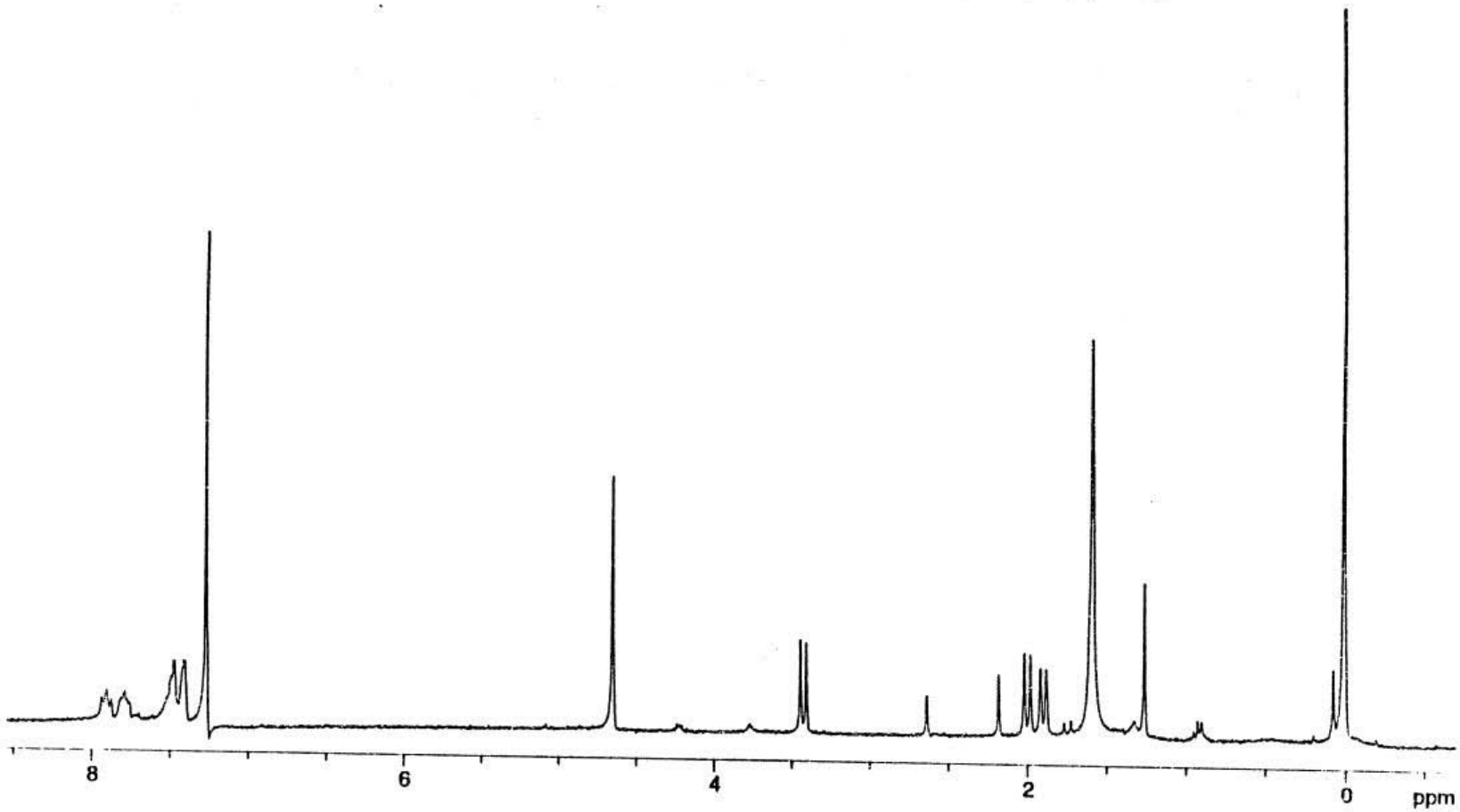

Figure A3. ^{1}H NMR of $(\eta^{5}\text{-}C_{5}H_{5})Co(C_{3}F_{7})(PPhMe_{2})(P(O)Ph(OMe))$ **(2-1c)**

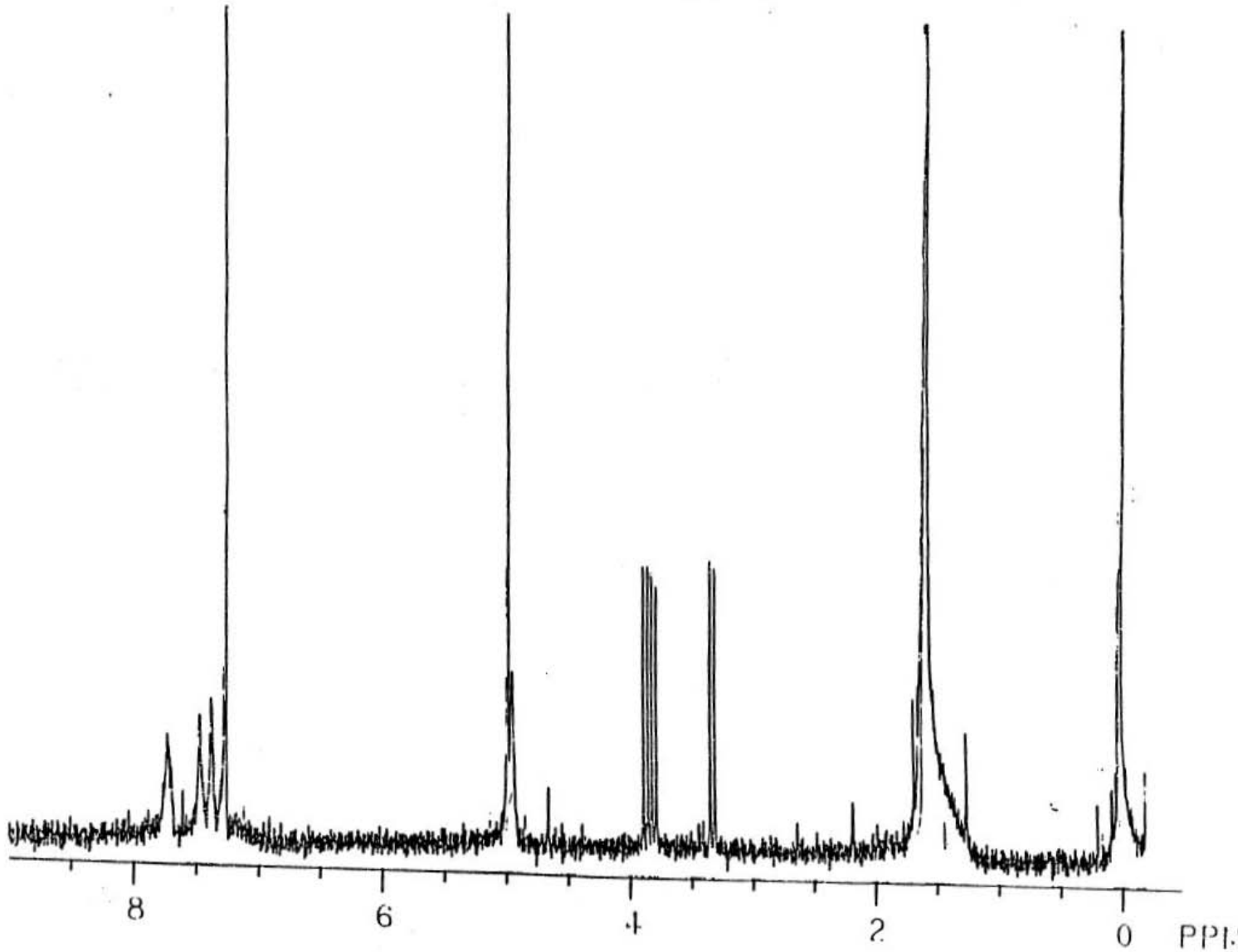

Figure A4 ^{1}H **NMR of** $(\eta^{5}\text{-Cp})Co(C_3F_7)(PPh(OMe)_2)(P(O)(OMe)Ph)$ **(2-1d)**

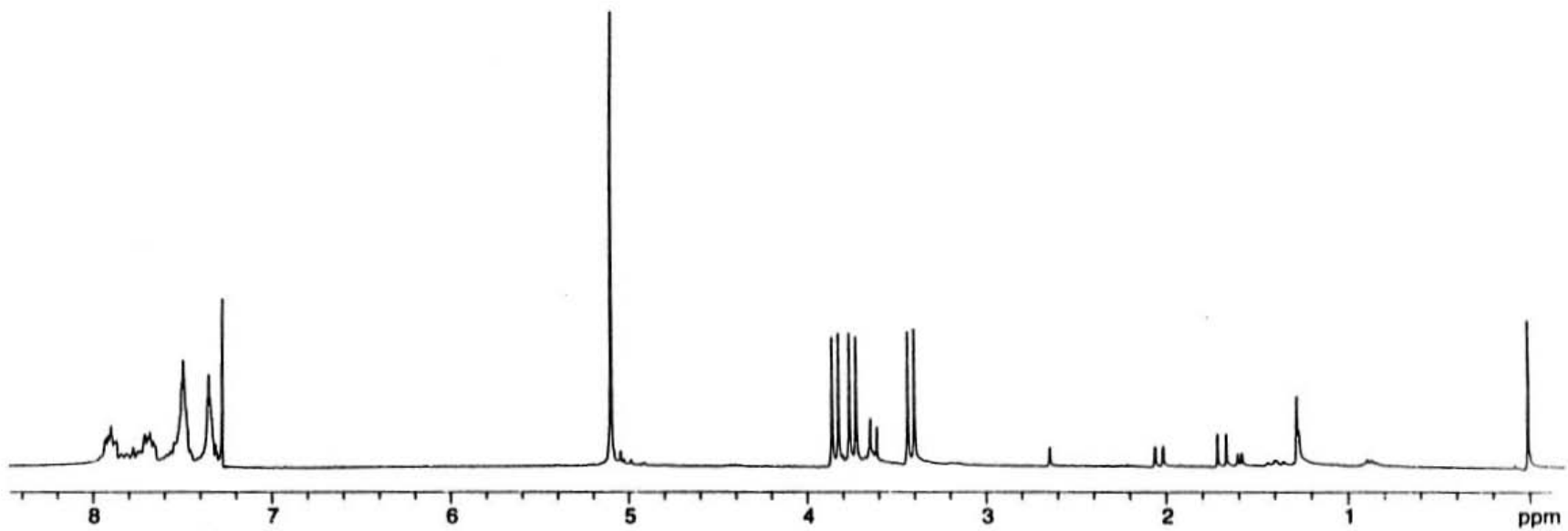

Figure A5 ^{1}H NMR of (S_C,S_{Co},R_P)-(η^5-Cp)Co(I)(PNH)(P(O)(OMe)(NEt$_2$)) **(2-2a)**

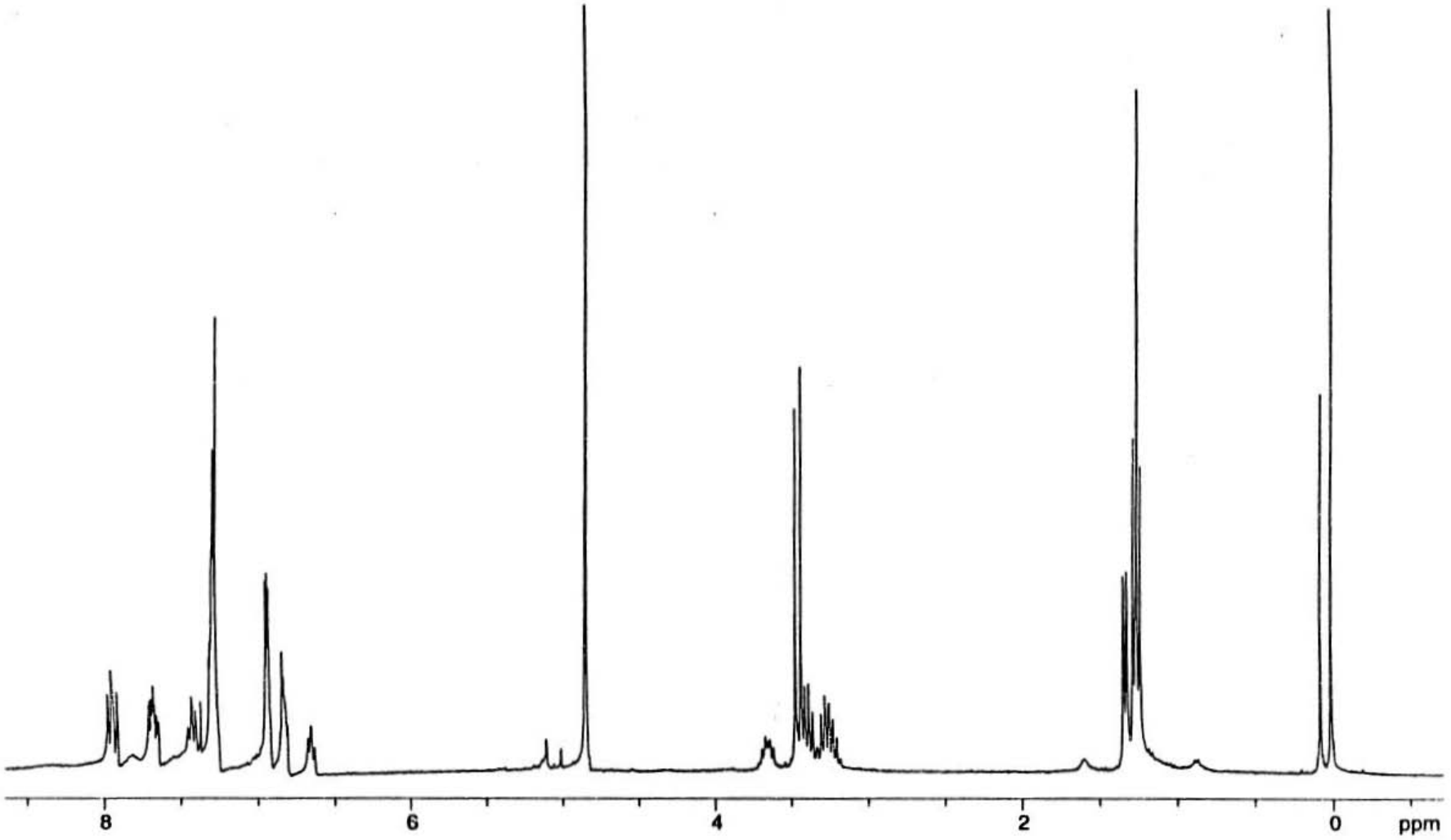

Figure A6 ^{1}H NMR of (S_C,S_{Co},S_P)-(η^5-Cp)Co(I)(PNH)(P(O)(OMe)(NEt_2)) **(2-2b)**

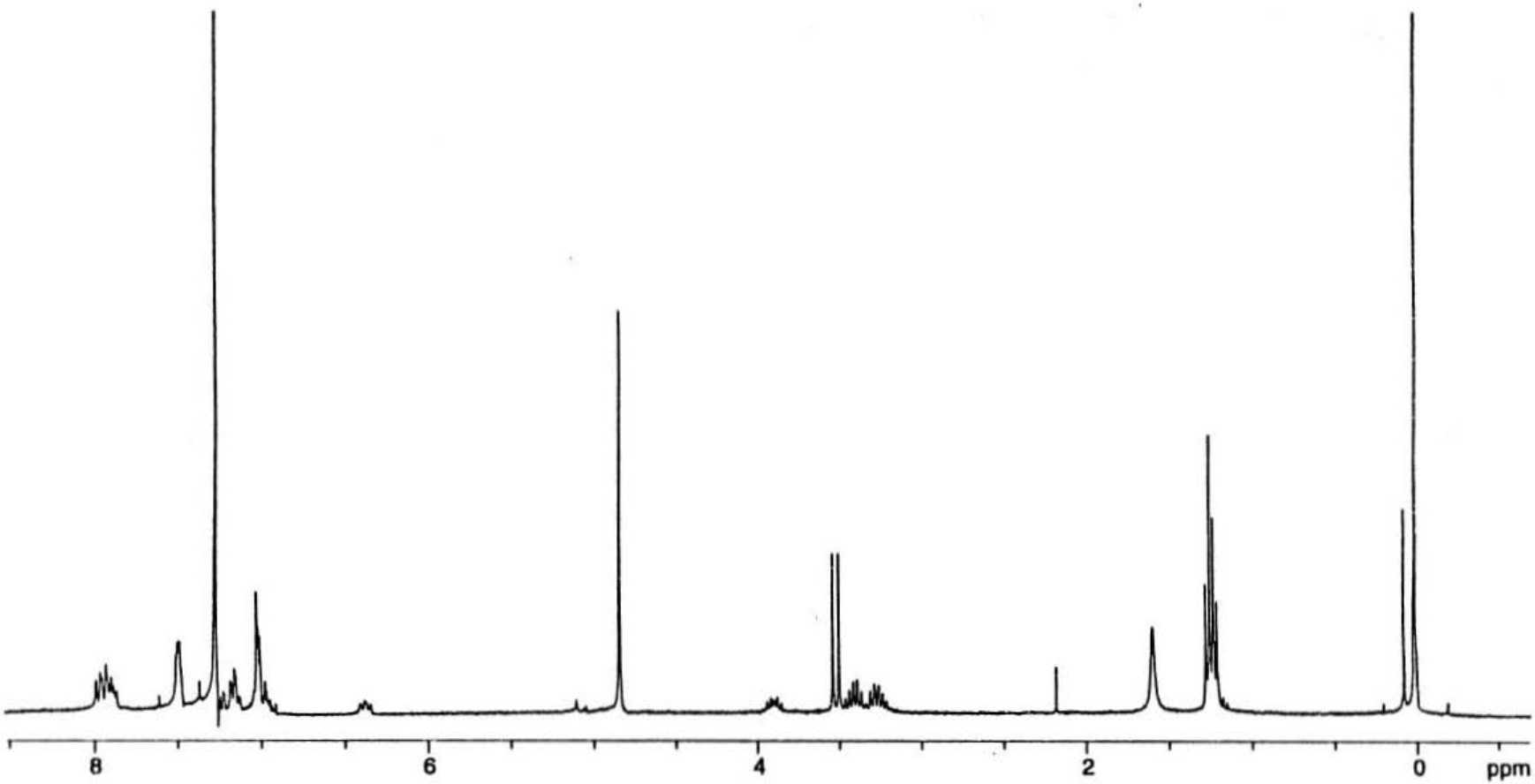

Figure A7 ^{1}H **NMR of** $(\eta^{5}\text{-Cp})Co(C_3F_7)(PPhMe_2)(P(O)(OMe)(NEt_2))$ **(2-3a)**

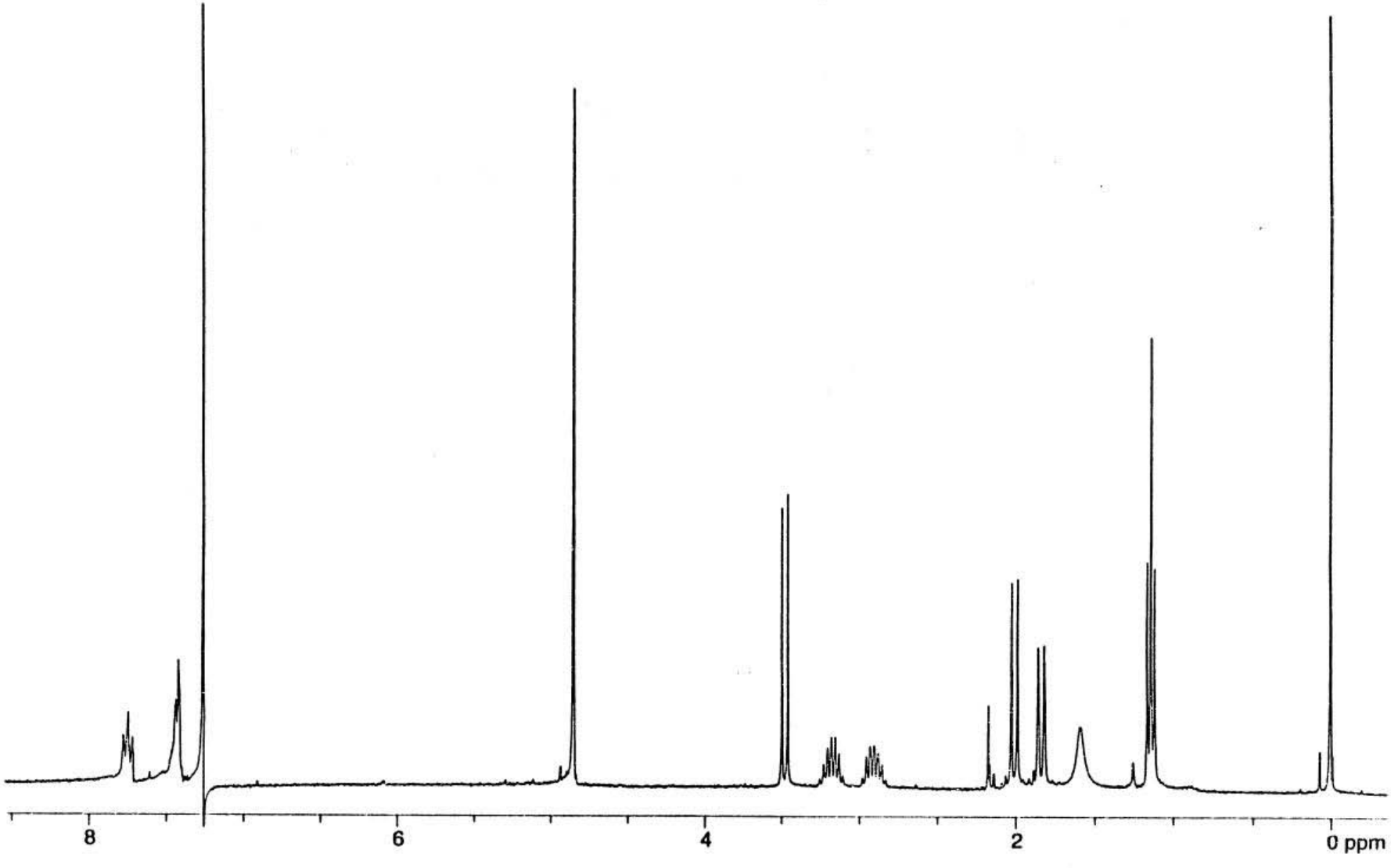

Figure A8 ^{1}H NMR of $(\eta^5\text{-Cp})Co(C_3F_7)(PPhMe_2)(P(O)(OMe)(NEt_2))$ **(2-3b)**

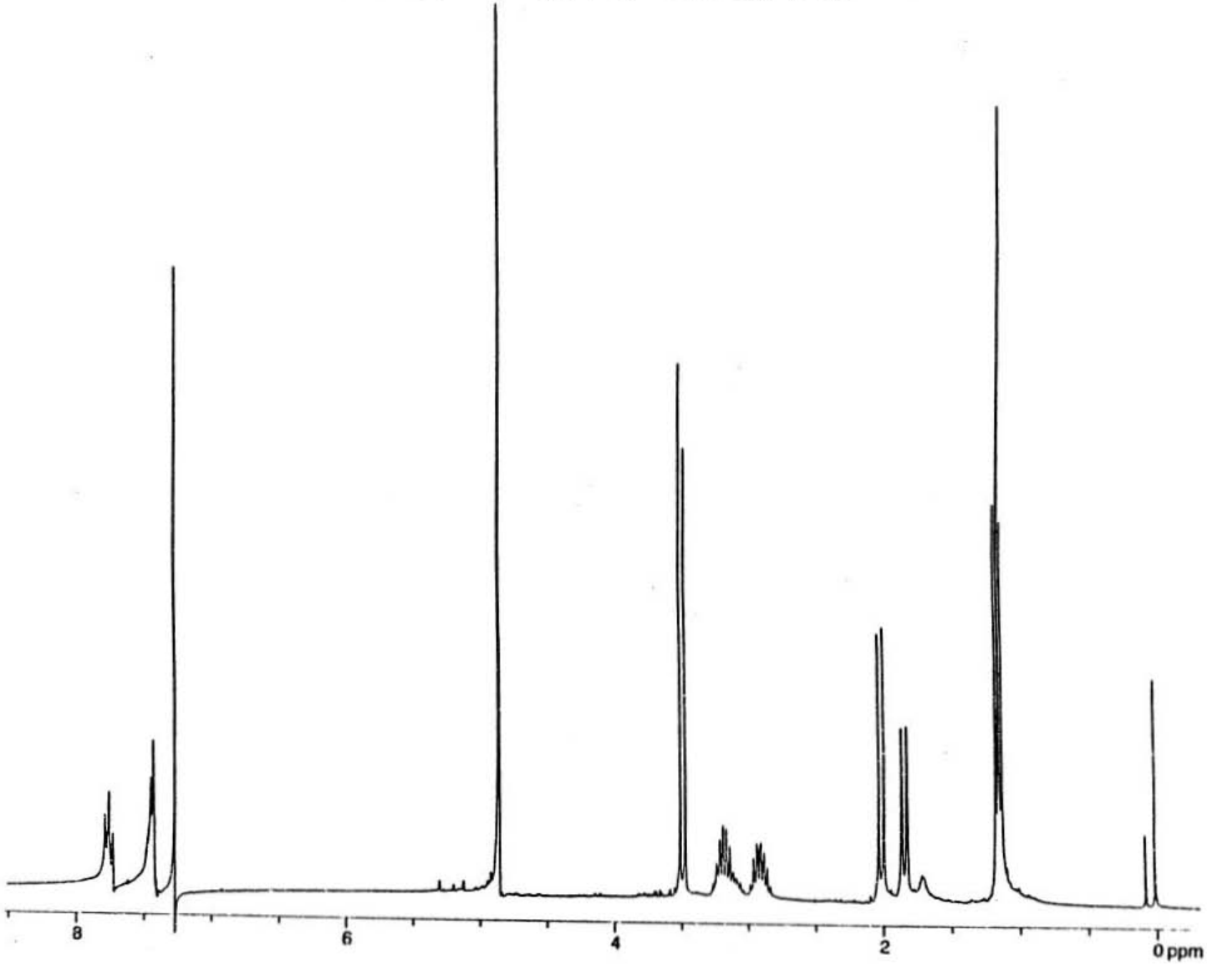

Figure A9 ^{1}H NMR of (S_{Co},R_P) / (R_{Co},S_P) -(η^5-Cp)Co(C_3F_7)(PPhMe$_2$)(P(O)(OEt)(SPh)) (2-4a)

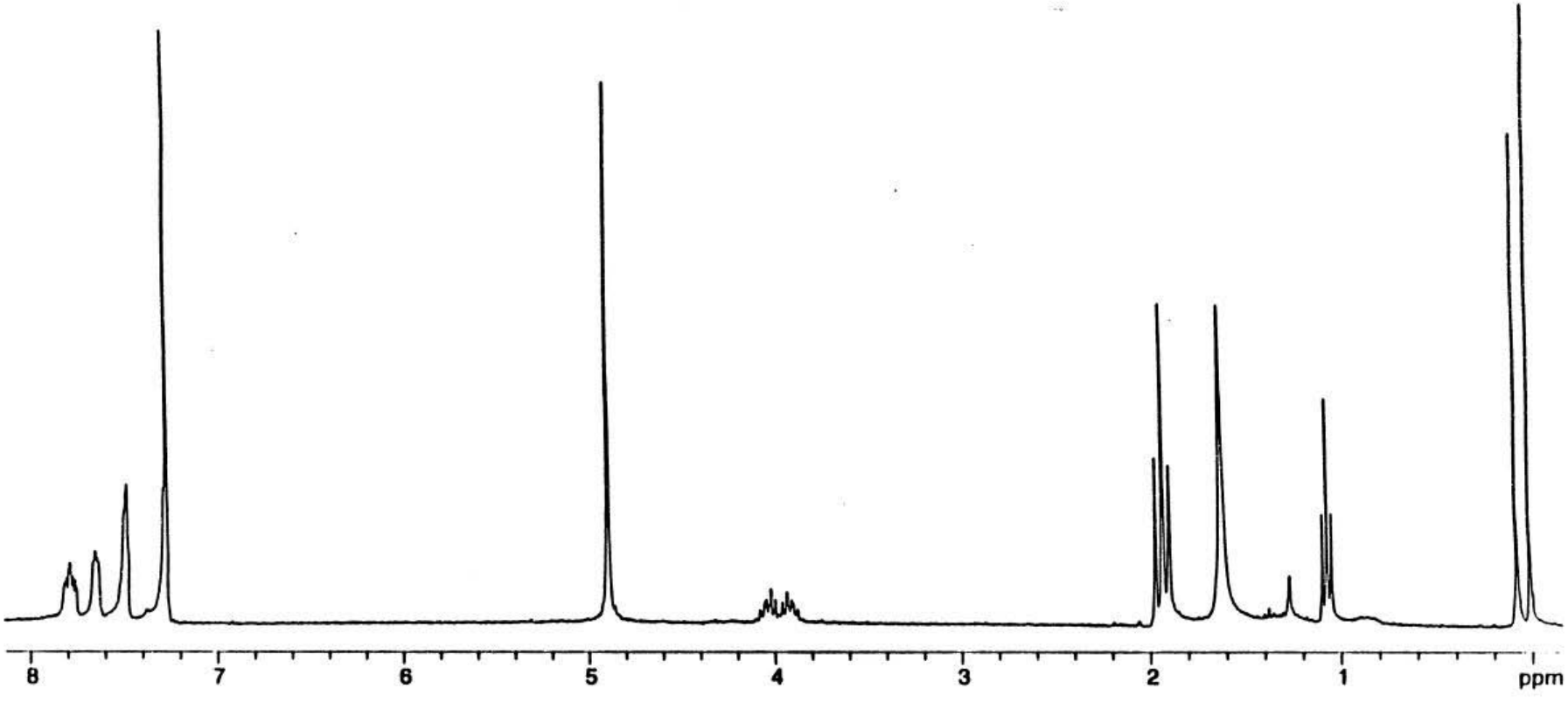

Figure A10 ^{1}H NMR of (S_{Co},S_P) / (R_{Co},R_P) -(η^5-Cp)Co(C_3F_7)($PPhMe_2$)(P(O)(OEt)(SPh)) **(2-4b)**

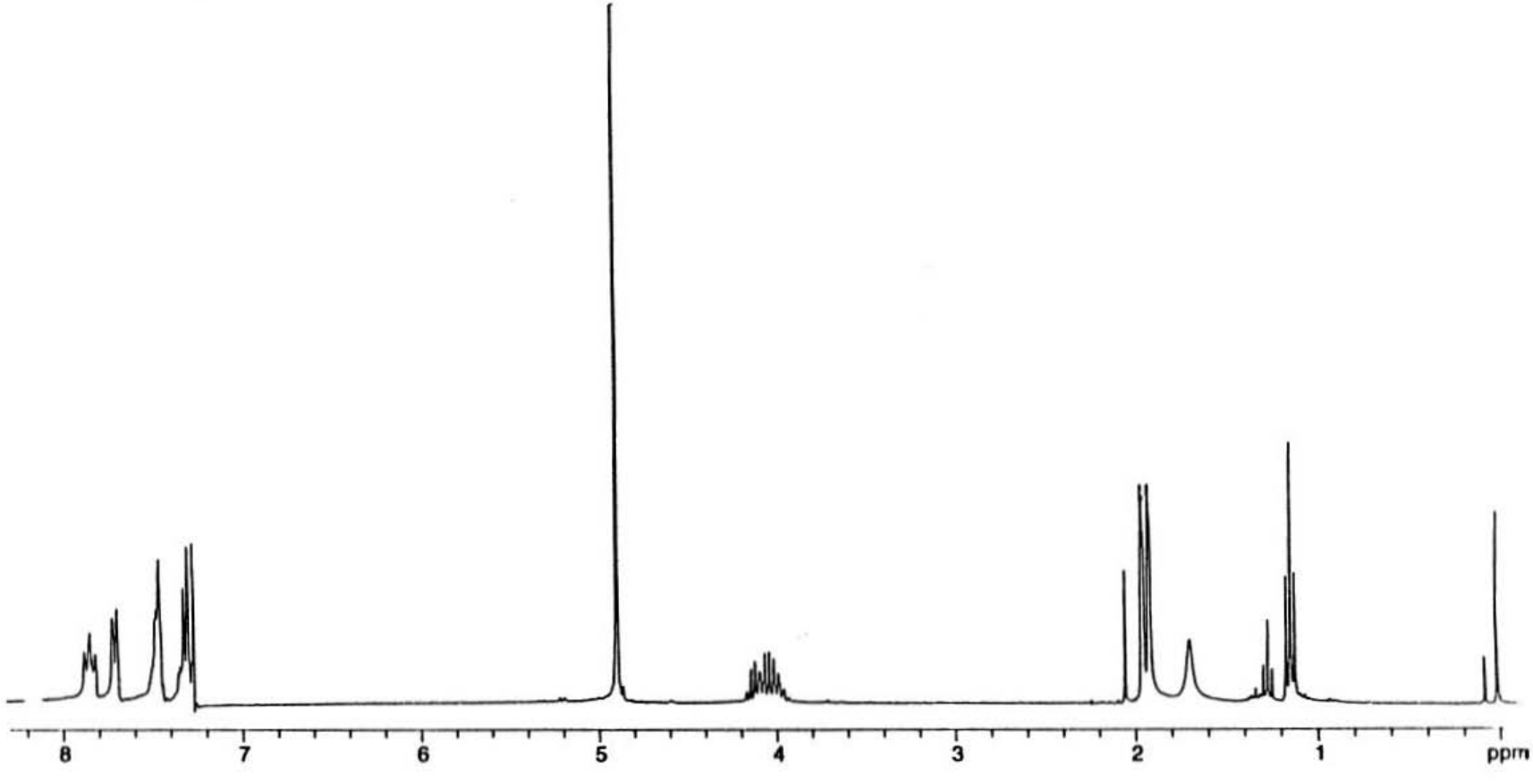

Figure A11 ^{1}H NMR of (η^5-Cp)Co(I)(PPh_2(OCD))(P(O)(OMe)(NEt_2)) **(3-1)**

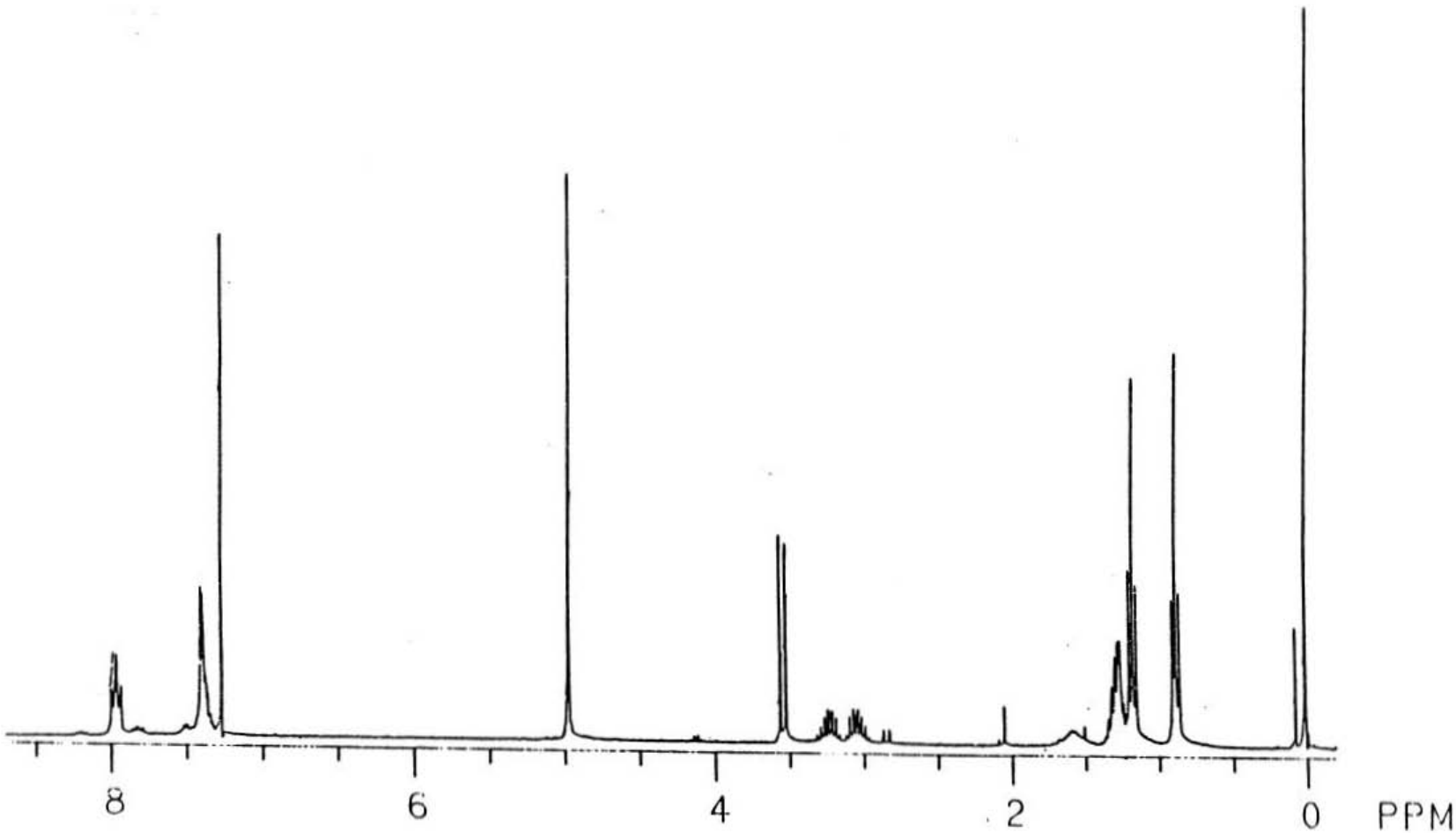

Figure A12 ^{1}H NMR of $[(\eta^{5}\text{-Cp})Co(C_3F_7)(PPhMe_2)(P(OH)(OMe)Ph)]^{+}Cl^{-}$ **(3-2)**

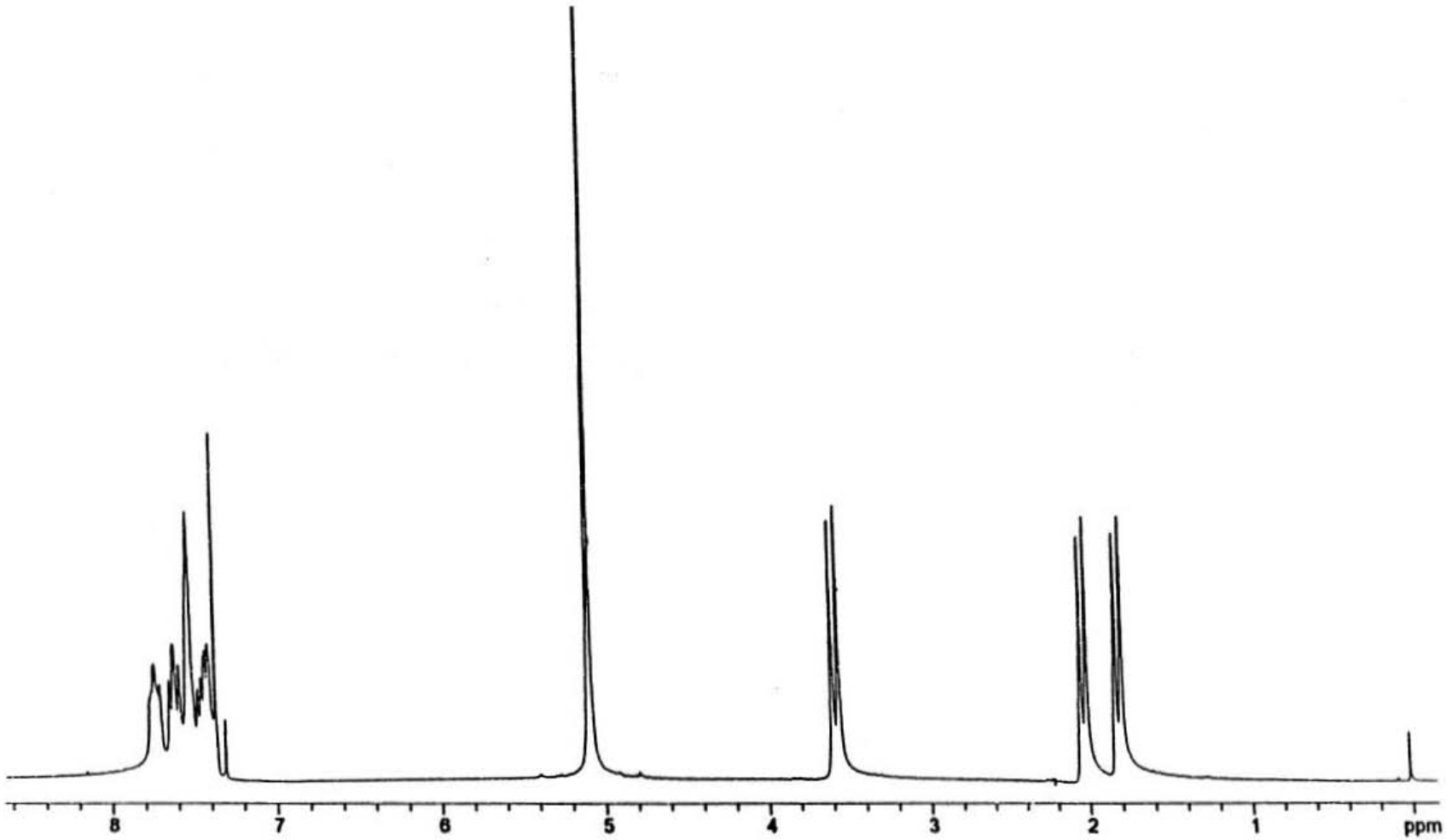

Figure A13 ^{1}H NMR of $(\eta^5\text{-Cp})Co(C_3F_7)(PPhMe_2)Cl$ **(3-3)**

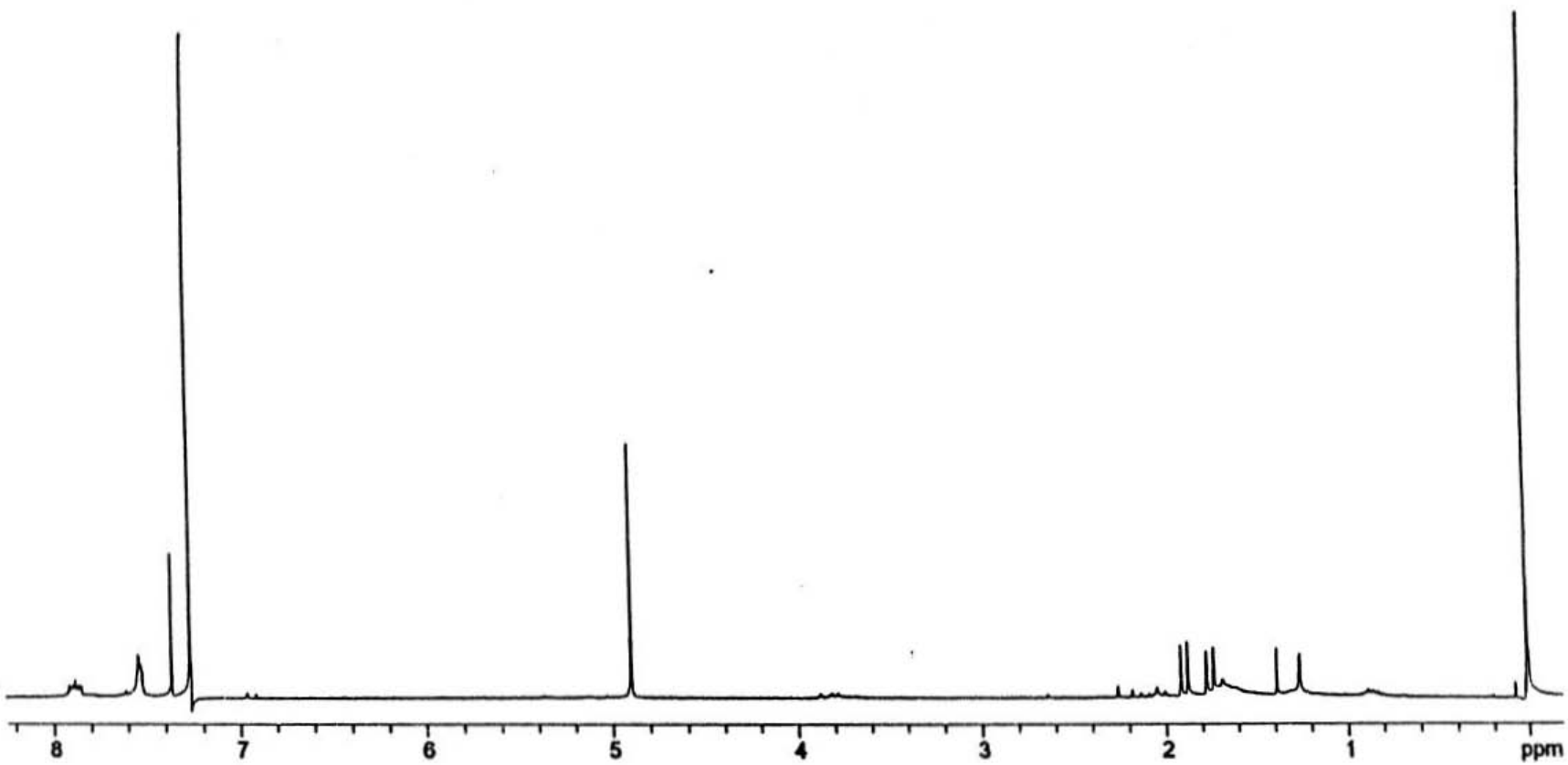

Figure A15 ^{19}F **NMR of** $(\eta^5\text{-Cp})Co(C(O)C_2F_5)(PPhMe_2)(P(O)(F)Ph)$ **(3-4)**